Title
Swelling and transport properties of hydrophobic polyelectrolyte gels

Author
Firestone, Bruce A.

Publication Date
1989

Peer reviewed|Thesis/dissertation

Swelling and Transport Properties of Hydrophobic Polyelectrolyte Gels

by

Bruce A. Firestone

B.S. University of California, Berkeley 1978

DISSERTATION

Submitted in partial satisfaction of the requirements for the degree of

DOCTOR OF PHILOSOPHY

in

Pharmaceutical Chemistry

in the

GRADUATE DIVISION

of the

UNIVERSITY OF CALIFORNIA

San Francisco

To
Mom, Hope and Chris for their love
and encouragement.

Acknowledgements

This dissertation is the culmination of a long journey that would have been impossible without the guidance, help and advice that I received from many outstanding people. I would like to convey my sincere thanks and appreciation to the following people who have contributed greatly to my development as a scientist:

My major professor Dr. Ron Siegel who agreed to take me on as his first graduate student. I will always be grateful to Ron for his valued input and guidance and for sharing with me his love of science.

Dr. C. Anthony Hunt for his interest and time for many insightful discussions concerning this work and for his constant reminders to consider alternative views and approaches.

My orals committee of Drs. Tom Tozer (chairman), Ken Dill, Richard Guy, Joe Bentz and Gerold Grodsky for seeing fit to let me pass without a repeat performance.

My thesis committee of Drs. Siegel, Hunt and Dill for valuable guidance and advice.

I would also like to sincerely thank Jim Wright whose enthusiasm for science I found very contagious during our days at Syntex and for his encouragement to attend graduate school (although at Wisconsin), Linda De Young and Seaung Oh for their friendship over the years and for the many valuable chalkboard sessions we had in HSE 1170.

The use of the DSC instrument at SRI International was made possible by Dr. Jorge Heller to whom I am grateful. I would also like to thank Barry Schwarz for his insights on polymer phase behavior, Ingegerd Johannes for her excellent technical assistance in the gel collapse experiments, José Manuel Cornejo Bravo for sharing his data on swelling equilibria in unbuffered solutions, J.P. for always being there in spirit and to all of the members of the Dill and Siegel groups for their help and feedback during my preparation for orals and for listening to my group meetings.

I would also like to express my gratitude to the Department of Pharmaceutical Chemistry at UCSF for selecting me to receive the ARCS Foundation Francis A Sooy Memorial Scholarship in 1987 and NIH Training Grant support from 1986 through 1989, to the Department of Pharmacy Faculty for awarding me the first Sydney Riegelman Prize in 1985-1986 and to Interphex USA for selecting me to receive the first Industrial Pharmacy Graduate Fellowship in 1987.

Bruce A. Firestone

April 1989

Swelling and Transport Properties of Hydrophobic Polyelectrolyte Gels

by

Bruce A. Firestone

Departments of Pharmacy and Pharmaceutical Chemistry
University of California, San Francisco

Abstract

This thesis project is concerned with the development and characterization of a class of hydrophobic gels that can undergo a reversible volume transition between swollen hydrophilic and collapsed hydrophobic states induced by solution pH. The gels employed are amphiphilic in nature and are based on a hydrophobic, water immiscible n-alkyl ester of methacrylic acid (nAMA) and a hydrophilic, ionizable monomer N,N-dimethylaminoethyl methacrylate (DMA). These gels remain collapsed and hydrophobic at, and above, neutral pH but generally undergo an abrupt swelling transition induced by lowering the pH into the acidic region. Increasing gel hydrophobicity significantly reduces the extent of equilibrium swelling and the pH of the swelling transition. The effects of solution pH, ionic strength and ionic valence on equilibrium swelling are shown to perturb the osmotic balance of the gels, and the observed changes in swelling are qualitatively predicted by the Donnan equilibrium theory, although the theory fails when applied quantitatively. The kinetics of gel water sorption and swelling from the dry state are generally non-Fickian, are believed to proceed via a moving front mechanism and are strongly influenced by the chemical nature of the ions in solution. Swelling and deswelling processes from the swollen state are rapid and completely reversible when pH remains below the pH of the swelling transition. When the transition pH is traversed, kinetics become more complicated and generally slow down considerably. Potential mechanisms for the slowing phenomena are investigated.

Table of Contents

List of Tables

List of Figures

Chapter 1.

Chapter 2.

Chapter 3.

Chapter 4.

Chapter 5.

Chapter 6.

Chapter 8.

Chapter 1.

Introduction

1.1 Background

A three dimensional network structure, composed of long chain polymer molecules that are periodically crosslinked together, is capable of absorbing a large amount of a suitable solvent in which it is immersed. The resulting form of matter is intermediate between a solid and a liquid and can vary in consistency from fluid-like to a rigid solid depending on the amount of solvent imbibed. The presence of crosslinks that connect one primary polymer chain to another can result from physical entanglements of the chains, ionic interactions between oppositely charged groups, or covalent bonds. Crosslinks prevent the network structure from ultimately dissolving in the solvent medium. Such systems are called gels and, as pointed out by Flory (1), are analogous to ordinary polymer solutions, but form elastic rather than viscous solutions.

The phenomenon of swelling in network structures has been studied since the early 1900s in a wide variety of natural and synthetic gels. The animal protein, gelatin, when dissolved in water, constitutes the most familiar of all gels. Many biological structures are, in fact, gels including the vitreous humor of the eye, synovial fluid of the joints, mucous, collagen and other connective tissues, and muscle tissue (2). The liquid component of these gels allows for the diffusion of oxygen and other nutrients while the network itself provides structural integrity and elasticity. Gels produced from the diverse array of synthetic polymers are the basis for many important processes in science and technology. Some of these include chromatographic separations and electrophoresis, solvent extraction

and solute recovery processes, as matrices and membranes in drug delivery, and in biosensors. Some of these applications will be briefly reviewed below.

1.2 Applications of Gels

The use of swellable gel systems in science and technology has become widespread over the past twenty years. Many of these applications have evolved from two important gel properties; 1) their three dimensional network structure and the effect it has on the transport properties of both small and large molecules, and 2) the sensitivity of gel swelling to local environmental conditions. Processes and techniques that exploit one or both of these properties constitute the most important applications of gels. The early interest in water swellable gels stemmed from their use as biocompatible materials, as was first reported by Wichterle and Lim (3). These applications include coatings for catheters (4) and surgical sutures (5), vitreous humor replacement (6), synthetic cartilage (7), hemodialysis membranes (8), contact lenses (9) and biosensors (10).

The most widespread use of gels today is in the area of chromatography and separation science. Gels are generally employed as stationary phases in separation techniques such as size exclusion or gel permeation chromatography (11), ion exchange chromatography (11) and gel electrophoresis (12).

A novel technique for concentrating dilute solutions of organic or biological molecules using gels as reusable size-selective extraction solvents was reported by Cussler and coworkers (13-15). The technique involves the addition of small spherical beads of pH-sensitive (partially hydrolyzed polyacrylamide) or temperature-sensitive (N,N-diethylacrylamide/sodium methacrylate) copolymer gels to a dilute solution of a macromolecule. Upon swelling in solution at slightly alkaline pH or at low temperature, low molecular weight solvent is absorbed by the gel while the macromolecule is excluded from entering the network. The resulting supernatant is concentrated with respect to the

macromolecule and can be separated from the swollen gel spheres by filtration. Acidifying the gel solution or increasing the temperature causes a reduction in gel volume and expulsion of the internal solvent. The gels can then be reused in further separation cycles.

The use of gels in drug delivery and controlled release applications has achieved popularity in the last ten years, and numerous reviews and accounts of this work have recently appeared (16-24). It is often desirable to control and prolong the administration of a single dose of an agent. The oscillatory blood levels that are observed with repeated dosing of a drug from a more traditional dosage form (tablet, capsule) can be avoided by administering the agent from a dosage form that slowly releases the agent. The extended and controlled release of drugs from a single device often leads to more constant blood levels that can be maintained for periods of months and years (20-24).

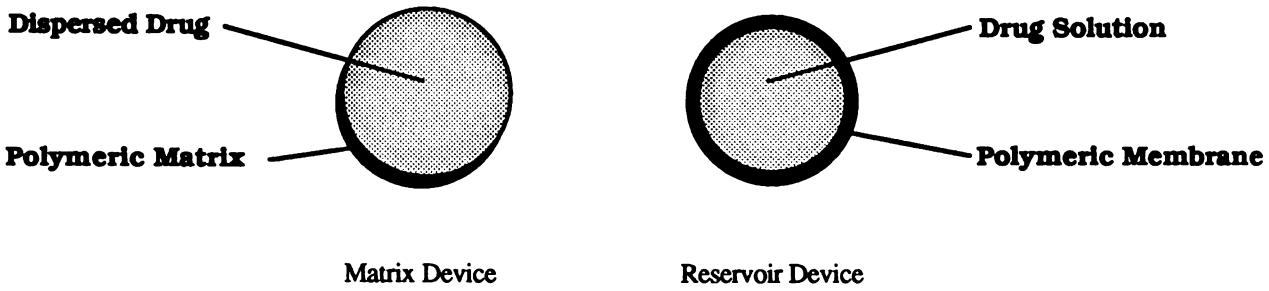

Figure 1.1. The two primary types of polymeric drug delivery devices; matrix and reservoir.

Gels and other polymeric materials are attractive for use in controlled release applications because they can be used as housings for incorporating and storing the drug in a device, as well as provide the rate-controlling mechanism for drug release from the device. Matrix devices, in which the drug is dispersed directly in the polymer, and reservoir devices, which contain a solution of drug separated from the outside environment by a rate-controlling polymeric membrane, are the two primary classes of polymeric delivery systems as shown in Figure 1.1. The principal release mechanisms from matrix

devices include diffusion, polymer erosion and polymer swelling, while diffusion through the rate-controlling polymer membrane is the usual release mechanism in reservoir devices (19,20). Release of the active agent is initiated by placing the device in a suitable release environment in the body, such as the buccal cavity, gastrointestinal tract, subdermally, intramuscularly, transdermally, vaginally or intranasally. Release proceeds until the device is either depleted of drug or is removed from the site of application.

Strategies in optimal drug delivery may require that drug release rates from a device be responsive to the local biological environment. Regional drug delivery in the gastrointestinal tract triggered by local pH differences, diffusional drug release from temperature-sensitive gels or delivery from an implanted device in response to the circulating level of an endogenous molecule (e.g. glucose in the diabetic patient) offers significant potential for improving the efficacy and bioavailability of therapeutic agents. Polymeric systems that have swelling properties that are responsive to their environment may have great utility in achieving stimulus-sensitive and self-regulating drug delivery strategies.

pH-sensitive gels and polymeric films that change their permeability properties in response to a change in solution pH have been reported by several groups. Kopecek et al. studied the pH-dependent permeability properties of hydrophilic ionizable gels, including acidic, basic and ampholytic, to NaCl (25). Salt permeability was found to be a strong function of the degree of ionization of the gel, as affected by both solution pH and the gel ionic monomer content. Alhaique et al. found that the permeability properties of poly(ethylene-co-vinyl N,N-diethylglycinate) random copolymer films to benzyl alcohol could be modulated by more than two orders of magnitude by adjusting the solution pH (26). They attributed the permeability enhancement at low pH to the increase in film hydration that accompanied the protonation of the copolymer amino groups.

In studies of poly(2-hydroxyethyl methacrylate-co-methacrylic acid) hydrogels, Kou et al. found that matrix hydration, as controlled by the solution pH, could be an effective modulator of the diffusional release of of phenylpropanolamine (PPA) (27). Diffusivity of PPA increased 52 fold as gel water weight fraction increased from 0.35 (at pH 1.0) to 0.88 (at pH 7.0). Siegel et al. reported the pH-sensitive swelling-controlled release of caffeine from hydrophobic copolymer gels based on methyl methacrylate and N,N-dimethylaminoethyl methacrylate (28). Caffeine release was controlled by the rate of water sorption into the gel and increased as pH decreased. At neutral pH, where minimal gel swelling occurs, caffeine release was virtually nonexistent.

In the development of self-regulating delivery devices, several groups have studied the use of temperature-sensitive gels such as poly(N-isopropylacrylamide) (pNIPAAm) (29,31), and its copolymers with methacrylic acid (29), acrylamide (30) and butyl methacrylate (32) . Gels based on N-isopropylacrylamide exhibit a lower critical solution temperature (LCST) of approximately 32 °C. Such gels reversibly shrink or swell when the solution temperature is raised or lowered through the LCST. Lowering the temperature below the LCST promotes gel expansion and reswelling. As a result of these temperature induced swelling changes, the release rates of substances initially in the gel matrix such as vitamin B12 (29,31), myoglobin (29), methylene blue (29) and indomethacin (32) can be accelerated by reducing the local temperature from 37 °C past the LCST.

Bae and coworkers showed that release of indomethacin from a poly(N-isopropylacrylamide-co-butyl methacrylate) gel could be turned on and off by cycling the temperature between 20 and 30 °C, which brackets the LCST of this gel (32). The release rate of indomethacin, essentially zero at 30 °C, increased to approximately 0.25 mg/hr with a step reduction in temperature to 20 °C. This pattern of release was fairly reproducible during subsequent temperature cycles, demonstrating the utility of this gel as a temperature-sensitive on-off switch for chemical delivery.

Dong and Hoffman demonstrated that the accessibility of a substrate to an enzyme (asparaginase) immobilized in poly(N-isopropyl acrylamide-co-acrylamide) gels could be modulated by changes in the local temperature (30). When the temperature was raised above the LCST, the activity of asparaginase was shut off, presumably due to the greatly reduced permeation rate of asparagine through the deswollen gel. A reduction in temperature below the LCST restored the asparaginase activity to essentially its original value. Temperature cycling experiments showed the process was reproducible. Such immobilized enzyme/gel systems were termed 'catalytic hydrogels' and their use in feedback control of temperature-sensitive reactions (30) and in medical diagnostics was proposed (33).

Other catalytic hydrogels have been reported where gel swelling is sensitive to the product of an immobilized enzyme-substrate reaction. Thus, the presence of substrate in the environment of the gel is transduced through the enzyme/substrate reaction to a change in gel swelling. Much of this work has been applied to the development of glucose-sensitive membranes for use in implantable self-regulating insulin delivery systems for the treatment of diabetes. Such a system would 'sense' the blood levels of circulating glucose and initiate the release of insulin when glucose levels become elevated. Upon return to normal glucose levels, the device would automatically decrease insulin release to a basal rate.

Ishihara and coworkers fabricated a glucose sensitive composite membrane by immobilizing the enzyme glucose oxidase (GO) in a polyacrylamide membrane and laminating it with a pH-sensitive polyamine membrane (34). In the presence of elevated levels of glucose in the external solution, glucose is oxidized to gluconic acid in the GO membrane as illustrated in Figure 1.2. Generation of gluconic acid causes a reduction in pH which induces the ionization and swelling of the polyamine membrane. The resulting permeability and diffusional release of insulin increases several fold due to the state of

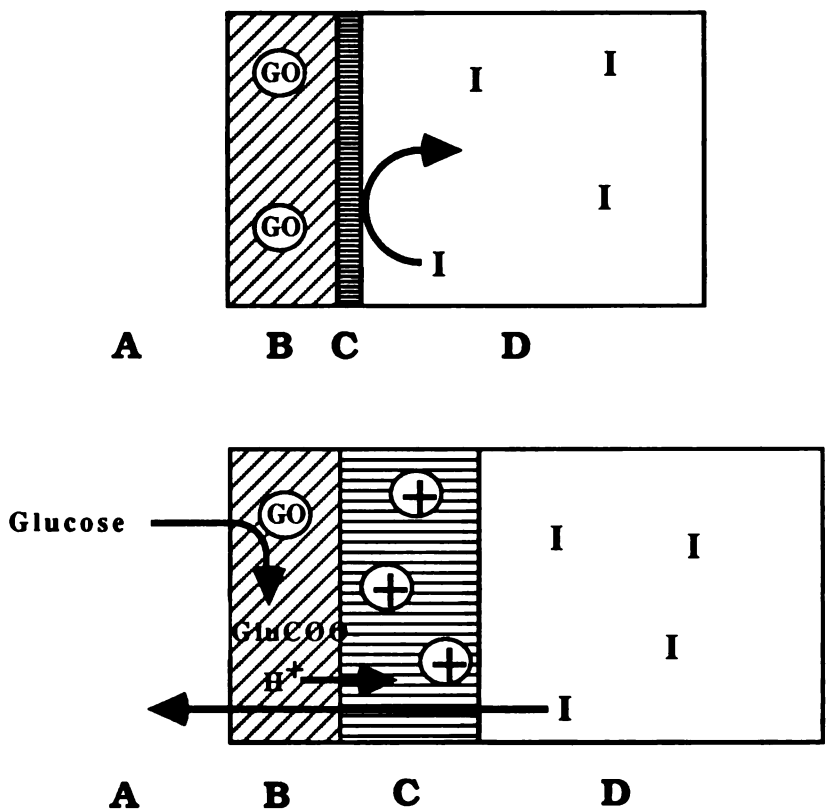

Figure 1.2. An illustration of a glucose-sensitive composite membrane. Top panel: in the absence of circulating glucose, the delivery of insulin (I) is minimal. The polyamine membrane (C) is unionized, moderately swollen, and has a low permeability to insulin. Bottom panel: in the presence of circulating glucose, gluconic acid is produced via oxidation by glucose oxidase (GO) in membrane B which reduces the local pH. This causes the ionization of the polyamine membrane (C), increases its permeability to insulin and initiates the diffusional release of insulin (34).

increased swelling in the polyamine membrane, compared with that in the absence of external glucose. Other similar glucose-sensitive membranes have been prepared with GO immobilized in hydrophilic pH-sensitive HEA/DMA/4-trimethylsilylstyrene (35) and HEMA/DMA (36) gels.

Clearly, the swelling state of network structures can be substantially altered by a variety of environmental changes. The increased understanding of such swelling phase behavior, from both a theoretical and experimental standpoint, will aid development of improved gel-based separation techniques, stimulus-sensitive drug delivery devices, biosensors and novel mechanochemical engines and pumps.

1.3 Scope of Thesis

Until now, the swelling behavior of polyelectrolyte gels has been studied largely in hydrophilic, crosslinked gel systems such as polyacrylamide, poly(HEMA) and poly(NIPAAm) containing ionizable comonomers. Because of their hydrophilic nature, these gels generally swell extensively in water or water-containing cosolvent mixtures, and retain appreciable solvent content even under 'collapsed' conditions. Consequently, efforts to employ the phase behavior of these hydrogels to control the diffusion and release of molecules has met with limited success. The development of crosslinked polymer systems that can undergo a sharp and reversible hydrophobic-hydrophilic transition, as controlled by solution properties, may be more effective in controlling the transport properties of small molecules compared with the hydrophilic polymer systems studied to date. Such gel systems could potentially be used in the design of improved self-regulating drug delivery devices and separation systems suitable for small and large molecules.

This thesis project is concerned with the development and characterization of a class of hydrophobic gels that can undergo a reversible volume transition between swollen hydrophilic

and collapsed hydrophobic states induced by solution pH. The gels employed in this work are distinct from those studied previously in that they are amphiphilic in nature. They are based on two principal types of monomeric units, a hydrophobic, water immiscible n-alkyl ester of methacrylic acid (nAMA) and a hydrophilic, ionizable monomer N,N-dimethylaminoethyl methacrylate (DMA). Because of the potential to become ionized in solution, these gels are polyelectrolytes. The structures of the monomers are shown in Figure 1.3, where the ester chain length of the nAMA monomer ranges from C1 (methyl, n=1) to C6 (hexyl, n=6). The gels are prepared via a free-radical initiated bulk copolymerization, and are crosslinked with a

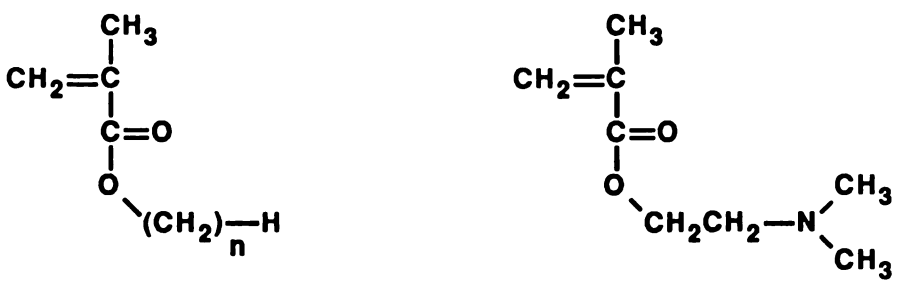

n-alkyl methacrylate (nAMA) N,N-dimethylaminoethyl methacrylate (DMA)

Figure 1.3. Structures of the two types of methacrylic acid esters used to make the copolymer gels in this work.

small amount of divinyl benzene (0.1 wt%). The structure of nAMA/DMA copolymer gels is shown in Figure 1.4, where the x and y subscripts refer to the relative molar contents of nAMA and DMA. Because the polymerization proceeds through the C2 and C3 carbon-carbon double bonds of each monomer, the ester groups become pendant chains to the main copolymer backbone. The various nAMA/DMA gels thus prepared differ only in their relative content of one pendent sidechain to the other as well as in the chain length of the nAMA sidechain.

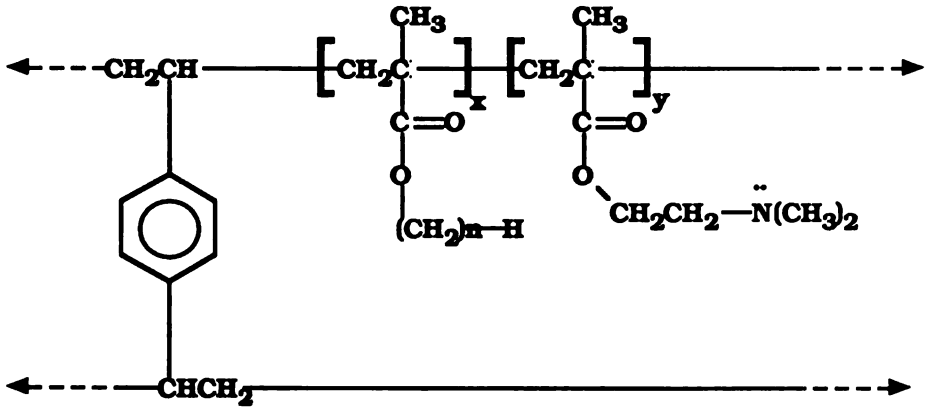

Figure 1.4. Network structure of nAMA/DMA gels crosslinked with divinyl benzene.

Chapter 2 of this thesis comprises an expanded review of the phenomenon of swelling in crosslinked network structures with particular emphasis on the swelling behavior of polyelectrolyte gels. A compilation of the materials and methods used in the preparation of nAMA/DMA copolymer gels in this work and their subsequent characterization is provided in Chapter 3.

The aqueous pH-dependent equilibrium swelling properties of these gels will be presented in Chapter 4. It will be shown that although these gels imbibe water to very limited extent (<10 wt% water) at, and above, neutral pH, they generally undergo abrupt swelling transitions to swollen structures induced by lowering the pH into the acidic region. The effects of both nAMA/DMA comonomer ratio and the nAMA sidechain length will be shown to significantly affect the equilibrium swelling properties.

Chapter 5 investigates the effects of solution ionic strength and ionic valence on equilibrium swelling. The results are compared with predictions of swelling based on the Donnan equilibrium theory. It will be shown that the theory qualitatively predicts most of the observed trends in the swelling data although it fails to work in a quantitative fashion.

The kinetic swelling properties of the gels from the dry state will be shown in Chapter 6 to be highly dependent on pH, ionic strength, ionic composition, temperature and gel composition. Initial sorption kinetics are generally non-Fickian in both glassy and rubbery gels and evidence is presented that swelling occurs by a moving front mechanism.

Chapter 7 focuses on swelling reversibility and the mechanism of deswelling given perturbations in pH. It is demonstrated that swelling and deswelling processes are rapid and completely reversible when pH remains below the pH of the swelling transition. When the transition pH is traversed, kinetics become more complicated and generally slow down considerably. Potential mechanisms for the slowing phenomena are investigated. And finally, unresolved issues and suggestions for future work are discussed in Chapter 8.

References

1. P.J. Flory, "Principles of Polymer Chemistry", Chapter XIII, Cornell University Press, 1953.

2. T. Tanaka, Gels, Sci. Am., 244, 1, 124 (1981).

3. O. Wichterle and D. Lim, Hydrophilic Gels for Biological Use, Nature, 185, 117 (1960).

4. R.A. Abrahams and S.H. Ronel, Factors Influencing the Biocompatibility of Hydrogels, Polym. Prep., 16, 535 (1975).

5. M. Tollar, M. Stol and M. Kliment, Surgical Structure Materials Coated with a Layer of Hydrophilic Hydron Gel, J. Biomed. Mat. Res., 3, 305 (1969).

6. M. Refojo in "Hydrogels for Medical and Related Applications", J. D. Andrade, Ed., ACS Symposium Series, Vol. 31, 1976.

7. B.D. Ratner in "Hydrogels for Medical and Related Applications", J. D. Andrade, Ed., ACS Symposium Series, Vol. 31, 1976.

8. P. Spacek and M. Kubin, Poly(Ethyleneglycol Methacrylate) as a Material for Hemodialysis, J. Biomed. Mat. Res., 7, 201 (1973).

9. B.J. Tighe in "Hydrogels in Medicine and Pharmacy", Vol. III, N.A. Peppas, Ed., Chapter 3, CRC Press, 1987.

10. "Biosensors, Fundamentals and Applications", A.P.F. Turner, I. Karube and G.S. Wilson, Eds., Oxford Science, 1987.

11. J.J. Kirkland and L.R. Snyder, "Introduction to Modern Liquid Chromatography", J. Wiley and Sons, 1974.

12. "Gel Electrophoresis, A Practical Approach", B.D. Barnes and D. Rickwood, Eds., IRL Press, 1981.

13. E.L. Cussler, M.R. Stokar and J.E. Varberg, Gels as Size Selective Extraction Solvents, AIChE. J., 30, 578 (1984).

14. S.H. Gehrke, G. P. Andrews and E. L. Cussler, Chemical Aspects of Gel Extraction, Chem. Eng. Sci., 41, 8, 2153 (1986).

15. R.F.S. Freitas and E.L. Cussler, Temperature Sensitive Gels as Extraction Solvents, Chem. Eng. Sci., 42, 1, 97 (1987).

16. "Recent Advances in Drug Delivery Systems", J.M. Anderson and S.W. Kim, Eds., Plenum Press, 1984.

17. "Hydrogels for Medical and Related Applications", J. D. Andrade, Ed., Chapters 12-14, ACS Symposium Series, Vol. 31, 1976.

18. W.E. Roorda, H.E. Boddé, A.G. de Boer and H.E. Juninger, Synthetic Hydrogels as Drug Delivery Systems, Pharmaceutisch Weekblad, Sci. Ed., 8, 165 (1986).

19. "Hydrogels in Medicine and Pharmacy", Vols. I-III, N.A. Peppas, Ed., CRC Press, 1986-87.

20. J. Heller in "Controlled Drug Delivery, Fundamentals and Applications", J.R. Robinson and V.H.L. Lee, Eds., Drugs and the Pharmaceutical Sciences, Vol. 29, Marcell Dekker, 1987.

21. "Medical Applications of Controlled Release", Vols. I-III, R.S. Langer and D.L. Wise, Eds., CRC Press, 1984.

22. "Controlled Release Technology, Pharmaceutical Applications", P.I. Lee and W.R. Good, Eds. Chapters 10-16, ACS Symposium Series, No. 348, ACS Press, 1987.

23. R.W. Baker, "Controlled Release of Biologically Active Agents", J. Wiley and Sons, 1987.

24. "Biopolymeric Controlled Release Systems", Vols. I-II, D.L. Wise, Ed., CRC Press, 1984.

25. J. Kopecek, J Vacik and D. Lim, Permeability of Membranes Containing Ionogenic Groups, J. Polym. Sci., A1, 9, 2801 (1971).

26. F. Alhaique, M. Marchetti, F.M. Riccieri and E. Santucci, A Polymeric Film Responding in Diffusional Properties to Environmental pH Stimuli: A Model for a Self-Regulating Drug Delivery Systems, J. Pharmacol., 33, 413 (1981).

27. J.H. Kou, G.L. Amidon and P.I. Lee, pH-Dependent Swelling and Solute Diffusion Characteristics of Poly(Hydroxyethyl Methacrylate-co-Methacrylic Acid) Hydrogels, Pharm. Res., 5, 9, 592 (1988).

28. R.A. Siegel, M. Falamarzian, B.A. Firestone and B.C. Moxley, pH-Controlled Release from Hydrophobic/Polyelectrolyte Copolymer Hydrogels, J. Contr. Rel., 8, 179 (1988).

29. A.S. Hoffman, A. Afrassiabi and L.C. Dong, Thermally Reversible Hydrogels: II. Delivery and Selective Removal Of Substances from Aqueous Solutions, J. Contr. Rel., 4, 213 (1986).

30. L.C. Dong and A.S. Hoffman, Thermally Reversible Hydrogels: III. Immobilization of Enzymes for Feedback Reaction Control, J. Contr. Rel., 4, 223 (1986).

31. A. Afrassiabi, A.S. Hoffman and L.C. Cadwell, Effect of Temperature on the Release of Biomolecules from Thermally Reversible Hydrogels, J. Memb. Sci., 33, 191 (1987).

32. Y.H. Bae, T. Okano, R. Hsu and S.W. Kim, Thermo-Sensitive Polymers as On-Off Switches for Drug Release, Makromol. Chem. Rapid Comm., 8, 481 (1987).

33. A.S. Hoffman, Applications of Thermally Reversible Polymers and Hydrogels in Therapeutics and Diagnostics, J. Contr. Rel., 6, 297 (1987).

34. K. Ishihara, M. Kobayashi, N. Ishimaru and I. Shinohara, Glucose Induced Permeation Through a Complex Membrane Consisting of Immobilized Glucose Oxidase and a Poly(Amine), Polym. J., 16, 8, 625 (1984).

35. K. Ishihara and K. Matsui, Glucose-Responsive Insulin Release from Polymer Capsule, J. Polym. Sci., Polym. Lett., 24, 413 (1986).

36. J. Kost, T.A. Horbett, B.D. Ratner and M. Singh, Glucose-Sensitive Membrane Containing Glucose Oxidase: Activity, Swelling and Permeability Studies, J. Biomed. Mat. Res., 19, 1117 (1985).

Chapter 2.

The Phenomenon of Swelling in Network Structures

2.1 Balance of Forces

As in solutions made up of linear polymer molecules, a system consisting of a network structure and excess solvent has an opportunity to increase its entropy by mixing the two components. Many more configurations of the solvent molecules are available if the two components mix. The resulting swelling process of the network is thus an inherently favorable process from an entropic standpoint (1).

The interaction of the solvent with the chains of the network, which arises from the effects of intermolecular forces, can also strongly affect the swelling process. These interactions may either increase or decrease the tendency to swell due to the entropy of mixing process. Under conditions of solvent/polymer compatibility, the interaction free energy augments the entropy of mixing in driving the system to swell. With an unfavorable solvent/polymer compatibility, the interaction free energy will disfavor mixing and will operate in opposition to the entropic component of mixing. Under these conditions, the relative magnitudes of these opposing forces determines the extent of network swelling. Thus, in direct parallel with the mixing of small molecules and/or polymers, the swelling process in neutral gels is driven by the free energy of mixing (1,2).

As the swelling process proceeds, the increase in gel volume leads to the stretching and elongation of the network chains. In response to this perturbation in chain conformation, an elastic retractile force develops in opposition to the swelling process. Once swelling equilibrium has been attained, and in the absence of any additional forces

(electrostatic, external pressure-volume, etc.), the mixing tendency of the network and solvent is exactly balanced by the elastic response of the crosslinked chains (2,3).

In polyelectrolyte gels, where the network chains contain fixed ionized groups, the swelling force can be greatly increased compared with an equivalent neutral gel. The basis for the influence of gel charge on the magnitude of swelling is derived from two equivalent effects: repulsive interactions between proximal charged groups on the gel and the ion osmotic pressure due to mobile counterions within the gel (1). Electrostatic repulsion becomes most important when the gel has a high charge density and the solution is of low ionic strength, so that screening of the fixed charges by the counterions is not appreciable. Under these conditions, the electrostatic repulsion between the fixed charged groups tends to stretch the chains of the gel which enhances swelling (4).

Procter and Wilson, in 1916, first realized that the swelling of protein gels is determined mainly by the osmotic pressure difference between the mobile ions in the gel and in the external solution (5). Osmotic pressures of several to tens of atmospheres can be generated by gels with moderate charge densities in solutions of low ionic strength. The origin of the ion osmotic pressure is schematically depicted in Figure 2.1 in which a swollen ionic gel is shown in equilibrium with an external electrolyte solution. Free exchange of mobile ions and solvent occurs between the gel and the external solution. Because the fixed charged groups of the gel are not free to leave the interior of the gel, a situation analogous to the Donnan membrane equilibrium develops in which at equilibrium there is an unequal distribution of mobile ions between the gel interior and the external solution. The concentration of mobile ions will be greater inside the gel due to the presence of the fixed charges on the network which require mobile ions to enter the gel to maintain electroneutrality. This disparity in mobile ion concentration generates a net osmotic pressure between the gel interior and the external solution which causes water to enter the

gel (1,8). The magnitude of the ion osmotic pressure increases with gel charge density, but diminishes as the solution ionic strength becomes much larger than the charge density.

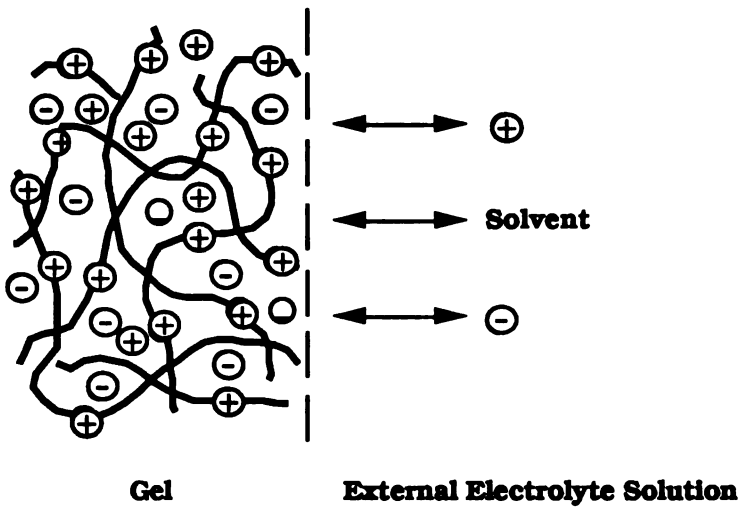

Figure 2.1. Schematic diagram of a polyelectrolyte gel in equilibrium with an electrolyte solution. Free exchange of mobile ions and solvent occurs between the gel and external solution. Adapted from (1).

The presence of charged groups on the gel, in conjunction with the polymer/solvent mixing entropy, drives the volume expansion of the network. Swelling equilibrium is achieved when the magnitudes of the osmotic pressure due to the charged groups, and the 'pressures' associated with the polymer/solvent mixing and the elastic retraction of the network chains, sum to zero. The equilibrium properties of neutral and polyelectrolyte gels are thus determined by a balance of opposing forces, that when perturbed, can bring about significant changes in the swelling state of gels.

2.2 Swelling Phase Transitions in Gels

A most significant discovery concerning the swelling behavior of gels was reported by Tanaka in 1978 (6). It was observed that large changes in the equilibrium volume of a hydrophilic polyacrylamide gel could be brought about by changes in the external

environment of the gel. Under certain conditions, varying the solvent composition or the temperature brought about a discontinuous and reversible volume change in the gel. Volume changes of up to three orders of magnitude could be caused by an infinitesimal change in the acetone/water solvent content or the temperature. These swelling transitions were reminiscent of the well known pressure-volume phase transitions observed in vapor-liquid equilibria. This work constituted the first demonstration of discrete phase transitions and critical phenomena in the swelling behavior of gels, a process that had been theoretically predicted by Dusek and Patterson nearly ten years earlier (7).

Since then, Tanaka and other workers have increased the understanding of swelling phase behavior in gels and have observed volume transitions in a wide variety of natural and synthetic polymers (8-14). Examples of discontinuous volume transitions in gels of biological origin include crosslinked DNA (13), crosslinked gelatin (13,15) and agarose (13). In each of these cases, the volume collapse of the gel was induced by increasing the acetone content in acetone/water cosolvent mixtures. Addition of a poor solvent for the polymer makes the solvent/polymer interaction less favorable for mixing. At the volume transition point, the solvent has become sufficiently poor so that polymer/solvent mixing is no longer favored. The gel thus collapses to minimize contact with solvent. This effect occurs, of course, at the expense of the mixing entropy, but the overall effect is to achieve a state with a minimized free energy.

The observation of volume phase transition in gels of widely varying chemical compositions such as polyvinyl gels (11), polynucleotide, polypeptide and polysaccharide gels (13) strongly suggests the universality of the phenomenon. Phase diagrams have been constructed for polyacrylamide (6,16) and poly(N-isopropylacrylamide) (17) gels that include coexistence curves and critical points. Similar phase behavior also exists for single polymer chains in solution where reversible collapse from the random coil to the more condensed state has been shown to occur (18-20).

2.3 Role of Network Ionization

As discussed above, ionic gels can become extensively swollen in aqueous systems due to the ion osmotic pressure that results from the presence of ionized groups on the gel. In a series of experiments involving the measurement of the equilibrium swelling behavior of partially hydrolyzed polyacrylamide gels and some of its derivatives, Tanaka et al. (8) and Nicoli et al. (21) demonstrated that network ionization plays a critical role in determining the existence of discrete, discontinuous volume phase transitions in these gels.

By subjecting prefabricated polyacrylamide gels to alkaline hydrolysis at pH 12, discontinuous and reversible volume transitions in acetone/water solutions were observed. As the duration of hydrolysis increased, the magnitude of the volume change increased and shifted to lower acetone concentration. Alkaline hydrolysis converts the pendant acrylamide groups to acrylic acid which ionizes in water or acetone/water solutions, as

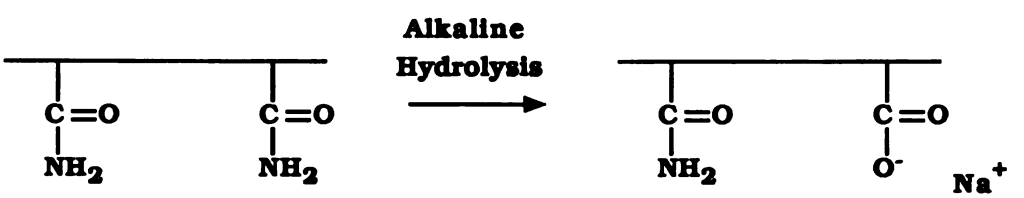

Figure 2.2. Alkaline hydrolysis of a polyacrylamide gel converts a fraction of the pendant acrylamide groups to acrylic acid, rendering the gel ionized.

shown in Figure 2.2. Increasing the duration of hydrolysis converts a greater fraction of the acrylamide groups to the corresponding acid and increases the gel charge density. Thus, the development of an ion osmotic pressure of sufficient magnitude in the gel can shift the system across the critical point which in turn results in a discontinuous volume transition.

Additional studies on other gel systems corroborate the role of ionization on volume transitions in both cationic and anionic gels (22-27). Poly(N-isopropylacrylamide) gels containing small amounts of ionizable sodium acrylate were prepared by Hirotsu and coworkers (22) and Hirose and coworkers (23). Continuous volume changes in pure water were observed for the gel containing no sodium acrylate as the temperature was varied. Gels containing increasing mole fractions of sodium acrylate underwent a discontinuous volume collapse as the temperature was raised past the transition temperature. The magnitude of the transition and the temperature at which it occurred increased with increasing sodium acrylate content.

Discrete volume phase transitions had thus been demonstrated in gels containing ionized groups as driven by changes in solvent composition and temperature. The corresponding neutral gels underwent volume changes under these same conditions, but they were continuous and of much smaller magnitude. The presence of ionized groups in gels significantly affects the balance of forces and the resulting phase properties.

2.4 Role of Solution Ionic Composition

Because ionic gels come to an osmotic equilibrium with the external solution, any change in the solution ionic composition can significantly alter the balance of forces. Changes in the solution salt concentration, valence of ionic species or in solution pH (for gels that contain weakly acidic or basic groups) can bring about differences in the resulting ion osmotic pressure.

Ohmine and coworkers found that partially hydrolyzed polyacrylamide gels in acetone/water solutions would undergo a volume transition when the solution salt concentration was increased (12). In solutions of low acetone concentrations containing a monovalent salt, the volume change was gradual and continuous, spanning three decades in salt concentration. In solutions of higher acetone concentrations, the volume transition

became discrete and shifted to lower salt concentration. In the presence of a divalent salt, the general trends were qualitatively similar to the monovalent case, but the transitions were shifted to lower salt concentration by several orders of magnitude.

In gels containing weakly acidic or basic groups, changes in the solution pH will influence the ionization state of the gel through proton mass action, as shown in Equations 2.1 and 2.2. The pH and ionic composition of the solution and ionization constants of the

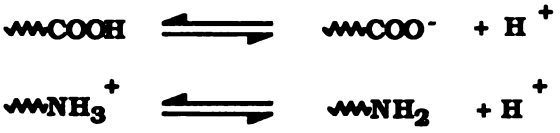

(2.1 and 2.2)

network will determine the charged state of these gels. Polypeptide gels containing ionizable amino acids such as histidine, aspartic acid, glutamic acid, lysine or hydroxylysine or in synthetic gels containing acrylic acid, methacrylic acid or amine containing groups can show pH-sensitive swelling behavior. Decreasing the solution pH decreases the charged state of polyacid gels and increases that of polybase gels, while increasing solution pH has the opposite effect. These types of weakly ionizable gels are distinct from the ion exchange resins that contain groups that are essentially permanently charged. These include resins that contain sulfonic acid ($-SO_3^-$), quaternary ammonium ($-NR_3^+$), quaternary phosphonium ($-PR_3^-$) or tertiary sulfonium ($-SR_2^+$) groups (28).

pH-dependent swelling properties have been reported for synthetic polyacid gels. In pure water, a partially hydrolyzed polyacrylamide gel undergoes a gradual and continuous volume reduction with a decrease in pH, while in acetone/water solution (50/50 v/v) a discrete volume transition is observed (8). Other hydrophilic polyacid

copolymer gels based on acrylic or methacrylic acid have been reported and show the expected behavior of increasing swelling as solution pH is raised (29-31).

Several accounts of pH-dependent swelling of synthetic hydrophilic polyamine gels have been reported (32-34). Ishihara and coworkers measured swelling of 2-hydroxypropyl methacrylate (HPMA)/N,N-dimethylaminoethyl methacrylate (DMA) copolymer gels (32). Swelling increased gradually and reversibly from approximately 30 wt% to 60 wt% when the pH was reduced from 7.4 to 6.5. Ishihara and Matsui prepared terpolymer gels from hydroxyethyl acrylate (HEA)/DMA/4-trimethylsilyl styrene and observed an increase in gel hydration from 30 wt% at pH 6.3 to 53 wt% at pH 6.15 (33). Kost et al. observed very weak pH-dependent swelling changes of about 20% in hydrophilic 2-hydroxyethyl methacrylate (HEMA)/DMA copolymer gels between pH 4 and 10 (34).

In work with inherently hydrophobic polyamine copolymer gels consisting of an n-alkyl ester of methacrylic acid (nAMA) and DMA, Firestone and Siegel found that these gels display aqueous swelling properties that are extremely sensitive to pH (35-36). In contrast to the hydrophilic pH-sensitive acrylamide gels, these gels adopt a collapsed hydrophobic state at, and above, neutral pH, but generally become highly swollen as the pH is lowered. The extent of swelling at lower pH values depends on the nAMA/DMA comonomer ratio as well as the nAMA ester side chain length. One gel, composed of methyl methacrylate/DMA, 70/30 mole%, undergoes a discrete volume transition from about 10 wt% to 70 wt% water at pH 6.6. In the swollen state, these gels respond rapidly and reproducibly to small perturbations in the external pH. In all cased cited above, the pH-dependent swelling behavior was attributed to alteration in the charged state of the gel through dissociation of the ionizable groups.

In addition to the pH-dependent dissociation of ionizable gel groups, variations in the ionic state of the gel can be brought about through proton-cation exchange processes between the gel and the external solution. Ricka and Tanaka found that the volume of a partially hydrolyzed polyacrylamide gel in an initially dilute salt solution first increased to a maximum and then decreased as the salt concentration was increased at constant pH (37). They explained this swelling behavior by noting that the charge density of the gel initially increases with the salt concentration due to the exchange of gel protons with solution cations. This exchange perturbs the proton dissociation equilibrium inside the gel and leads to the ionization of more of the acidic groups, as illustrated in Figure 2.3. The maximum swelling corresponds to the point

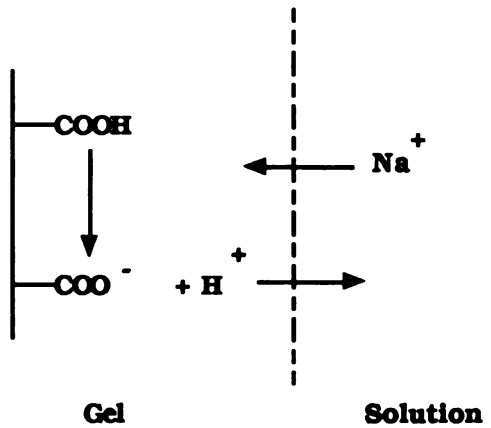

Figure 2.3. The process of proton/cation exchange can lead to an increase in the charge density of the gel through a shift in the proton dissociation equilibrium.

where all acidic groups are ionized giving the maximum gel charge density. A further increase in the salt concentration merely reduces the ion osmotic pressure difference between the gel interior and the solution, thereby reducing swelling. The maximum in the salt dependent swelling disappeared when the experiment was repeated at higher pH, where all the acid groups are dissociated regardless of the salt concentration. This work provided additional evidence in support of the ion exchange mechanism.

Swelling equilibria in ionic gels have been found to be affected by externally applied electric fields (38) and by complex formation with counterions (39).

The increased understanding of the swelling phase behavior of ionic networks has enabled the development of gel systems with very specific properties for use in the drug delivery and separation sciences. However, most of this work has been devoted to hydrophilic ionic gels (e.g. those based on polyacrylamide, pNIPAAm and pHEMA) which generally remain appreciably swollen even when unionized. Very little work has been devoted to ionic gels that can undergo reversible expansion-collapse transitions reminiscent of the helix-coil transition of single polymer chains such as globular proteins. The swelling and transport properties of inherently hydrophobic nAMA/DMA polyelectrolyte gels will be investigated in this work. The understanding of the equilibrium and transport properties of such gels will be the key to developing new polymer-based materials for use in self-regulating drug delivery systems, biosensors and highly efficient separation systems.

References

1. P.J. Flory, "Principles of Polymer Chemistry", Chapter XIII, Cornell University Press, 1953.

2. P.J. Flory and J. Rehner, Statistical Mechanics of Cross-Linked Polymer Networks II. Swelling, J. Chem. Phys., 11, 521 (1943).

3. P.J. Flory, Statistical Mechanics of Swelling of Network Structures, J. Chem. Phys., 18, 108 (1950).

4. A. Katchalsky, Polyelectrolyte Gels, Prog. Biophys., 4, 1 (1954).

5. H.R. Procter and J.A. Wilson, The Acid-Gelatin Equilibrium, J. Chem. Soc., 109, 307 (1916).

6. T. Tanaka, Collapse of Gels and the Critical Endpoint, Phys. Rev. Lett., 40, 12, 820 (1978).

7. K. Dusek and D. Patterson, Transitions in Swollen Polymer Networks Induced by Intramolecular Condensation, J. Polym. Sci., A-2, 6, 1209 (1968).

8. T. Tanaka, D. Fillmore, S.-T. Sun, I. Nishio, G. Swislow and A. Shah, Phase Transitions in Ionic Gels, Phys. Rev. Lett., 45, 1636 (1980).

9. M. Ilavsky, Phase Transition in Swollen Gels. 2. Effect of Charge Interactions on the Collapse and Mechanical Behavior of Polyacrylamide Networks, Macromolecules, 15, 782 (1982).

10. J. Hrouz, M. Ilavsky, K. Ulbrich and J. Kopecek, The Photoelastic Behavior of Dry and Swollen Networks of Poly(N,N-Diethylacrylamide) and of Its Copolymer with N-Tert-Butylacrylamide, Eur. Polym. J., 17, 361 (1981).

11. Y. Hirokawa and T. Tanaka, Volume Phase Transition of a Nonionic Gel, J. Chem. Phys., 81, 6379 (1984).

12. I. Ohmine and T. Tanaka, Salt Effects on the Phase Transition of Ionic Gels, J. Chem. Phys., 77, 5725 (1982).

13. T. Amiya and T. Tanaka, Phase Transitions in Cross-Linked Gels of Natural Polymers, Macromolecules, 20, 1162 (1987).

14. M. Ilavsky, J. Hrouz, J. Stejskal and K. Bouchal, Phase Transition in Swollen Gels. 6. Effect of Aging on the Extent of Hydrolysis of Aqueous Polyacrylamide Solutions and on the Collapse of Gels, Macromolecules, 17, 2868 (1984).

15. T. Tanaka and G. Swislow and I. Ohmine, Phase Separation and Gelation in Gelatin Gels, Phys. Rev. Lett., 42, 23, 1556 (1979).

16. A. Hochberg, T. Tanaka and D. Nicoli, Spinodal Line and Critical Point of an Acrylamide Gel, Phys. Rev. Lett., 43, 3, 217 (1979).

17. S. Hirotsu, Critical Points of the Volume Phase Transition in N-isopropyl acrylamide Gels, J. Chem. Phys., 88, 1, 427 (1988).

18. H.L. Frisch and S. Fesciyan, DNA Phase Transitions: The Ψ Transition of Single Coils, J. Polym. Sci., Polym. Lett., 17, 309 (1979).

19. C.B. Post and B. H. Zimm, Internal Condensation of a Single DNA Molecule, Biopolymers, 18, 1487 (1979).

20. G. Swislow, S.-T. Sun, I. Nishio and T. Tanaka, Coil-Globule Phase Transition in a Single Polystyrene Chain in Cyclohexane, Phys. Rev. Lett., 44, 12, 796 (1980).

21. D. Nicoli, C. Young, T. Tanaka, A. Pollack and G. Whitesides, Chemical Modification of Acrylamide Gels: Verification of the Role of Ionization in Phase Transitions, Macromolecules, 16, 887 (1983).

22. S. Hirotsu, Y. Hirokawa and T. Tanaka, Volume-Phase Transitions of Ionized N-isopropylacrylamide Gels, J. Chem. Phys., 87, 1392 (1987).

23. Y. Hirose, T. Amiya, Y. Hirokawa and T. Tanaka, Phase Transition of Submicron Gel Beads, Macromolecules, 20, 1342 (1987).

24. S. Katayama, Y. Hirokawa and T. Tanaka, Reentrant Phase Transition in Acrylamide-Derivative Copolymer Gels, Macromolecules, 17, 2641 (1984).

25. S. Katayama and A. Ohata, Phase Transition of a Cationic Gel, Macromolecules, 18, 2781 (1985).

26. Y. Hirokawa, T. Tanaka and E. Sato, Phase Transition of Positively Ionized Gels, Macromolecules, 18, 2782 (1985).

27. M. Ilavsky, J. Hrouz and K. Ulbrich, Phase Transition in Swollen Gels 3. The Temperature Collapse and Mechanical Behavior of Poly(N,N-diethylacrylamide) Networks in Water, Polym. Bull., 7, 107 (1982).

28. F. Helfferich, "Ion Exchange", Chapter 5, McGraw-Hill, New York, 1962.

29. H.S. Ch'ng, H. Park, P. Kelly and J.R. Robinson, Bioadhesive Polymers as Platforms for Oral Controlled Release Drug Delivery II. Synthesis and Evaluation of Some Swelling, Water-Insoluble Bioadhesive Polymers, J. Pharm. Sci., 74, 4 (1985).

30. J.H. Kou, G.L. Amidon and P.I. Lee, pH-Dependent Swelling and Solute Diffusion Characteristics of Poly(Hydroxyethyl Methacrylate-co-Methacrylic Acid) Hydrogels, Pharm. Res., 5, 9, 592 (1988).

31. J. Hasa and M. Ilavsky, Deformational, Swelling and Potentiometric Behavior of Ionized Poly(Methacrylic Acid) Gels. II. Experimental Results, J. Polym. Sci., Polym. Phys., 13, 263 (1975).

32. K. Ishihara, M. Kobayashi, N. Ishimaru and I. Shinohara, Glucose Induced Permeation Through a Complex Membrane Consisting of Immobilized Glucose Oxidase and a Poly(Amine), Polym. J., 16, 8, 625 (1984).

33. K. Ishihara and K. Matsui, Glucose-Responsive Insulin Release from Polymer Capsule, J. Polym. Sci., Polym. Lett., 24, 413 (1986).

34. J. Kost, T.A. Horbett, B.D. Ratner and M. Singh, Glucose-Sensitive Membrane Containing Glucose Oxidase: Activity, Swelling and Permeability Studies, J. Biomed. Mat. Res., 19, 1117 (1985).

35. B.A. Firestone and R.A. Siegel, Dynamic pH-Dependent Swelling Properties of a Hydrophobic Polyelectrolyte Gel, Polym. Comm., 29, 204 (1988).

36. R.A. Siegel and B.A. Firestone, pH-Dependent Equilibrium Swelling Properties of Hydrophobic Polyelectrolyte Copolymer Gels, Macromolecules, 21, 3254 (1988).

37. J. Ricka and T. Tanaka, Swelling of Ionic Gels: Quantitative Performance of the Donnan Theory, Macromolecules, 17, 2916 (1984).

38. T. Tanaka, I. Nishio, S.-T. Sun and S. Ueno-Nishio, Collapse of Gels in an Electric Field, Science, 218, 467 (1982).

39. J. Ricka and T. Tanaka, Phase Transition in Ionic Gels Induced by Copper Complexation, Macromolecules, 18, 83 (1985).

Chapter 3.

Gel Preparation and Characterization

3.1 Introduction

The purpose of this chapter is to describe the methods and apparatus used to prepare, purify and characterize n-alkyl methacrylate/N,N-dimethylaminoethyl methacrylate copolymer gels. Methods are described for monomer storage and purification, initiator recrystallization and gel preparation and characterization by elemental analysis and differential scanning calorimetry.

3.2 Materials

All chemicals and reagents have been used 'as received' unless otherwise indicated. The vinyl monomers methyl methacrylate (MMA), ethyl methacrylate (EMA), n-propyl methacrylate (PMA), n-butyl methacrylate (BMA), n-hexyl methacrylate (HMA), N,N-dimethylaminoethyl methacrylate (DMA) and the free radical initiator 2,2' azobisisobutyronitrile (AIBN) were obtained from Polysciences, Inc. The crosslinking reagent divinyl benzene (DVB) was purchased from Pfaltz and Bauer, Inc. Water was double distilled and deionized using the Barnstead Nanopure System. Methanol (Fisher Scientific, A.C.S. grade), absolute ethanol (Gold Shield Chemical Company), toluene (Eastman, scintillation grade), dichlorodimethylsilane (Aldrich, 99%) and the antioxidant Ethanox 330 (1,3,5-trimethyl-2,4,6-tris[3,5-di-tertbutyl-4-hydroxybenzyl] benzene) (Ethyl Corporation) were all used as received.

3.3 Monomer Storage

Commercially supplied vinyl monomers contain polymerization inhibitors or stabilizers which prevent polymerization during shipment and storage (1). Methacrylate monomers usually contain the inhibitor hydroquinone (1,4-dihydroxybenzene, HQ) or hydroquinone methyl ether (MEHQ) at levels of 10-2000 ppm (2). HQ or MEHQ is removed prior to the use of each monomer in gel preparation to ensure complete and

HQ

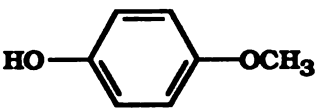

MEHQ

reproducible polymerization. After the inhibitor has been removed, the monomer is used immediately or stored under an inert atmosphere (nitrogen or argon) in a tightly sealed container at -20 °C. Otherwise, the monomers are kept stabilized with HQ or MEHQ and are stored at 4 °C.

3.4 Monomer Purification

All n-alkyl methacrylates, N,N-dimethylaminoethyl methacrylate and divinyl benzene are liquids at room temperature and are purified (separated from hydroquinone and/or polymer) by vacuum distillation. The apparatus used in this procedure is shown in Figure 3.1. The antioxidant Ethanox 330 is added to the crude monomer to retard heat-induced polymerization during the distillation. The boiling points of the monomers are listed in Table 3.1. All distilled monomers are colorless, transparent liquids. As a qualitative check for the presence of polymer, a few drops of distilled monomer can be added to methanol. Turbidity indicates the presence of polymer.

Table 3.1. Boiling Points of Monomers.

Monomer	Formula Weight	Boiling Point (°C)	Reference
methyl methacrylate	100.1	99-100 (760 mm Hg)	(2)
ethyl methacrylate	114.2	118-119 (760 mm Hg)	(2)
n-propyl methacrylate	128.2	140-141 (760 mm Hg)	(2)
n-butyl methacrylate	142.2	163-164 (760 mm Hg)	(2)
n-hexyl methacrylate	170.3	88-89 (14 mm Hg)	(2)
N,N-dimethylaminoethyl methacrylate	157.2	75-77 (13 mm Hg)	(2)
divinyl benzene	130.2	195 (760 mm Hg)	(3)

Procedure:

1) Monomers are brought to room temperature prior to distillation. Monomer is poured into the distillation flask via a glass funnel. The distillation flask is filled to not more than 50-60% of capacity.

2) Ethanox 330 is added (approximately 100 mg/100 ml monomer) along with a magnetic stir bar. The distillation head is connected. The solution is vigorously stirred.

3) A vacuum pump equipped with a cold trap (dry ice/ethanol) is attached to the system.

4) The temperature is gradually raised. This is done slowly and only after the vacuum has been applied. Monomers begin to reflux and then distill.

5) The first distillate fraction (5-10 ml) is discarded. Collection of the major fraction is done after the temperature has stabilized.

6) Distillation is stopped by removing the heating mantle from the distillation flask. This is done before the distillation flask has gone to dryness. The system is purged with argon. The collection flask is removed and monomer is poured into a clean bottle (preferably amber) under argon. The bottle is tightly capped and Parafilm is wrapped around the cap to ensure the exclusion of moisture. The bottle is stored in the freezer at -20 °C.

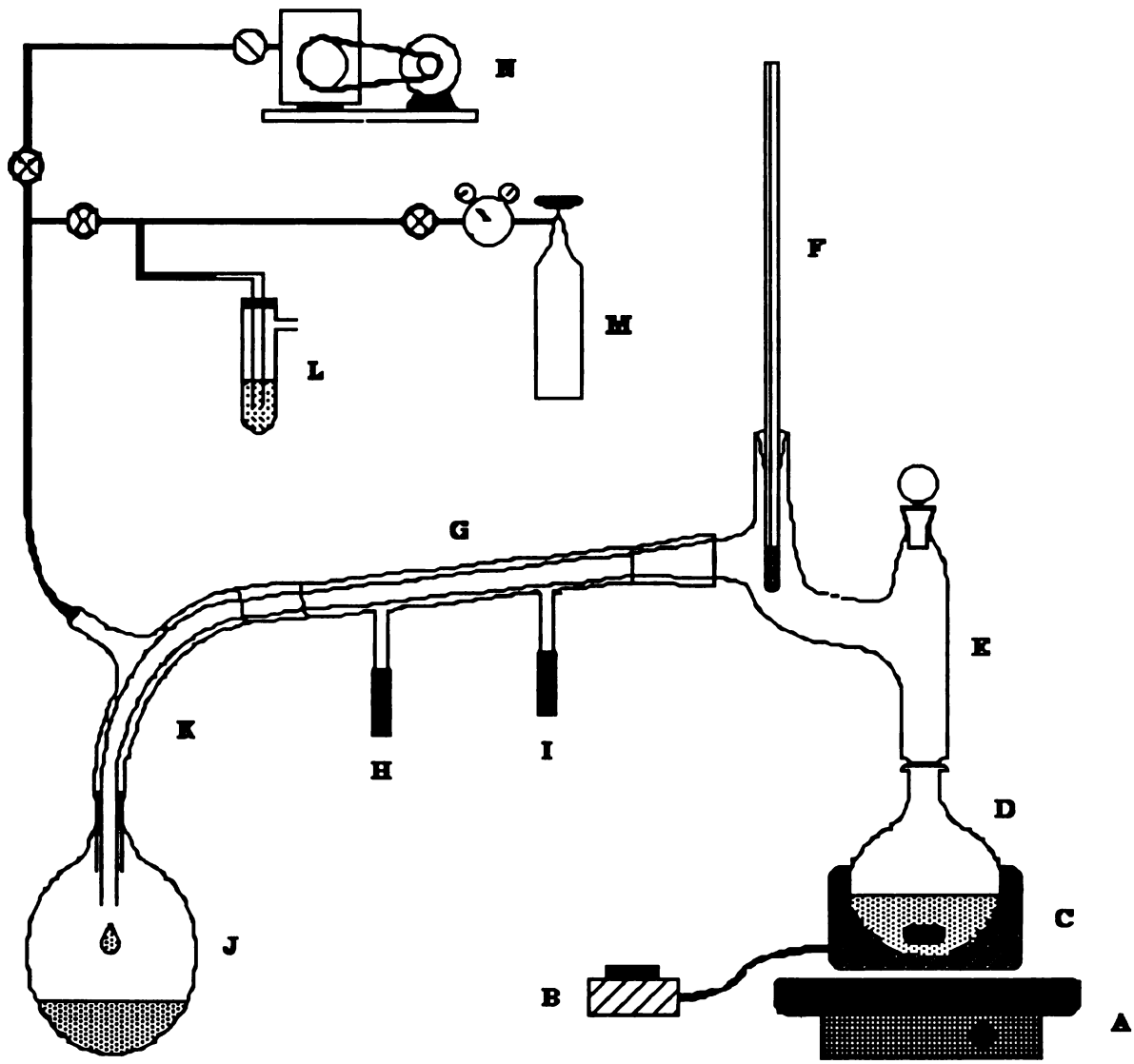

Figure 3.1. Apparatus for the vacuum distillation of monomers. A, magnetic stirrer; B, Variac voltage regulator; C, heating mantle; D, distillation flask; E, Claisen head; F, thermometer; G, condenser; H, water inlet; I, water outlet; J, receiving flask; K, vacuum adapter; L, bubbler; M, argon tank; N, vacuum pump.

3.5 Recrystallization of AIBN

Commercial grade AIBN from Polysciences is a granular slightly off white solid. Purification of AIBN by recrystallization from absolute ethanol/water is done before use in gel preparation.

Procedure:

1) A solution of crude AIBN in absolute ethanol (approximately 25 mg/ml) is prepared. Sonication is usually necessary to get complete dissolution (solution should not be heated due to the tendancy of AIBN to decompose at elevated temperatures).

2) Solution is gravity filtered through a Whatman 'Qualitative' filter. Filtrate is collected.

3) Water is added to the filtrate with stirring until the solution first becomes turbid (solution composition at this point is approximately 7/10 water/ethanol (v/v)).

4) Solution is stirred in an ice bath at 0 °C for 2-3 hours. Crystallization of AIBN occurs.

5) Solution is gravity filtered as in step 2 to isolate crystals. Filtrate can be collected and steps 4 and 5 repeated.

6) Crystals are air dried at 25 °C for 4 hours and then dried under vacuum at 25 °C for 24 hours. Drying is never done at elevated temperatures. Recrystallized AIBN is stored at 4 °C in a tightly sealed bottle wrapped with Parafilm to ensure exclusion of moisture.

Recrystallized AIBN consists of shiny fine white needles. Typical mass recovery of AIBN after recrystallization is 70-80%.

3.6 Gel Preparation

Each nAMA/DMA copolymer gel was prepared as a thin sheet by a free radical bulk polymerization carried out between two silanized glass plates (13 cm x 13 cm). A Teflon gasket (between 0.10 and 0.835 mm thick) was inserted between the plates near the edges to provide a uniform internal cavity for the monomer solution as shown in Figure 3.2. The glass plate assembly was held together from the outside by metal clamps. Silanization was

accomplished by immersing the plates in a 2% (v/v) solution of dichlorodimethyl silane in toluene for two minutes. The plates are then removed from the solution, rinsed with toluene and air dried. Silanization derivatizes the residual silanol groups of the glass plates rendering the surface hydrophobic, as diagrammed below (4). This procedure facilitates subsequent separation of the plates and gel removal.

Procedure:

1) The purified monomers are removed from the freezer and allowed to come to room temperature. A solution containing an nAMA monomer, DMA, DVB (0.1% w/w) and AIBN (0.5% w/w) at the desired composition is prepared in a round bottom flask.

2) The flask is fitted with a manifold and degassed for 5 minutes by applying light vacuum while stirring as illustrated in Figure 3.3.

3) The monomer solution is drawn into a glass syringe fitted with a 24 gauge needle and then injected into the vertically oriented glass plate assembly (Figure 3.4).

4) The assembly is incubated at 60 °C for 18 hours in the vertical position in an oven filled with argon.

5) After incubation, the assembly is removed from the oven and allowed to cool to room temperature. The glass plates are separated by prying the corners apart with a razor blade. The gel sheet will adhere to one of the plates and is removed by peeling it off with the razor blade.

6) Circular disks are cut out of the sheet using a 7.0 or 9.5 mm diameter punch.

7) The disks are swollen in stirred methanol for two days. The methanol is changed several times during this period. Small molecules (residual monomer, crosslinker or initiator) that are present in the gel after polymerization are extracted during this washing process. The disks are then transferred to a stirred methanol/water solution (50/50 v/v) and left overnight. Partial collapse of the disks occurs which enables them to be handled with forceps without damage.

8) The washed, partially collapsed disks are dried at room temperature for 24 hours and then at 50 °C *in vacuo* for an additional 24 hours.

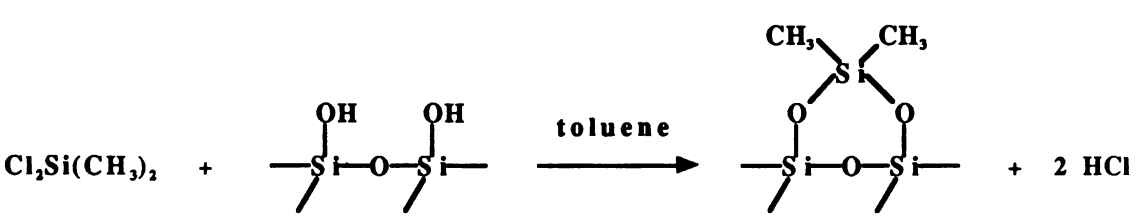

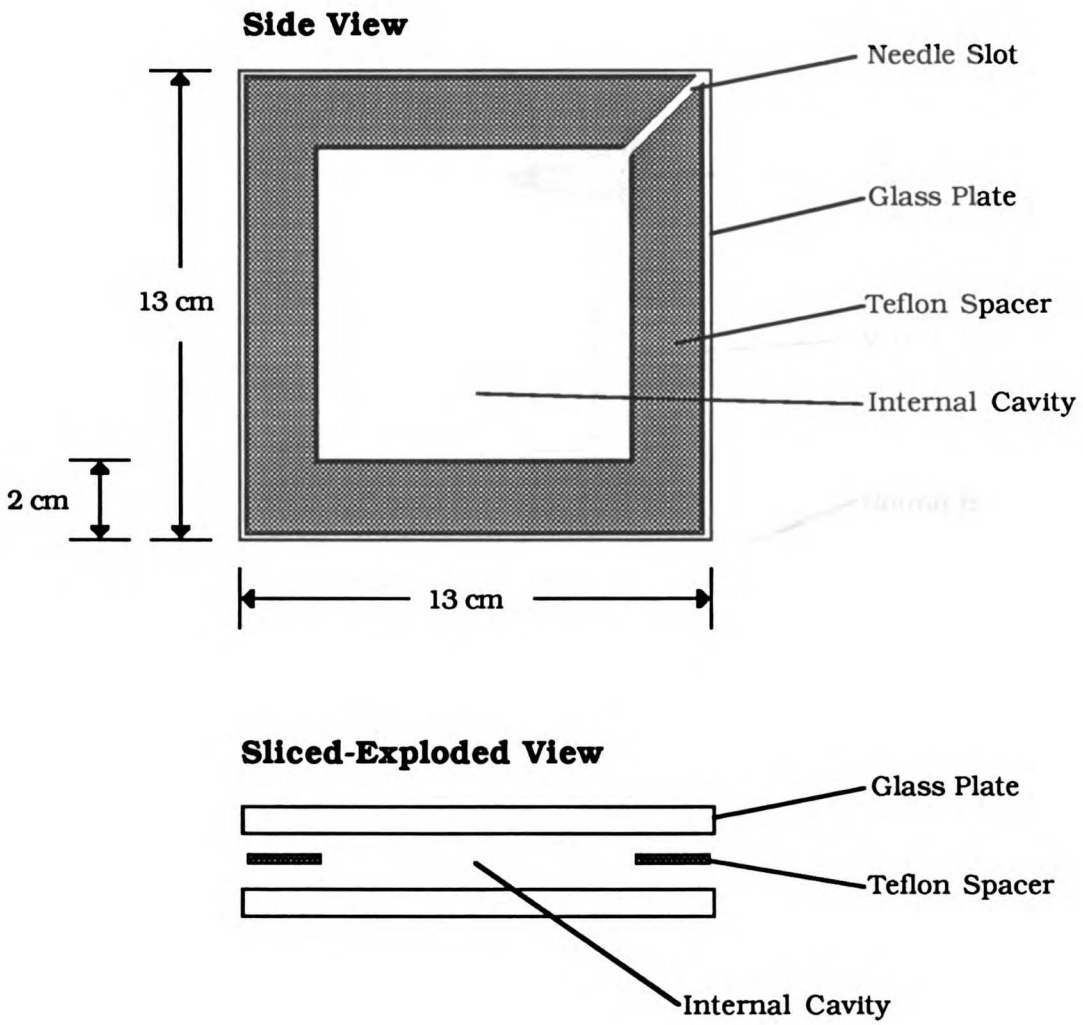

Figure 3.2. Diagram of the glass plate assembly used to make copolymer gels.

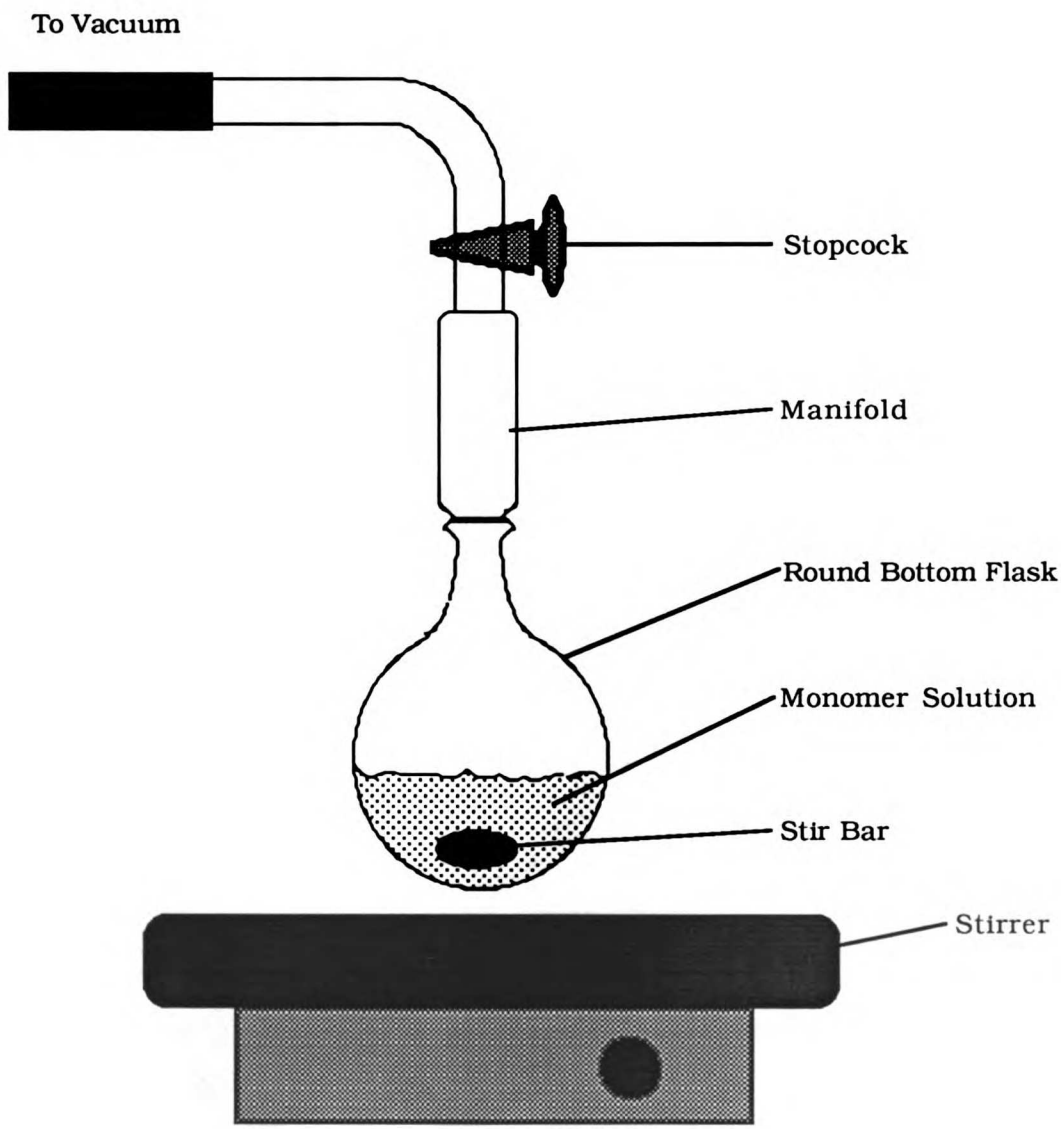

Figure 3.3. Setup for degassing monomer solution.

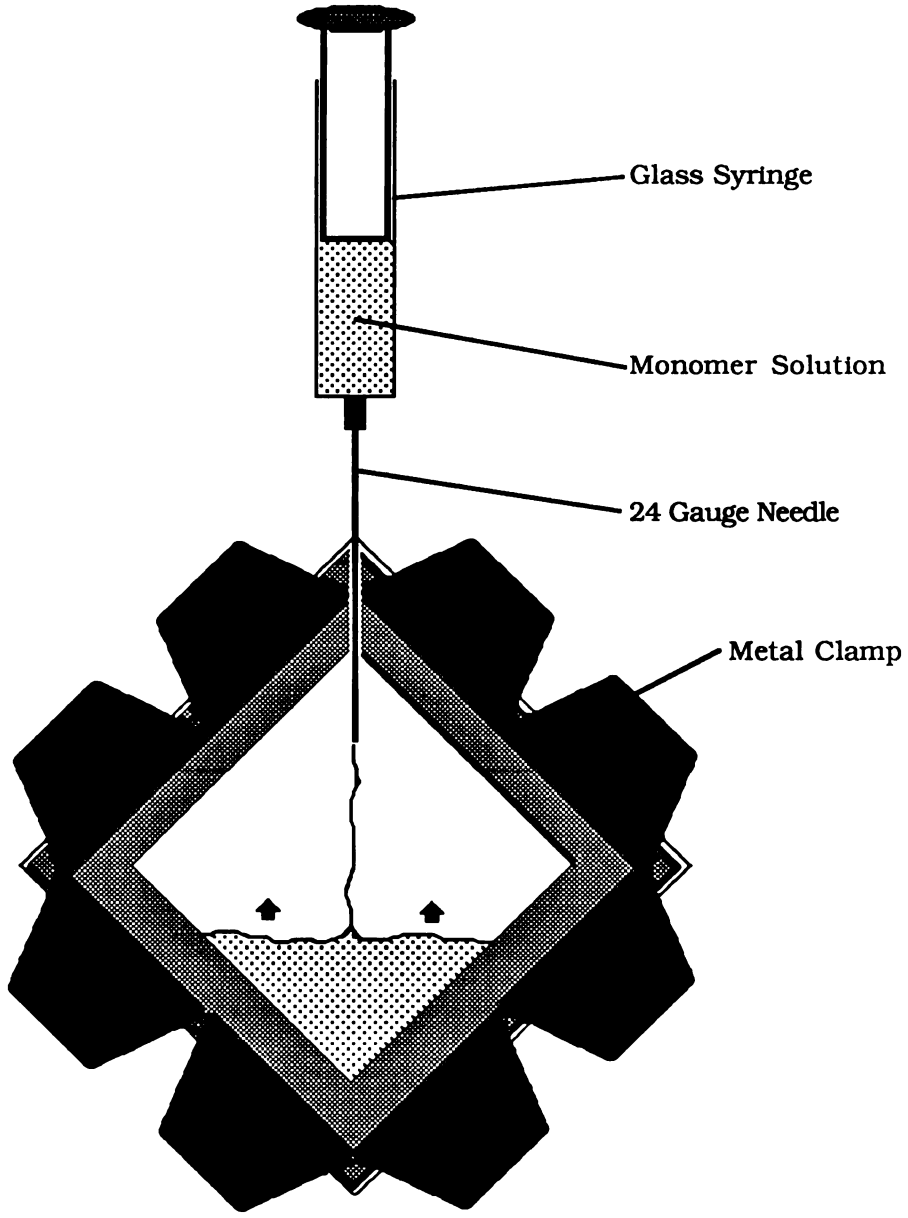

Figure 3.4. Technique for filling the glass plate assembly with monomer solution.

The resulting gel disks were hard, transparent and colorless. Disk thicknesses were generally the same or slightly smaller (approximately 5-10%) than the thickness of the Teflon gasket.

3.7 Gel Characterization

3.7.1 Elemental Analysis

Washed copolymer gel samples were sent to the Microanalytical Laboratory in the Department of Chemistry, University of California, Berkeley for carbon, hydrogen and nitrogen (CHN) elemental analysis.

The theoretical weight percents of CHN for a copolymer gel can be computed from the known composition of the original monomer solution (assuming complete monomer incorporation). The CHN weight percents are computed as follows:

$$\text{wt\% element i} = (W_{i,a})\,(X_a) + (W_{i,b})\,(X_b)$$

where $W_{i,a}$ and $W_{i,b}$ are the weight percents of element i in monomers a and b, respectively, and X_a and X_b are the mole fractions of monomers a and b, respectively, in the monomer feed solution. The contributions from the other components (AIBN and DVB) are ignored in the above calculations since they are present in very small quantities (0.5 and 0.1% w/w, respectively). The computed and actual CHN contents were

Table 3.2. Results of CHN Analysis for a MMA/DMA 70/30 mole% Gel.

Element	Wt% Computed	Wt% Found
C	60.2	60.0
H	8.3	8.7
N	1.9	2.5

compared for gels representing each composition prepared in this work. Typical results of a CHN analysis are shown in Table 3.2 for the case of the MMA/DMA 70/30 mole% gel indicate that the polymerization procedure of Section 3.6 results in the complete incorporation of the monomer feed solutions into the gel. Gel content thus reflected the monomer feed solution in each case.

3.7.2 Glass Transition Temperature

It is a general property of all amorphous polymeric materials that at sufficiently low temperature, the polymer takes on the properties of a glass. This is characterized by hardness, brittleness and rigidity (5,6). The glass transition temperature (T_g) is commonly defined as the temperature below which the polymer is glassy and above which it is rubbery (1).

On a molecular basis, T_g marks the onset of large scale motion of the polymer chain segments. At low temperature ($T<<T_g$), the motion of atoms in amorphous materials is confined to low amplitude vibrations about fixed positions, similar to that in the crystalline state (but with no long range structural order). As the temperature of the sample is increased, vibratory motions of the polymer segments increase. At T_g, rotational and translational motions become significant and the polymer takes on the properties of a rubbery material.

T_g is affected by structural features such as molecular weight, extent of crosslinking, bulkiness and rigidity of the chains and pendant groups, and the extent of interactions between the chains (6). Material properties including heat capacity and thermal expansion coefficient change abruptly in the vicinity of T_g, which provides a basis by which the glass transition can be detected experimentally. Many techniques are available for determining the glass transition temperature including differential scanning calorimetry (DSC), dilatometry, stress relaxation measurements and refractometry (1). DSC was used

in this work. The instrument was a Dupont 910 Differential Scanning Calorimeter equipped with a Model 1090 Programmer located in the Polymer Sciences Department at SRI International in Menlo Park, California.

Typically, 5-10 mg of dry gel is sealed into an aluminum pan and placed on the heating block. An identical empty pan is placed on an adjacent heating block. The system is cooled to approximately -60 °C, and then heated at a programmed rate (15 °C /minute in this work). During the run, the calorimeter supplies heat to one pan or the other via a feedback circuit such that the rate of temperature increase in each pan is kept constant. The differential power required to accomplish this heating reflects the heat capacity of the polymer and is recorded as a function of temperature during the run. At the glass transition, the change in sample heat capacity is indicated by a sigmoidal shift in the DSC tracing, as exemplified by the heating curve of the MMA/DMA 70/30 mole% copolymer gel shown in Figure 3.5. The glass transition typically occurs over a finite temperature interval (approximately 85-95 °C in Figure 3.5). It is customary to report T_g as the inflection temperature of the transition, as shown in Figure 3.6. The computation of inflection temperature was performed directly after the acquisition of the DSC scan by the Model 1090 Programmer.

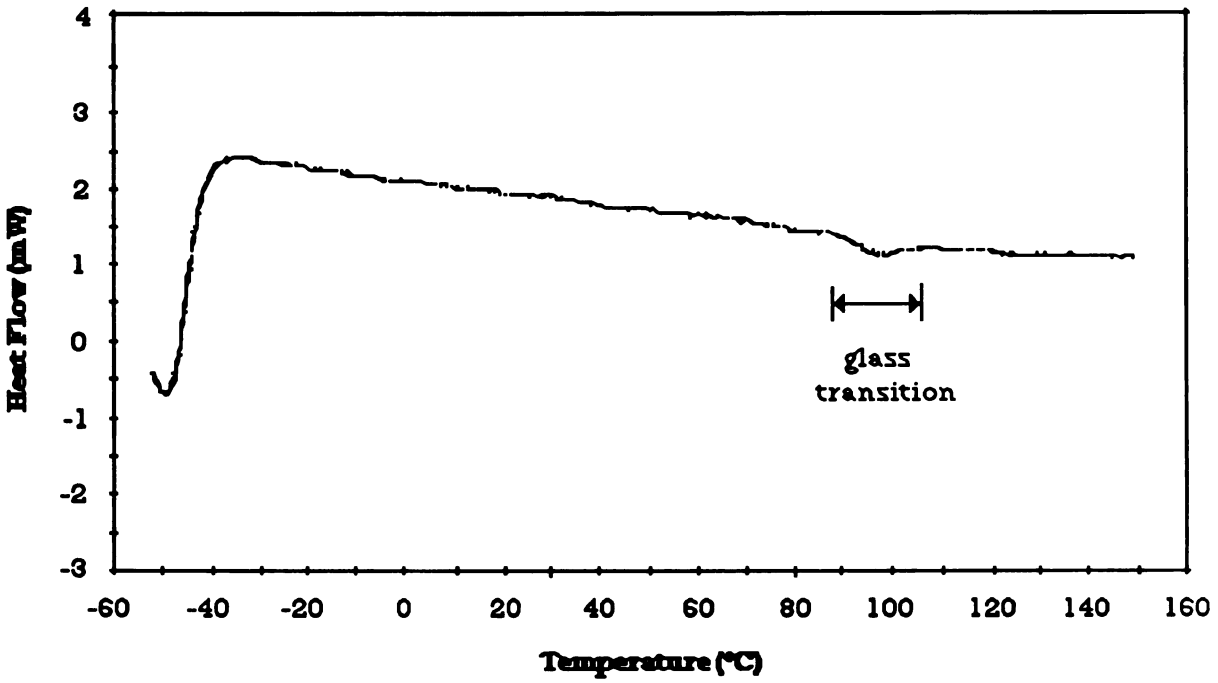

Figure 3.5. DSC scan of the MMA/DMA 70/30 mole% gel in the dry state from -50 to 150 °C. The heating rate was 15 °C per minute.

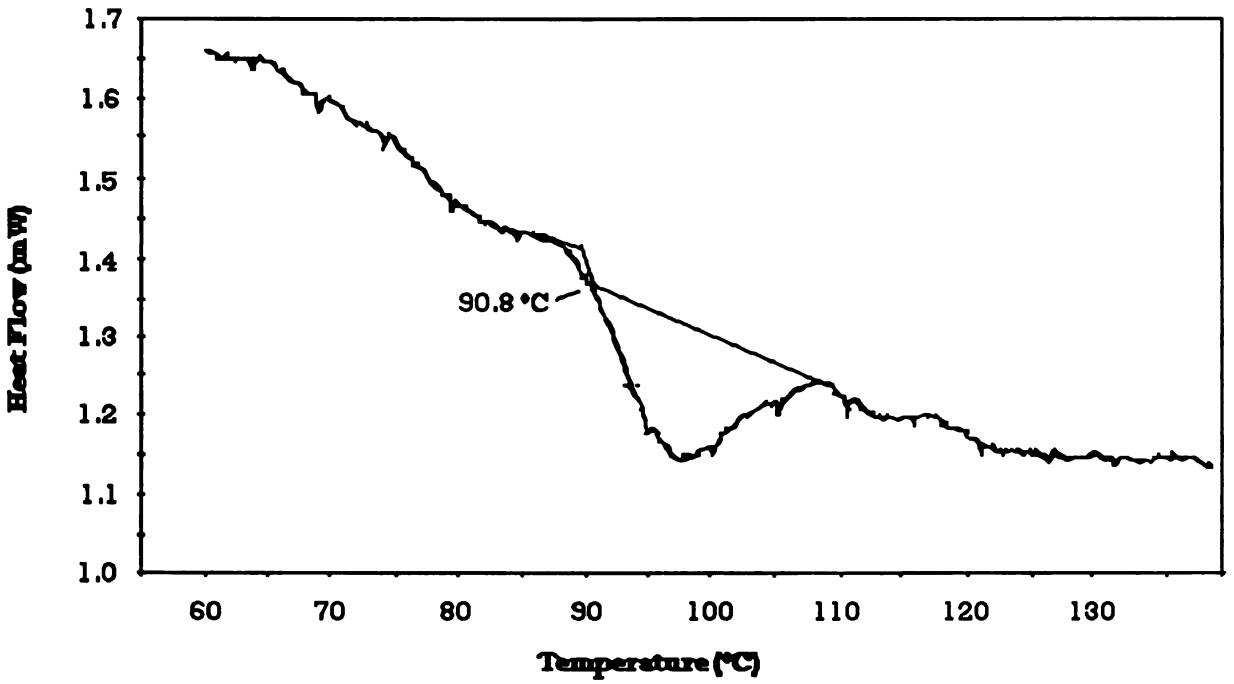

Figure 3.6. Expanded DSC scan of the MMA/DMA 70/30 mole% gel in the vicinity of the glass transition. Lines indicate the computed T_g as computed by the Model 1090 Programmer.

References

1. E.A. Collins, J. Bares and F.W. Billmeyer, Jr., "Experiments in Polymer Science", Chapter 3, J. Wiley & Sons, 1973.

2. Chemical and Supply Catalog, Polysciences, Inc., 1988-89.

3. Catalog Handbook of Fine Chemicals, Aldrich Chemical Company, 1988-89.

4. B. Arkles, Tailoring Surfaces with Silanes, CHEMTECH, 766, December, 1977.

5. F.W. Billmeyer, Jr., "Textbook of Polymer Science", Third Ed., Chapter 11, J. Wiley & Sons, 1984.

6. P.J. Flory, "Principles of Polymer Chemistry", Chapter II, Cornell University Press, 1953.

Chapter 4.

pH - Dependent Swelling Equilibria in nAMA/DMA Gels

4.1 Introduction

It has long been known that a crosslinked polymer gel containing weakly acidic and/or basic pendant groups will imbibe solvent to an extent that depends on the pH and ionic composition of the bathing solution. When the gel is relatively solvophilic and contains acidic pendant groups, gel swelling increases as solution pH increases (1,2). Similarly, a weakly basic solvophilic gel undergoes a volume expansion as the solution pH is decreased (3,4).

In recent years, considerable attention has been drawn to systems in which the polyelectrolyte gel and the solvent do not interact favorably. In such cases, the polyelectrolyte gel remains in a collapsed state until the external solution reaches a critical pH, at which point the gel abruptly increases its equilibrium swelling (5). These transitions in gel volume can also be induced by changes in the solution ionic composition (6), temperature (7,9,10), or solvent composition (5,10,11). This has stimulated research on the feasibility of such gels for use as artificial muscles and/or switches (5), as components in chemical separation systems (1,8), and as physiologically sensitive drug delivery devices (3,4,9).

In the present chapter, the equilibrium swelling properties of a class of lightly crosslinked, hydrophobic, tertiary amine-containing copolymer gels in aqueous solution of various pHs is presented. These gels consist of an n-alkyl ester of methacrylic acid (nAMA) copolymerized with N,N-dimethylaminoethyl methacrylate (DMA). Gel

characteristics were varied by altering the nAMA/DMA comonomer ratio as well as the length of the n-alkyl ester sidechain.

4.2 Experimental

4.2.1 Materials, Gel Preparation and Characterization

The methods for the purification of the monomers methyl methacrylate (MMA), ethyl methacrylate (EMA), n-propyl methacrylate (PMA), n-butyl methacrylate (BMA), n-hexyl methacrylate (HMA), N,N-dimethylaminoethyl methacrylate (DMA) and divinyl benzene (DVB), and the radical initiator 2,2'-azobisisobutyronitrile (AIBN) and the method for nAMA/DMA copolymer gel preparation are described in detail in Chapter 3. Water used in the swelling studies was double distilled and deionized. Sodium dihydrogen phosphate, NaCl (Mallinckrodt, Inc.) and citric acid (Fisher Scientific) were analytical reagent grade and were used as received. nAMA/DMA gel characterization by elemental analysis and the determination of gel glass temperatures in the dry state by differential scanning calorimetry are described in Chapter 3.

4.2.2 Equilibrium Swelling Studies

Dry copolymer disks in triplicate were immersed in either 0.01 M citric acid buffer (pH 2.0-7.0) or 0.01 M phosphate buffer (pH>7.0) at 25 °C. The total ionic strength (I') of each buffer was adjusted to 0.1 M by the addition of a calculated amount of NaCl. Periodically, the disks were withdrawn from the buffer solution, the surface water removed by lightly blotting with a laboratory tissue, and weighed. The disk weights were individually monitored in this way until they reached a constant value. This typically required from several hours to three weeks depending on the copolymer composition and pH. The extent of swelling for each copolymer sample at equilibrium is expressed as the hydration (H), where H = (g water)/(g swollen disk) and is calculated as:

$$H = (W_S - W_d)/W_S$$

where W_S and W_d are the fully swollen (equilibrium) and dry disk weights, respectively. H simply indicates the weight fraction of water in the gel sample at equilibrium. Excellent reproducibility in the hydration values was obtained for each set of triplicate samples with a relative standard error of 1% or less.

4.3 Results

4.3.1 Gel Glass Temperatures

The comonomer composition and the glass temperatures (T_g) of the various nAMA/DMA copolymer gels prepared are listed in Table 4.1. For the purpose of comparison, the literature glass temperatures of the corresponding homopolymers are given. In general, glass temperatures for a given polymer can vary widely depending on the polymerization conditions and the method of determination. It is usually difficult to compare results across both polymers and methods. The data are presented for the purpose of identifying qualitative trends. It is apparent from Table 4.1 that the MMA/DMA, EMA/DMA and PMA/DMA gels all have T_gs well above ambient temperature and thus exist in the glassy state when dry. T_gs for the BMA/DMA gels are quite close to ambient temperature. The glass temperature of nAMA/DMA gels is a strong function of both the comonomer ratio and the nAMA sidechain length. In general, increasing the ratio of the monomer with the higher homopolymer T_g (Table 4.2) serves to increase the T_g of the copolymer. For example, in MMA/DMA gels, the T_g increases as the gel MMA content increases as shown in Table 4.1. The homopolymers poly(BMA) and poly(DMA) have similar T_g values and the corresponding BMA/DMA T_gs are virtually insensitive to the comonomer composition. The effect of the nAMA sidechain length can be seen by comparing T_gs of the the homologous 70/30 mole% nAMA/DMA gels (Table 4.1) and the nAMA homopolymers (Table 4.2). Increasing the number of carbons in the nAMA

Table 4.1. Compositions and Glass Temperatures of the Various nAMA/DMA Copolymer Gels Prepared.

Gel	Comonomer Ratio (mole%)	Glass Temperature (°C)
MMA/DMA	70/30	90.8
MMA/DMA	78/22	108.5
MMA/DMA	86/14	114.4
MMA/DMA	93/7	not determined
EMA/DMA	70/30	67.9
PMA/DMA	70/30	51.6
BMA/DMA	70/30	31.1
BMA/DMA	77/23	31.7
BMA/DMA	86/14	34.7
HMA/DMA	70/30	not determined

Table 4.2. Glass Temperatures of Some Relevant Homopolymers.

Homopolymer	Method	Reference	Glass Temperature (°C)
poly(MMA)	dilatometry	13	104
	"	14	105
poly(EMA)	dilatometry	13	66
	"	14	65
poly(PMA)	dilatometry	14	35
poly(BMA)	dilatometry	13	19
	"	14	20
	"	8	15
poly(DMA)	dilatometry	12	19

sidechain decreases T_g. In the case of the nAMA/DMA 70/30 gels, T_g is reduced by about about 20° for each additional sidechain methylene group.

4.3.2 pH-Dependent Swelling Equilibria

Figures 4.1 and 4.2 show the equilibrium swelling behavior for four MMA/DMA and the three BMA/DMA gels measured as a function of pH at 25 °C and a total ionic strength of 0.1 M. Citrate buffer was used between pH 2 and 7 because a triprotic acid (pK_1=3.15, pK_2= 4.78 and pK_3=6.40) has a large buffer capacity over this pH range, while phosphate buffer was used above pH 7. Each symbol in these figures represents the mean of three samples and the corresponding standard deviations are, in general, smaller than the symbols shown.

It is apparent that the gels are all compact and hydrophobic at pH values greater than 6.6 regardless of monomer composition, containing 10% (w/w) water or less at equilibrium. At lower pH values, a point is reached where the hydration abruptly increases, sometimes discontinuously, giving rise to highly swollen hydrophilic gels. At still lower pHs, gel hydration continues to gradually increase. For example, the 70/30 mole% MMA/DMA gel has an equilibrium hydration of about 0.10 (10% water by weight) in the pH range 6.6-7.2. For a small decrease in pH at 6.6, a discontinuous jump to 70% water is observed. Gel hydration further increases to values in excess of 90% as the pH is reduced to 2.0. Swelling transitions are also observed for the 78/22 and 86/14 MMA/DMA gels and the 70/30, 77/23 and 86/14 BMA/DMA gels, but is absent for the 93/7 MMA/DMA gel, which remained collapsed and hydrophobic at all pH values tested.

The gel comonomer composition impacts significantly on the equilibrium swelling behavior of the MMA/DMA and BMA/DMA gels as is evident in Figures 4.1 and 4.2, respectively. As the proportion of nAMA to DMA increases, gel hydrophobicity increases and amine group density decreases, and two effects are observed: 1) the pH of the

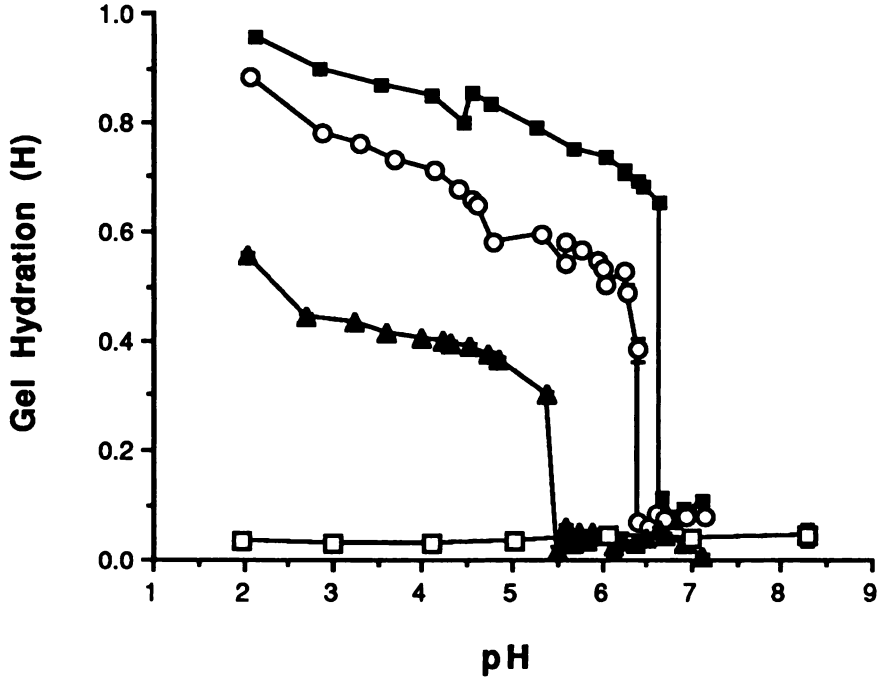

Figure 4.1. Swelling isotherms for a series of MMA/DMA copolymer gels of different comonomer ratios as a function of pH in 0.01 M citrate buffer (pH<7) or 0.01 M phosphate buffer (pH>7). Measurements were made at 25 °C and a total ionic strength of 0.1 M. 70/30 mole% (■), 78/22 mole% (○), 86/14 mole% (▲) and 93/7 mole% (□).

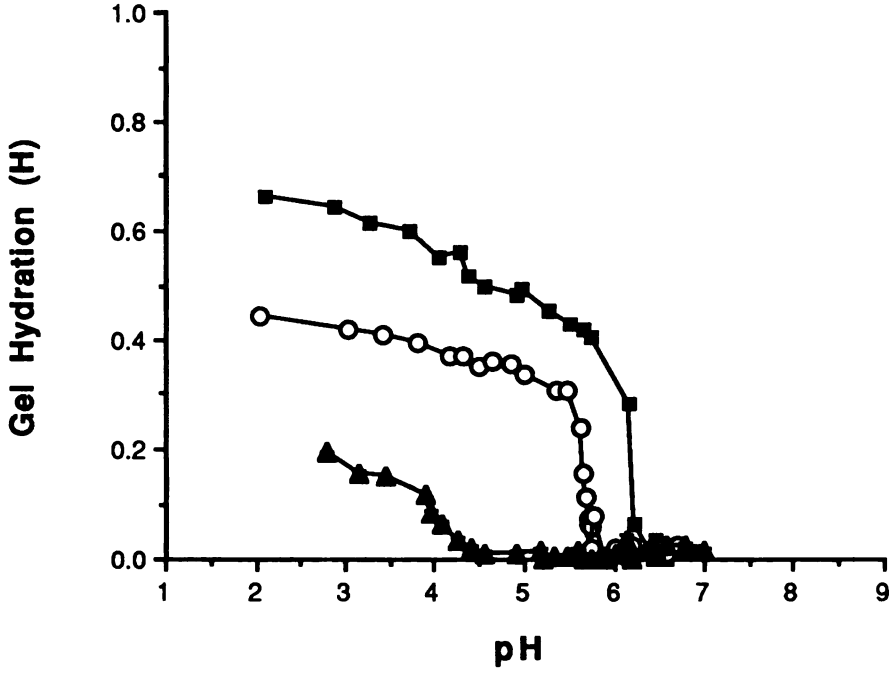

Figure 4.2. Swelling isotherms for a series of BMA/DMA copolymer gels of different comonomer ratios as a function of pH in 0.01 M citrate buffer. Measurements were made at 25 °C and a total ionic strength of 0.1 M. 70/30 mole% (■), 78/22 mole% (○) and 86/14 mole% (▲).

swelling transition shifts to lower pH, and 2) the extent of the swelling transition is decreased. For example, changing the MMA/DMA proportion from 70/30 to 86/14 mole% shifts the transition pH from 6.5 to 4.8, and gel hydration in the low pH range decreases from 90% to 40%. Also, the transition for the 70/30 gel appears to be discrete, occurring over a very small interval in pH.

The influence of the n-alkyl ester sidechain length on the pH-dependent equilibrium swelling properties at 25 °C and ionic strength 0.1 M is shown in Figure 4.3 for a homologous series of nAMA/DMA gels each containing 30 mole% DMA. The nAMA monomers include the methyl, ethyl, propyl, butyl and hexyl esters of methacrylic acid. Here again, each point represents the mean of three samples. All gels in this series display a swelling transition. The extent of the transition and the pH at which it occurs are affected by the pendant chain length. As the pendant chain length increases from C_1 to C_6, the water content at pH 2-3 decreases from 90% for the methyl to about 50% for the hexyl gel. The width of the pH interval of the swelling transition broadens with increasing side chain length and shifts progressively to lower pH for the methyl, ethyl and propyl esters. The latter trend does not, however, continue for the butyl and hexyl gels.

The question of whether the low hydrations observed at pH values above the swelling transition reflect true equilibria or are determined by slow sorption kinetics is considered. Figure 4.4 shows representative swelling kinetics for MMA/DMA 70/30 and EMA/DMA 70/30 gels from the initially dry state in 0.01 M citrate buffer at pH 7 and ionic strength 0.1 M. Water sorption appears to be complete after one day with hydration remaining constant out to 13 days. There is no evidence for a slow secondary phase of sorption, at least over this time-scale.

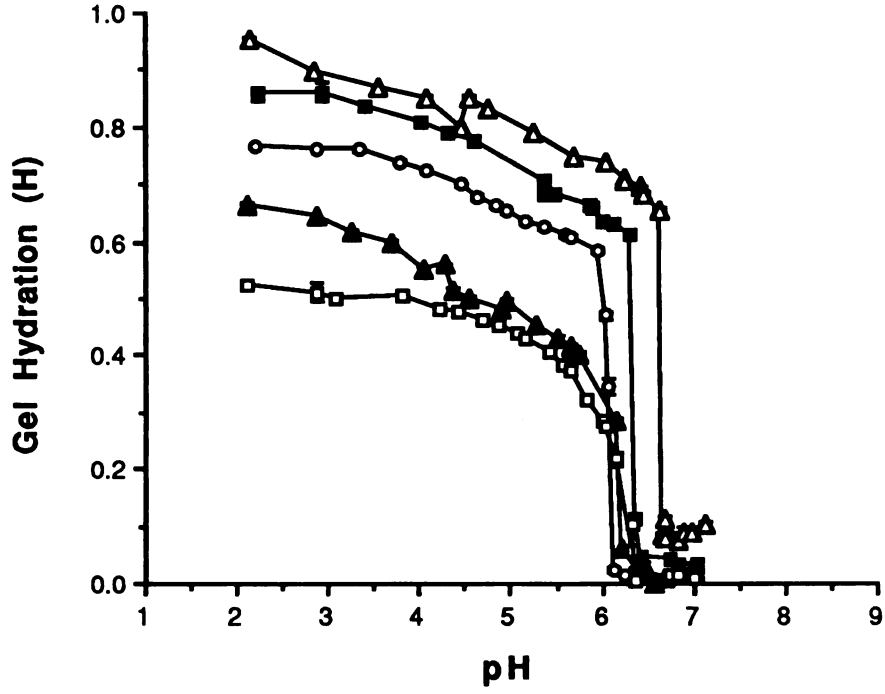

Figure 4.3. Swelling isotherms for a series of 70/30 mole% nAMA/DMA copolymer gels of various nAMA sidechain lengths as a function of pH in 0.01 M citrate buffer. Measurements were made at 25 °C and a total ionic strength of 0.1 M. MMA/DMA (Δ), EMA/DMA (■), PMA/DMA (○), BMA/DMA (▲) and HMA/DMA (□).

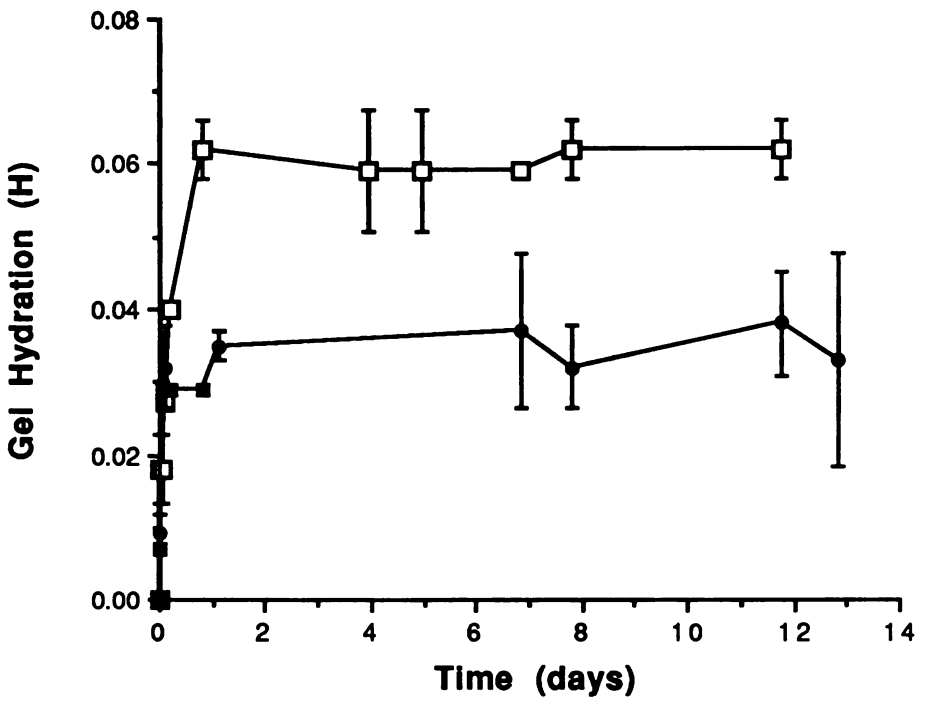

Figure 4.4. Sorption kinetics of the MMA/DMA 70/30 mole% (❑) and the EMA/DMA 70/30 mole% (●) gels at pH 7.0. Measurements were made at 25 °C and a total ionic strength of 0.1 M.

The influence of buffer type on the equilibrium swelling of the 70/30 MMA/DMA gel is shown in Table 4.3 for the pH interval of 5.8 to 6.6. Swelling in both 0.01 M phosphate and 0.01 M citrate buffers at several pH values was determined at 25 °C. The

Table 4.3. Effect of Buffer Type on the Equilibrium Hydration of the MMA/DMA 70/30 mole% Gel at 25 °C and 0.1 M Ionic Strength.

pH	Equilibrium Hydration (H) [a]	
	0.01 M Citrate	0.01 M Phosphate
5.84	0.749 (0.0012)	0.866 (0.0007)
6.02	0.736 (<0.0001))	0.859 (<0.0001)
6.42	0.694 (0.0040)	0.826 (0.0007)
6.64	0.656 (0.0046)	0.771 (0.0014)

[a] Values in parentheses represent the standard deviation of the mean.

total ionic strength for each buffer was adjusted to 0.1 M with NaCl. These results show that the equilibrium swelling for the MMA/DMA copolymer is higher for the phosphate buffer at any pH. Thus, pH and ionic strength are not sufficient to determine the equilibrium hydration in these gels. The identity of buffer ions plays a significant role.

4.4 Discussion

Swelling equilibria of polyelectrolyte networks are determined by a balance of three primary forces: 1) the free energy of mixing of the network chains with solvent, 2) the net osmotic pressure within the network resulting from the mobile counterions surrounding the fixed charged groups (ion swelling pressure), and 3) the elastic retractile response of the network (network swelling pressure) (5,16,17). The hydrophobic character of the methacrylate copolymer gels dominates the overall swelling behavior in water at pH values near, and above, neutrality. The unfavorable interaction between the network chains and

water in this pH range forces the gels to prefer a collapsed conformation with the resulting exclusion of water.

The hydrophobic character of these gels is contrasted with the relatively hydrophilic gels that have been studied by other workers (1-11,16-18). The observed swelling changes in this work are accordingly less extensive than those obtained with lightly crosslinked hydrogels [e.g. poly(acrylamide-*co*-acrylic acid) (5)].

The external pH has a profound effect on the balance of forces that determine equilibrium swelling. As the pH is lowered into the acidic region, the amine sidechains of the DMA residues become protonated, thus increasing the charge density in the network. The concomitant increase in mobile counterion content of the network sharply increases the internal osmotic pressure which, in turn, induces the observed swelling transitions.

Varying the ratio of nAMA to DMA for a given comonomer system (Figures 4.1 and 4.2) or varying the n-alkyl sidechain length of nAMA from C_1 to C_6 while at constant comonomer ratio (70/30 mole%, Figure 4.3) appears to affect both the extent and nature of the swelling transition. An explanation is that an increase in nAMA content or in nAMA sidechain length has two concomitant effects. First, the concentration of ionizable amine groups decreases, lowering the osmotic pressure that can be generated by the counterions. Second, the overall hydrophobicity of the gel increases. These two effects generally combine to lower the extent of equilibrium swelling in these gels.

The systematic reduction in pH at which the swelling transition occurs as nAMA content increases (Figures 4.1 and 4.2) is explained in a similar way. A transition will occur when a balance of osmotic and hydrophobic forces is achieved. As network hydrophobicity increases, a greater degree of ionization is required to enable the transition. The concomitant decrease in ionizable group concentration that occurs as DMA content decreases must be countered by a further increase in degree of ionization, requiring a lower

pH. Another factor which may contribute to the lowering of the transition pH is a decrease in the dielectric coefficient of the gel interior which likely accompanies an increase in nAMA content. This will serve to lower the effective pK_a of the ionizable DMA groups. In view of the observed swelling isotherms, it is somewhat puzzling that the transitions for the homologous nAMA/DMA series (Figure 4.3) do not show similar behavior. The downward shift of the transition pH as the nAMA sidechain length increases from C_1 to C_3 is halted and reversed somewhat for C_4 and C_6. Moreover, the discontinuous transitions observed for the C_1-C_3 gels become continuous.

One plausible explanation for these results is that the swelling data observed for the C_1-C_3 gels at high pH do not represent true thermodynamic equilibria. Since these gels are glassy in the dry state at ambient temperature, it is conceivable that the swelling data actually represent completion of the first stage of a 'dual-sorption' process (19). That is, water is initially sorbed into the 'free volume' of the glassy polymer, but the process of chain relaxation leading to the final swelling equilibrium in incomplete. The sorption kinetics shown in Figure 4.4 carried out at pH 7 argue against this explanation, however. After 2 days, sorption appears to be complete. If a secondary, relaxation controlled process exists, it must be extremely slow.

The buffer effect on swelling (Table 4.3) can be explained by considering the distribution of polyvalent anions in the citrate and phosphate buffer systems. Since the MMA/DMA gel itself is a polycation, the Donnan effect will favor uptake of polyanions over monoanions. In addition, fewer polyanions are required to neutralize an equivalent amount of charge on the gel. As the concentration of polyanions in the solution increases, these two factors will combine to lessen the concentration of counterions inside the gel, reducing the counterion osmotic pressure, and gel swelling. The pK_a's for citric acid are 3.15, 4.78 and 6.40, while those for phosphoric acid are 2.15, 7.10 and 12.12. At any pH, there will be more multivalent ions in citrate buffer than in phosphate buffer for a given

total buffer concentration. Thus, at constant ionic strength and buffer concentration, phosphate buffer should permit greater gel swelling than citrate buffer, as was observed. The influence of solution ionic strength and ionic valence on equilibrium swelling will be investigated more comprehensively in Chapter 5.

4.5 Conclusions

It has been demonstrated that abrupt pH-driven swelling transitions can occur in the class of hydrophobic nAMA/DMA copolymer gels. Characteristic features of the swelling isotherms of these weakly basic gels such as the extent, pH, and type of transition (continuous or discontinuous) are particularly sensitive to gel comonomer ratio and nAMA sidechain length. The principal determinant of the swelling equilibrium for any gel is the hydronium ion concentration with secondary contributions from the solution ionic strength and ion valences.

References

1. E.L. Cussler, M.R. Stokar and J.E. Varberg, Gels as Size Selective Extraction Solvents, AIChE. J., 30, 578 (1984).

2. J. Grignon and A.M. Scallan, Effects of pH and Neutral Salts Upon the Swelling of Cellulose Gels, J. Appl. Polym. Sci., 25, 2829 (1980).

3. J. Kost, T.A. Horbett, B.D. Ratner and M. Singh, Glucose-Sensitive Membrane Containing Glucose Oxidase: Activity, Swelling and Permeability Studies, J. Biomed. Mat. Res., 19, 1117 (1985).

4. K. Ishihara, M. Kobayashi, N. Ishimaru and I. Shinohara, Glucose Induced Permeation Through a Complex Membrane Consisting of Immobilized Glucose Oxidase and a Poly(Amine), Polym. J., 16, 8, 625 (1984).

5. T. Tanaka, D. Fillmore, S.-T. Sun, I. Nishio, G. Swislow and A. Shah, Phase Transitions in Ionic Gels, Phys. Rev. Lett., 45, 1636 (1980).

6. I. Ohmine and T. Tanaka, Salt Effects on the Phase Transition of Ionic Gels, J. Chem. Phys., 77, 5725 (1982).

7. S. Katayama, Y. Hirokawa and T. Tanaka, Reentrant Phase Transition in Acrylamide-Derivative Copolymer Gels, Macromolecules, 17, 2641 (1984).

8. R.F.S. Freitas and E.L. Cussler, Temperature Sensitive Gels as Extraction Solvents, Chem. Eng. Sci., 42, 1, 97 (1987).

9. A.S. Hoffman, A. Afrassiabi and L.C. Dong, Thermally Reversible Hydrogels: II. Delivery and Selective Removal Of Substances from Aqueous Solutions, J. Contr. Rel., 4, 213 (1986).

10. S. Katayama and A. Ohata, Phase Transition of a Cationic Gel, Macromolecules, 18, 2781 (1985).

11. Y. Hirokawa, T. Tanaka and E. Sato, Phase Transition of Positively Ionized Gels, Macromolecules, 18, 2782 (1985).

12. S. Krause, J.J. Gromley, N. Rowan, J.A. Shetter and W.H. Watanabe, Glass Temperatures of Some Acrylic Polymers, J. Polym. Sci., Part A, 3, 3573 (1965).

13. J.A. Shetter, Effect of Stereoregularity on the Glass Temperatures of a Series of Poly Acrylates and Methacrylates, J. Polym. Sci., B1, 209 (1963).

14. S.S. Rogers and L. Mandelkern, Glass Formation in Polymers. I. The Glass Transitions of the Poly(n-alkyl Methacrylates), J. Phys. Chem., 61, 985 (1957).

15. F. Bueche, Viscoelasticity of Polymethacrylates, J. Appl. Phys., 26, 738 (1955).

16. P.J. Flory, "Principles of Polymer Chemistry", Chapter XIII, Cornell University Press, 1953.

17. A. Katchalsky, Polyelectrolyte Gels, Prog. Biophys., 4, 1 (1954).

18. J. Ricka and T. Tanaka, Swelling of Ionic Gels: Quantitative Performance of the Donnan Theory, Macromolecules, 17, 2916 (1984).

19. W.R. Vieth, J.M. Howell and J.H. Hsieh, Dual Sorption Theory, J. Membr. Sci., 1, 177 (1976).

Chapter 5.

Swelling Equilibria in Electrolyte Solutions and the Donnan Equilibrium Theory

5.1 Introduction

Ionic gels eventually come to an osmotic equilibrium with the solution in which they are immersed. Because exchange of solvent (usually water) and mobile ions occurs between the gel and the external electrolyte solution, changes in the ionic composition of the solution (e.g. pH, ionic strength, ionic valence) can perturb the osmotic balance and cause profound effects on the swelling equilibrium of the gel. Accounts of these effects are discussed in Chapter 2. The mechanisms governing the swelling behavior of ionic gels in simple and complex electrolyte solutions should be understood if these materials are to be used in devices that are intended for biological environments.

Theories of swelling in ionic gels have generally been based on the description of the expansive and contractile forces of the neutral network (network swelling pressure) and the electrostatic interactions between ions in the gel, both fixed and mobile (ion swelling pressure) (1). These pressures sum to zero under conditions of swelling equilibrium. The network swelling pressure has contributions from the free energy of mixing of polymer chains of the gel network and solvent, which is usually described by the Flory-Huggins theory of polymer solutions (2), and the elastic free energy associated with the elongation of the network chains during swelling (2). Such theories are, in general, quite complex and involve parameters whose experimental estimation is difficult. Furthermore, the theories at present only provide a semi-quantitative description, so that evaluation of the theory parameters typically does not lead to quantitative predictions (3).

A particularly simple theory to describe the effects of the solution electrolyte composition on the swelling of ionic gels without considering contributions from the network swelling pressure was first reported by Proctor and Wilson (4,5) in their studies of gelatin gels, and has since been advocated by others (2,6,8-9,17,19). This theory attributes the ion swelling pressure to the mobile ion 'osmotic pressure' difference between the gel interior and the external solution. The concentration of mobile ions will be greater in the gel phase due to the necessity of neutralizing the fixed charges of the network, and resembles the classic Donnan equilibrium as diagrammed in Figure 5.1 (7). Actually, the presence of excess mobile ions in the gel acts to reduce the chemical potential of water which will cause water entry and swelling. Swelling will eventually be opposed by the elastic retraction of the network which serves to increase the chemical potential of water to its level in the external solution (2). The osmotic pressure difference can be computed from the van't Hoff law (eqn. 5.1) for

$$\Pi_{ion} = RT \sum(C_i - C_i') \qquad (5.1)$$

the osmotic pressure of dilute solutions, where in eqn. 5.1, C_i and C_i' are the concentrations of the i^{th} mobile ion inside the gel and in the external solution, respectively, R is the gas constant and T is the absolute temperature, and the summation is taken over all mobile ions. The use of eqn. 5.1 for the computation of Π_{ion} for any equilibrated gel requires the knowledge of all the ionic concentrations in the gel interior (all C_i terms). Although difficult to measure when complex ionic equilibria are involved, the gel ion concentrations can be estimated from the known concentrations in the external solution by applying the Donnan equilibrium theory (2-9,15-19).

Within the scope of this theory, the ionic contribution to swelling in polyelectrolyte gels depends on the ionic composition of the external solution and on the fixed charge

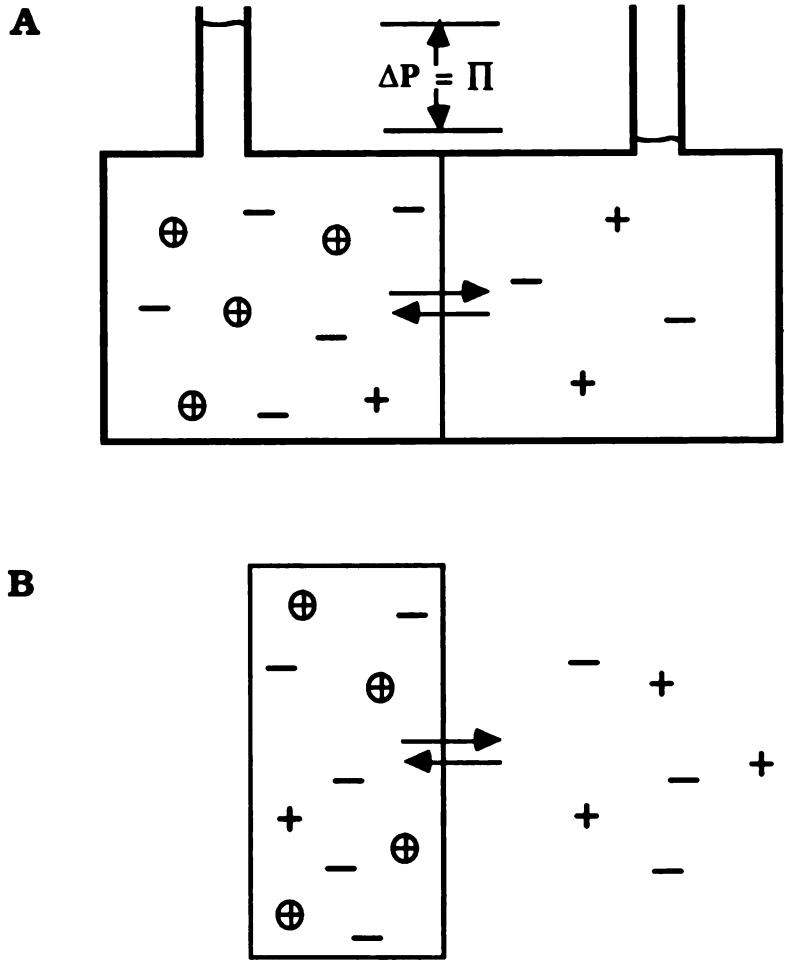

Figure 5.1. Illustration of the analogy between the Donnan equilibrium and equilibria in ionic gels. A, Classic Donnan equilibrium experiment involving a semipermeable membrane separating a solution of colloidal macroions from a solution containing a simple electrolyte solution. The membrane is permeable to small ions and water but is impermeable to macroions. Small ions concentrate in the macroion chamber and this leads to an osmotic pressure gradient which is balanced by the hydrostatic pressure-head (ΔP). B, Due to the presence of fixed charges in the gel, mobile ions concentrate in the gel interior and cause an osmotic pressure gradient between the gel interior and the external solution. This induces swelling and is eventually opposed by the elastic retraction of the network.

density of the network. Contributions from other ionic effects such as electrostatic repulsion between the fixed charges (which would enhance swelling) or ionic interactions between fixed ions and their counterions (which would reduce swelling either by reducing the osmotic activity of the counterions or by the formation of ionic crosslinks (8)) are not considered. The Donnan theory, although providing a rather simplistic description of the effects of gel ionization on swelling, has been very successful in quantitatively predicting the swelling behavior of lightly ionized polyacrylamide gels as a function of solution ionic composition (8,9,17).

In this chapter, the effect of solution electrolyte composition on the equilibrium swelling properties of the MMA/DMA 70/30 mole% gel is discussed. We are particularly interested in the effects of pH and ionic strength of simple solutions containing monovalent ions as well as in more complex solutions of multivalent ions. The results of these experiments are compared with predictions based on the Donnan theory. Validity of the Donnan theory, as it applies under these conditions, is assessed.

5.2 Theory

5.2.1 Derivation

Consider a polyelectrolyte gel placed in an excess of an aqueous electrolyte solution. The equilibrium condition for each mobile ion in the system is that its electrochemical potential must be the same inside the gel as in the external solution, and is written as:

$$\mu^{\circ}_i + RT \ln a_i + z_i F\Phi = \mu^{\circ}_i + RT \ln a_i' \qquad (5.2)$$

where μ_i^o is the standard state chemical potential of ion i at infinite dilution in water, z_i is the valence of ion i, F is the Faraday constant, a_i and a_i' are the thermodynamic activities of ion i in the gel and in the solution, respectively, and Ø is the electric (Donnan) potential of the gel phase with respect to the external solution (zero potential). The Donnan potential arises due to the unequal ionic activities between the gel and the solution. As counterions diffuse from the gel to the solution down the gradient in activity (diffusion flux), a minute charge separation develops creating the Donnan potential. This potential creates a counterion current (drift flux) which draws counterions back to the gel, and eventually exactly counterbalances the diffusion flux. Eqn. 5.2 can be rearranged to give:

$$a_i = a_i' e^{-z_i F\emptyset /RT} \tag{5.3}$$

Under conditions of dilute salt concentration and extensive swelling in the gel phase, we assume $a_i = C_i$ and $a_i' = C_i'$ and eqn. 5.3 simplifies to:

$$C_i = C_i' e^{-z_i F\emptyset/RT} \tag{5.4}$$

Because Ø is identical for all ions in the system (as only one potential can exist), it is customary to define the Donnan ratio (λ) as:

$$\lambda = e^{-F\emptyset/RT} \tag{5.5}$$

Substituting this expression into eqn. 5.4, we obtain:

$$C_i = C_i' \lambda^{z_i} \tag{5.6}$$

Eqn. 5.6 applies to all mobile ionic species in a given system and describes the ideal (Donnan) partitioning of ions between the gel interior (C_i) and the external solution (C_i'). For gel counterions (mobile ions whose charge is opposite to that of the gel), z_i and Ø are of opposite sign, so that $\lambda^{z_i} > 1$ and the concentration of a given counterion inside the gel will exceed its bulk solution concentration ($C_i > C_i'$). For gel coions (mobile ions whose charge is the same as that of the gel), z_i and Ø have the same sign, $\lambda^{z_i} < 1$, and the concentration of a given coion in the gel will be less than its bulk solution concentration ($C_i < C_i'$). The latter situation is known as the Donnan exclusion of coions. From eqn. 5.6, it is seen that the Donnan partitioning properties of ions become more unequal as the magnitude of the ion valence z_i increases.

In order to solve for λ it is necessary to apply the condition of bulk electroneutrality, in the gel phase. Electroneutrality must be obeyed for any macroscopic phase of uniform electric potential since charge separation cannot exist over distances larger than several tens of angstroms. The only location were electroneutrality does not strictly apply is in the vicinity of the gel/solution interface where the potential decays with distance in an approximately exponential fashion from its value in the gel interior toward zero in the bulk solution. The theory assumes that the potential changes as a step-function at the interface. The spatial decay occurs over molecular scales (several Debye lengths) and can be neglected when applying electroneutrality to the macroscopic gel phase.

Applying electroneutrality to the gel phase is accomplished by summing up the total charge density (equivalents/volume) within the gel due to both mobile ions and the fixed charges of the gel, and equating to zero:

$$\sum (z_i C_i) + \rho_{net} = 0 \qquad (5.7)$$

The first term on the left hand side of eqn. 5.7 accounts for the charge density of the mobile ions within the gel and the second term (ρ_{net}) represents the charge density of the fixed charged groups (gel charge density). For gels that contain permanently charged groups (e.g. quaternary ammonium or sulfonic acid groups), ρ_{net} is computed by dividing the equivalents of charged groups by the gel volume that contains them. For gels that contain weakly ionizable groups, ρ_{net} will depend on the degree of ionization of these groups as determined by the internal pH of the gel which, in general, will not be the same as in the external solution due to the Donnan partitioning of hydronium ions. Addition of a term for simple proton mass action into the expression for ρ_{net}, we obtain for weak acid gels (8):

$$\rho_{net} = \rho^{\circ}_{net} \left(\frac{K}{K + C_H} \right) \tag{5.8}$$

and for weak base gels:

$$\rho_{net} = \rho^{\circ}_{net} \left(\frac{C_H}{K + C_H} \right) \tag{5.9}$$

where ρ^{o}_{net} is the total concentration of ionizable groups in the swollen gel at equilibrium, C_H is the hydronium ion concentration inside the gel and K is the acid dissociation constant of the gel's ionizable groups. The terms in parentheses in eqns. 5.8 and 5.9 represent the fraction of groups of the gel that are ionized.

The term ρ^{o}_{net} can be expressed in terms of the equilibrium swelling of the gel as:

$$\rho^{\circ}_{net} = (1 - H) \frac{f_w}{M_m} [H \rho_w + (1 - H) \rho_g] \; 1000 \tag{5.10}$$

where H is the equilibrium hydration of the gel (g water/g swollen gel), f_w is the weight fraction of the ionizable monomer in the dry gel (at synthesis), M_m is the formula weight of the ionizable monomer, and ρ_w and ρ_g are the densities of the gel water phase (assumed to 1.0 for simplicity) and the dry gel (estimated to be 1.2, see Chapter 8), respectively. The term in square brackets represents the density of the swollen gel as a weighted average of the water density and the dry gel density, assuming additivity of volume. Substituting the expression for ρ_{net} (eqn. 5.8 or 5.9) into the electroneutrality equation (eqn. 5.7), we obtain for the case of a basic gel:

$$\sum z_i C_i' \lambda^{z_i} + \rho^\circ_{net} \left(\frac{C_H' \lambda}{C_H' \lambda + K} \right) = 0 \qquad (5.11)$$

where all C_i terms have been replaced by $C_i' \lambda^{z_i}$ from eqn. 5.6.

When eqn. 5.11 is written for a given equilibrium situation and simplified, a polynomial in λ is obtained whose order depends on the valences (z_i) of the mobile ions. For example, in a simple monovalent electrolyte solution such as NaCl in water, the summation is taken over four ionic species (Na^+, Cl^-, H_3O^+ and OH^-) and results in a third order polynomial. Higher order polynomials are generated when multivalent ions are present. Eqn. 5.11 can be solved for λ using a numerical procedure such as the Newton-Raphson method (28).

Once λ is determined, Π_{ion} can be computed from the following modification of eqn. 5.1:

$$\frac{\Pi_{ion}}{RT} = \sum C_i' \left(\lambda^{z_i} - 1 \right) \qquad (5.12)$$

Thus, for an ionic gel of a given (measurable) equilibrium hydration (H) in an electrolyte solution of known composition, λ can be obtained by solving the electroneutrality equation, which is then used to compute Π_{ion} from eqn. 5.12.

5.2.2 Limiting Cases

There are two important limiting cases of the theory that predict markedly different swelling behavior (2,3). In the first case, we consider a situation where the counterion concentration in the external solution is very small compared with the charge density of the gel (i.e., $C' << \rho_{net}$). Under such conditions the gel will absorb a sufficient number of counterions to neutralize ρ_{net} (equivalents/liter) of gel charge. This will amount to a concentration of counterions of $C = |\rho_{net}/z|$, where z is the counterion valence. This gives:

$$\lambda = \left(\frac{C}{C'}\right)^{1/z} = \left(\frac{|\rho_{net}|}{|z|C'}\right)^{1/z} \tag{5.13}$$

Because $C' << \rho_{net}$, we see from eqn. 5.13 that the Donnan ratio will differ significantly from unity, and results in a difference in hydronium ion activity between the gel interior and the external solution. The contribution to Π_{ion} becomes, approximately:

$$\frac{\Pi_{ion}}{RT} = \sum C_i' \left(\lambda^{z_i} - 1\right) \tag{5.12}$$

$$\cong C'\left[\left(\frac{|\rho_{net}|}{|z|C'}\right) - 1\right]$$

$$\cong \frac{|\rho_{net}|}{|z|} \tag{5.14}$$

Eqn. 5.14 indicates that in the dilute electrolyte regime, Π_{ion} is highly dependent on the gel charge density (ρ_{net}) and the counterion valence (z). An increase in z will strongly reduce Π_{ion}.

The second limiting case of interest arises when the concentration of mobile ions in the external solution greatly exceeds the gel charge density ($\rho_{net} << \Sigma C_i'$). Then, it can be shown (3) that λ approaches 1 - $\rho_{net}/2I'$ (essentially unity) and:

$$\frac{\Pi_{ion}}{RT} \cong \frac{\rho_{net}^2}{4\,I'} \tag{5.15}$$

where I' is the ionic strength of the external solution defined as:

$$I' = \frac{1}{2}\sum\left(z_i^2\, C_i'\right) \tag{5.16}$$

Thus, in solutions of high ionic strength Π_{ion} is effectively determined by the ionic strength (I') of the external solution and is insensitive to ionic valence, except as it contributes to I'. Increasing the solution ionic strength in this concentration regime swamps out the imbalance in the mobile ion concentration due to Donnan partitioning, and strongly reduces Π_{ion} towards zero.

5.2.3 Theory Assumptions and Conditions of Applicability

The equations developed in Section 5.2.1 contain several simplifying assumptions that were either stated explicitly or implied and will limit the applicability of the theory. These assumptions are enumerated below along with the conditions under which the theory is expected to be most valid.

Assumptions:

1) **Ideal Solution Behavior of Ions.** It has been explicitly assumed in writing eqn. 5.4 that all ions behave ideally (activity = concentration) and retain full osmotic activity in both the external solution phase and the gel interior. Electrostatic interactions between ions (both mobile and fixed) are ignored as are the dielectric effects in the gel interior on ionic activities.

2) **Ionization Constants of the Gel and Other Weak Electrolytes are Constant.** The dissociation constants of the gel amine groups and all other weak electrolytes (each citrate species) in the gel interior are constant and independent of the extent of swelling and the magnitude of the network charge density (ρ_{net}).

3) **No Electrostatic Contribution to Π_{ion}.** Repulsive electrostatic interactions between the fixed charges of the network are ignored. Under conditions of high gel charge density, such interactions may contribute significantly to Π_{ion} and the Donnan potential cannot be assumed constant throughout the gel phase, as is implicit in eqn. 5.2 (10-12).

In view of the above assumptions, the Donnan theory should be most applicable under conditions of high gel swelling and small gel charge density at dilute salt concentrations. We apply the theory to the swelling behavior of the MMA/DMA 70/30 mole% gel, which is the most extensively swollen of the nAMA/DMA gels studied.

5.2.4 Calculations

Calculations of Π_{ion} based on the Donnan theory were carried out using two different simulated conditions. In the first, the equilibrium gel hydration (H) was held constant (thus ρ^{o}_{net} is constant by eqn. 5.10) and Π_{ion} was computed as a function of solution pH or ionic strength. The calculations with constant H correspond to a situation where the gel is constrained to constant volume (such as a gel confined in a rigid container) but develops an internal net ion osmotic pressure as determined by the electrolyte

composition of the external solution. In the second case, Π_{ion} was computed based on an observed value of gel hydration for the MMA/DMA 70/30 mole% gel under conditions of known solution pH and ionic strength. These calculations comprise a more robust test of the theory because they enable a realistic value of ρ^{o}_{net} to be used and correspond to the actual experimental conditions in which free swelling of the gels occur. Table 5.1 lists the parameter values used. The values of the parameters f_w and ρ_g correspond to the MMA/DMA 70/30 mole% gel and the value of K used corresponds to the reported ionization constant of the DMA monomer (13).

Table 5.1. Parameter Values Used in All Calculations.

Parameter	Definition	Value Used
f_w	wt. fraction of DMA in gel	0.40
M_m	formula weight of DMA	157.2
ρ_w	density of gel water	1.0
ρ_g	density of dry gel	1.2
K	ionization constant of gel	$10^{-7.7}$

5.3 Experimental

5.3.1 Materials

Sodium chloride, potassium chloride (Mallinckrodt, Inc.); sodium sulfate, sodium bromide, sodium thiocyanate (J.T. Baker); sodium iodide, cesium chloride, lithium chloride (Aldrich) and citric acid (Fisher Scientific) were analytical reagent grade and were used without further purification. Water used in the swelling studies was double distilled and deionized.

5.3.2 Equilibrium Swelling Studies

MMA/DMA 70/30 mole% gels were prepared as thin circular disks (0.28 x 7mm) according to the method described in Chapter 3. The pH-dependent equilibrium swelling properties were measured in 0.01 M citrate buffer at 25 °C as described in Chapter 4. The ionic strength of each buffer solution was adjusted to 0.1 M by the addition of a calculated amount of NaCl. The ionic strength dependent swelling properties of the same gel were determined as described in Chapter 4 in either dilute HCl solution or 0.01 M citrate buffer at pH 4.0. The ionic strength of the HCl solutions were adjusted to the desired level by the addition of NaCl, whereas the citric acid solutions were adjusted with either NaCl or Na_2SO_4.

5.4 Results

5.4.1 Effect of Solution pH

The equilibrium hydrations of the MMA/DMA 70/30 mole% gel in both citrate buffer solutions and dilute HCl solutions are shown in Figure 5.2 as a function of pH. The ionic strength of each solution was adjusted to 0.1 M by the addition of a calculated amount of NaCl. The swelling data in citrate solution was presented in Chapter 4, and the data below pH 6.6 (swollen regime) are shown again here for comparison. The results show that although this gel swells to significant extent in both solutions, there are significant differences at the same pH and ionic strength in solutions containing different ions. Swelling in unbuffered solutions between pH 2.0 and 6.0 results in an essentially constant equilibrium hydration (H) of approximately 0.85, whereas in citrate buffer solutions, hydration generally decreases with increasing pH from H=0.95 at pH 2.0 to H=0.66 at pH 6.6. Differences in gel hydration at the same pH and ionic strength were also observed for this gel in citrate and phosphate buffer solutions as presented in Table 4.3. There exists a

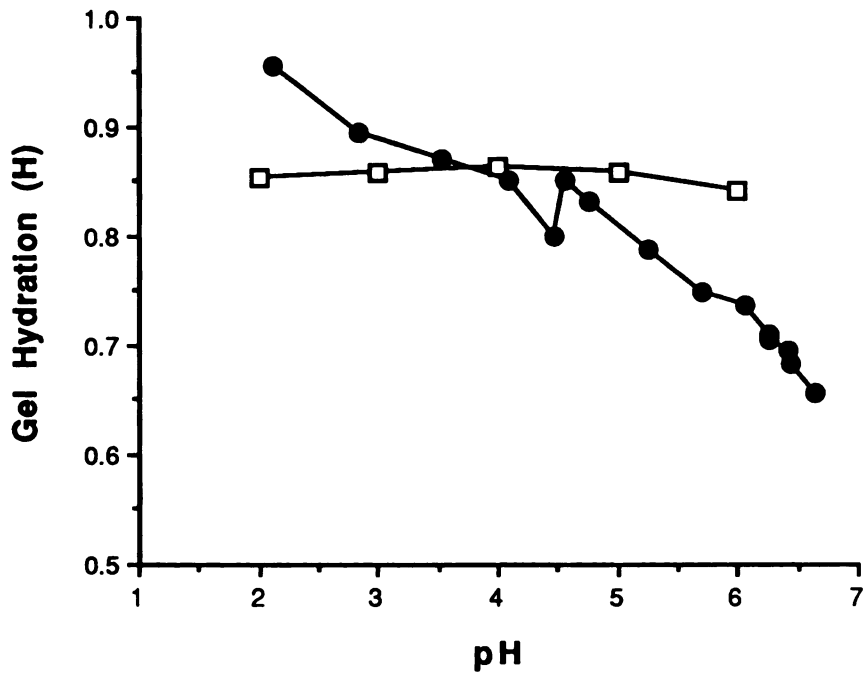

Figure 5.2. Equilibrium swelling of the MMA/DMA 70/30 mole% gel as a function of pH in 0.01 M citrate/NaCl solutions (●) and HCl/NaCl solutions (❑). Measurements were made at 25 °C and a total ionic strength of 0.1 M.

secondary but significant contribution to the extent of gel hydration from the ionic composition of the electrolyte solution.

5.4.2 Effect of Solution Ionic Strength

Figure 5.3 shows the effects of varying the total ionic strength (I') (defined as in eqn. 5.16) and valence of various electrolyte solutions on the equilibrium hydration of the MMA/DMA 70/30 mole% gel, all at a constant pH of 4.0. Gel swelling was measured in three different electrolyte solutions, each as a function of ionic strength: 1) dilute HCl (pH 4.0) with NaCl added to adjust I', 2) 0.01 M citrate buffer (pH 4.0) with NaCl added to adjust I', and 3) 0.01 M citrate buffer (pH 4.0) with Na_2SO_4 added to adjust I'.

The HCl/NaCl solutions are composed of only monovalent ions and contain Cl^- as the single gel counterion (OH^- can be neglected at pH 4.0). The citrate/NaCl solutions contain gel counterions of several valencies as follows: citrate monoanion (Cit^-), citrate dianion (Cit^{-2}), citrate trianion (Cit^{-3}) and increasing amounts of Cl^- to adjust I'. At pH 4.0, citric acid is 91% ionized with 77% of the total acid as Cit^-, 14% as Cit^{-2} and 0.056% as Cit^{-3} (see Appendix 5.A for calculations). The citrate/Na_2SO_4 solutions contain the same distribution of citrate anions (the pH is the same), but contain the dianion SO_4^{-2} in increasing amounts depending on I' (sulfuric acid, H_2SO_4, has a very low pK_1 (<0) and a pK_2 of 1.90. Thus at pH 4.0, greater than 99% of sulfate species exist as the dianion, SO_4^{-2}). It should be pointed out that the two citrate curves of Figure 5.3 share a common data point at I'=0.013 M (the lowest ionic strength), which corresponds to 0.01 M citrate buffer at pH 4.0 with no added salt. As indicated in Figure 5.3, there are marked differences in swelling in the various solutions at low ionic strength, while swelling appears to converge at high ionic strength. The gel equilibrium hydration in HCl/NaCl solutions monotonically decreases as the ionic strength is increased. In citrate/NaCl solutions at low ionic strength, gel hydration is significantly lower than that in

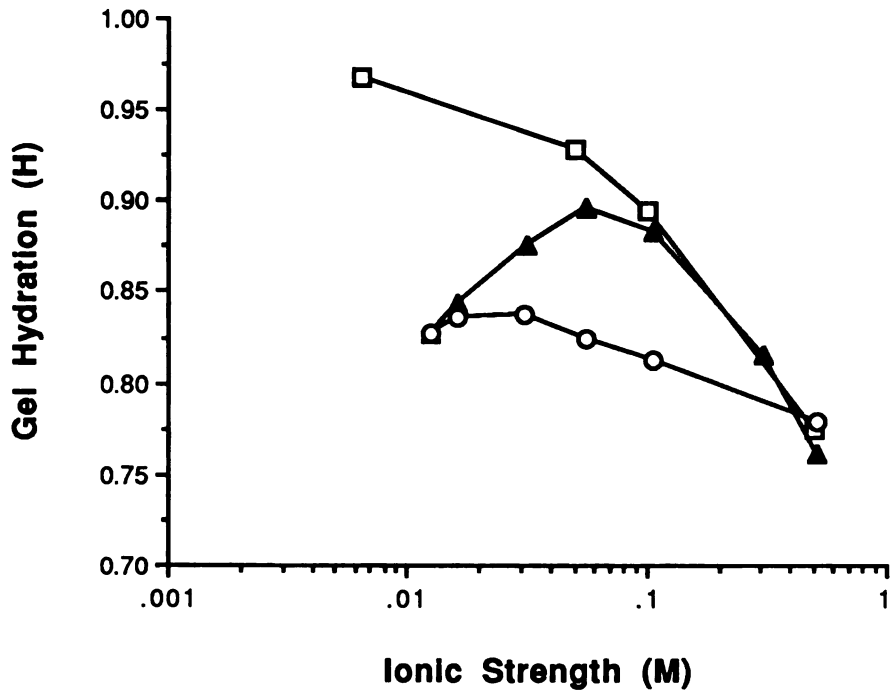

Figure 5.3. Equilibrium swelling of the MMA/DMA 70/30 mole% gel as a function of ionic strength at pH 4.0 and 25 °C in HCl/NaCl solutions (□), 0.01 M citrate/NaCl solutions (▲) and 0.01 M citrate/Na_2SO_4 (○).

HCl/NaCl and increases to a maximum at about I'=0.05 M. Further increases in I' causes a decline in gel hydration in parallel with that in HCl/NaCl solutions. In citrate/Na_2SO_4 solutions, gel hydration increases slightly as I' is increased, but then decreases in the high ionic strength region.

5.4.3 Effects of Other Strong Electrolytes

In order to assess the effects of ion-specific interactions on gel swelling not predicted by the Donnan theory, swelling was measured in a series of four chloride salts (representing different gel coions) and six sodium salts (representing different gel counterions) were each prepared as I'=0.1 M solutions at pH 4.0. Figure 5.4A indicates that the identity of the gel coion has minimal impact on the gel swelling, whereas swelling is strongly affected by the identity of the counterion as shown in Figure 5.4B, where a difference in swelling of approximately 15-fold across the series of sodium salts is observed.

5.5 Discussion

5.5.1 Qualitative Predictions

Calculations were performed employing a value of H=0.70 which corresponds to a swollen gel containing 70% water by weight. The exact value of H used in the model is not critical as long as it represents an appreciably swollen gel. Values of other parameters are listed in Table 5.1.

Results of calculations of Π_{ion}/RT as a function of solution pH are shown in Figure 5.5 for swelling in HCl/NaCl solutions and 0.01 M citrate buffer solutions with added NaCl. The calculations for citrate buffer took into account its multiple equilibria (pK_a values for citric acid are pK_1=3.15, pK_2=4.78 and pK_3=6.40). For swelling in HCl/NaCl solutions, Π_{ion}/RT is essentially constant up to pH 5.0 where it declines rapidly thereafter.

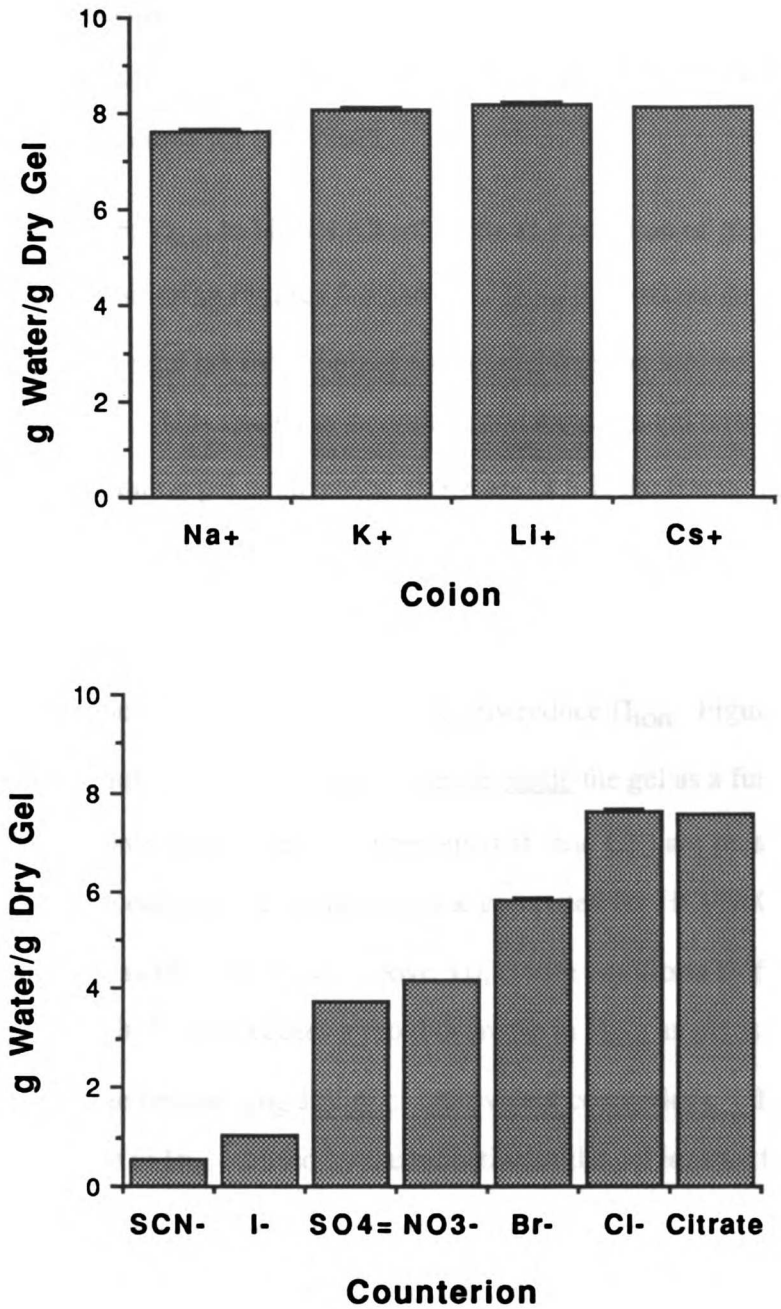

Figure 5.4. Effect of specific ions on the equilibrium swelling of the MMA/DMA 70/30 mole% gel at pH 4.0 and a total salt concentration of 0.1 M. A (top), various gel coions; and B (bottom), gel counterions. Measurements were made at 25 °C.

For citrate solutions, Π_{ion}/RT is constant up to pH 3.1, where it superimposes the curve for HCl/NaCl, but declines in a nearly linear fashion at pHs above 3.1 where it falls appreciably below the curve for HCl/NaCl.

The behavior of Π_{ion} in HCl/NaCl solutions as a function of pH in Figure 5.5 can be understood by considering Figures 5.6 and 5.7. Π_{ion} is constant up to pH 5.1 because the amine groups of the gel are fully ionized (computed fraction ionized =1.0) in this region as shown in Figure 5.6. This results in a constant and maximal gel charge density (ρ_{net}) and thus Π_{ion}. As solution pH is increased above about 5.1, the fraction of gel amine groups that are ionized decreases, which reduces ρ_{net} and thus Π_{ion}.

Swelling in citrate/NaCl solutions is somewhat more complicated due to the formation of multivalent ions which tend to strongly reduce Π_{ion}. Figure 5.7 shows the computed concentrations of ions of a given valence inside the gel as a function of solution pH. Below pH 3.0, only monovalent counterions (Cit^- and Cl^-) are present in the gel, so the predicted Π_{ion} is constant and identical to that computed for HCl/NaCl solution in this pH range. However, as pH is increased above 3.0, citrate equilibria shifts to produce Cit^{-2} and, above pH 5.0, Cit^{-3}. This causes a rapid decrease in Π_{ion} as pH is increased due to the efficient gel charge neutralizing ability of multivalent counterions. This occurs in addition to the decline in Π_{ion} caused by the reduction in the gel ionized fraction above pH 5.0 (Figure 5.6). It is worthwhile to point out in passing the exceedingly small concentrations of coions (Na^+ and H_3O^+) indicated in Figure 5.7. This is the so-called Donnan exclusion effect as discussed in Subsection 5.2.1.

In comparing Π_{ion} of Figure 5.5 with the results of Figure 5.2, it is apparent that some trends are qualitatively observed. For instance, the constant swelling in HCl/NaCl solutions up to pH 5.0 is indeed observed, as is the decline in swelling in citrate/NaCl

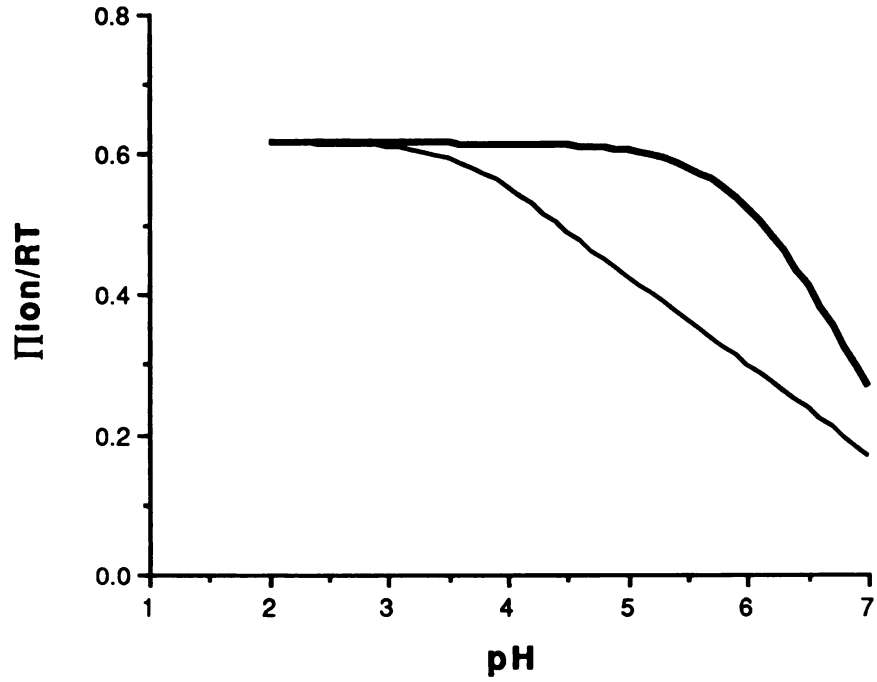

Figure 5.5. Π_{ion} computed as a function of pH for HCl/NaCl solutions (heavy line) and 0.01 M citrate/NaCl solutions (thin line). A constant value of H=0.70 was used in the calculations. Other parameter values are listed in Table 5.1.

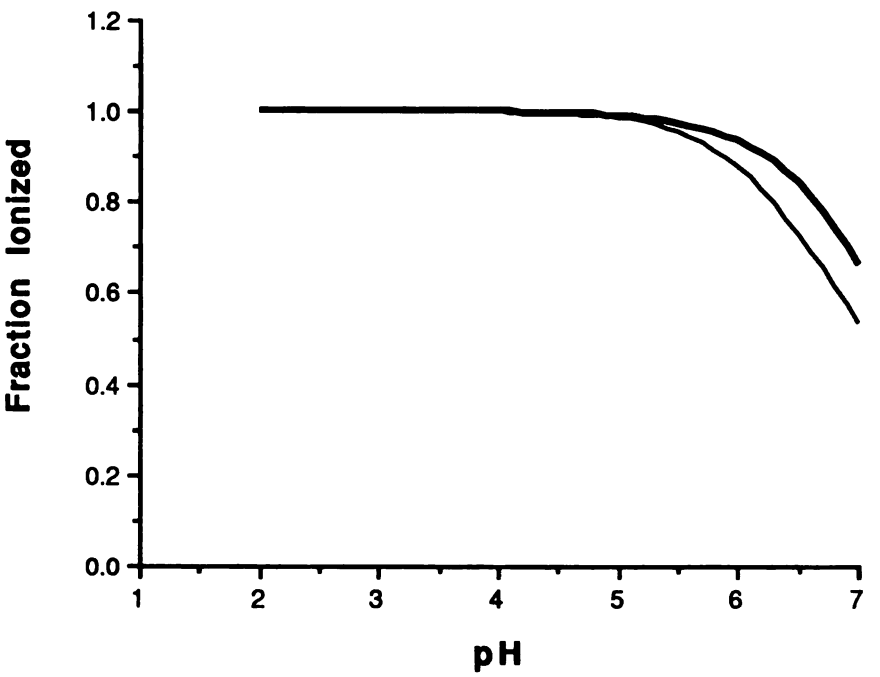

Figure 5.6. Fraction of gel amine groups ionized computed as a function of pH from the Donnan theory using a simple proton mass action law (eqn. 5.9). Electrolyte solutions are 0.01 M citrate/NaCl (heavy line) and HCl/NaCl (thin line).

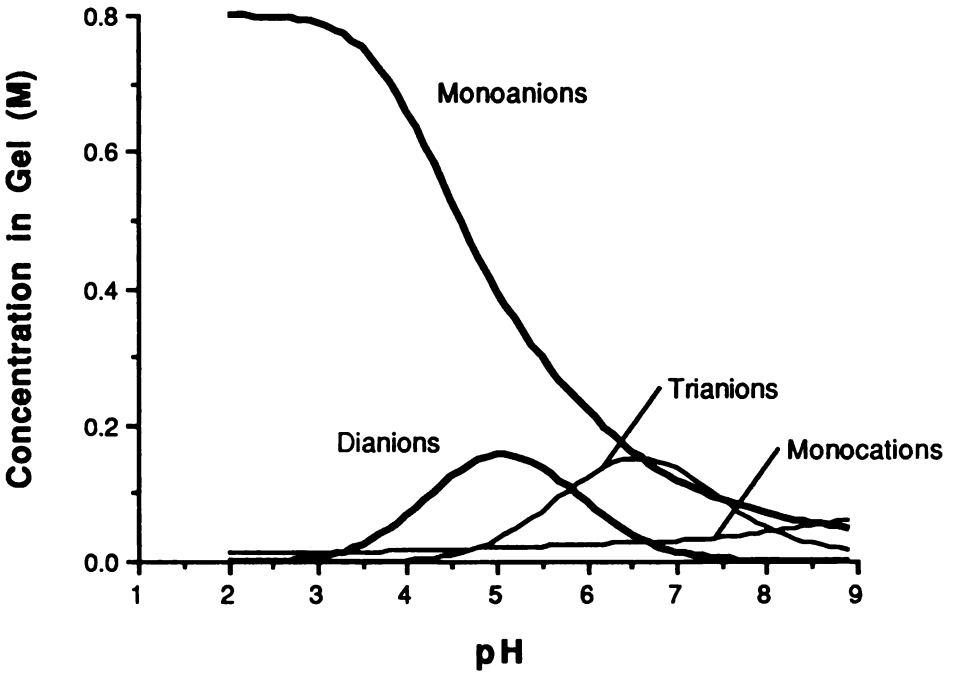

Figure 5.7. Concentrations of mobile ions of a given valence inside the gel computed from the Donnan theory as a function of solution pH for 0.01 M citrate/NaCl solutions at an ionic strength of 0.1 M. Monocations are Na^+ and H_3O^+, monoanions are Cl^- and Cit^-, dianions are Cit^{-2}, and trianions are Cit^{-3}.

solutions above pH 3.0. However, swelling in citrate/NaCl solutions below pH 3.0 continues to increase as pH is reduced, and lies above the data for HCl/NaCl. Such behavior, although not predicted by the Donnan theory, may be caused by the conversion of the pendant ester groups of the gel to form methacrylic acid groups by general acid catalyzed hydrolysis.

Calculations of Π_{ion}/RT as a function of ionic strength at a constant pH of 4.0 are indicated in Figure 5.8 for the three different electrolyte solutions considered (HCl/NaCl, 0.01 M citrate/NaCl and 0.01 M citrate/Na_2SO_4). The ionic strength was varied in the calculations down to 10^{-4} M in the HCl/NaCl solutions, and down to 0.013 M in the citrate solutions. Results of calculations in Figure 5.8 indicate that the ion swelling pressure is a sensitive function of ionic strength and ionic valence, and shows highly nonmonotonic behavior. At low ionic strength (I') in HCl/NaCl solution, increasing I' by the addition of NaCl results in an increase in Π_{ion}. This increase is shown in Figure 5.9 to be due to the increase in the ionized fraction of the gel. At very low ionic strength, the availability of gel counterions ultimately limits the extent of ionization of the gel. The addition of more NaCl permits the ionized fraction to increase, thereby increasing ρ_{net} and thus Π_{ion}, which is qualitatively consistent with eqn. 5.14. The maximum in Π_{ion} at approximately I'=0.008 M corresponds to the calculated plateau in gel ionization (Figure 5.9). At this point, all amine groups are ionized and an increase in I' past this level simply decreases the ion osmotic pressure difference between the gel and solution, in accord with eqn. 5.15. The observed swelling in HCl/NaCl solution (Figure 5.3) monotonically decreases over the same ionic strength range as predicted in Figure 5.8.

The maximum in the citrate/NaCl curve of Figure 5.8 is shifted to higher ionic strength and arises by a different mechanism than in the HCl/NaCl case. At the lowest ionic strength and pH 4.0, the distribution of citrate species is 77% Cit^-, 14% Cit^{-2} and

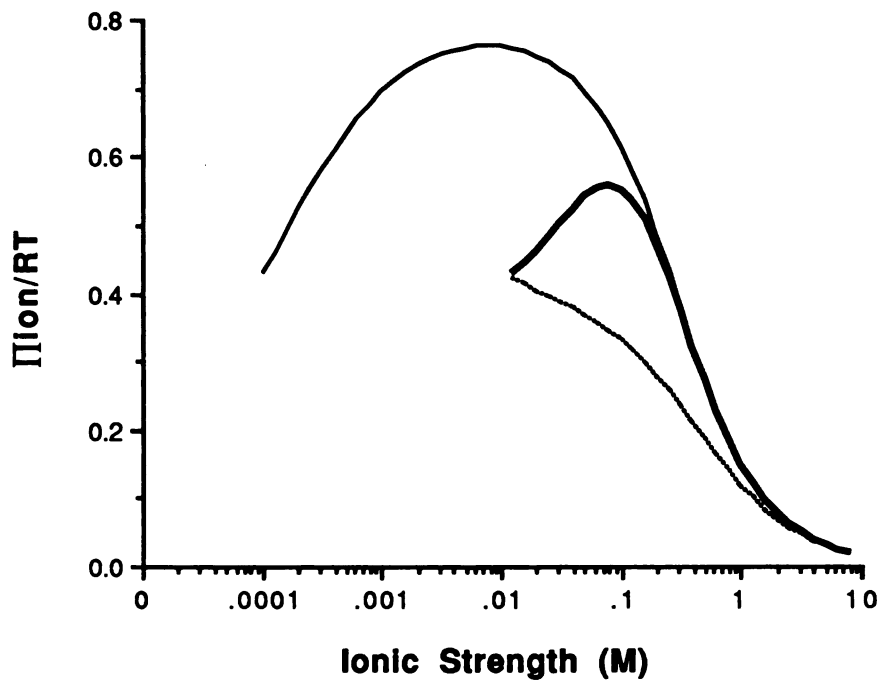

Figure 5.8. Π_{ion} computed as a function of solution ionic strength at pH 4.0 for three types of electrolyte solutions: HCl/NaCl (thin line), 0.01 M citrate/NaCl (heavy line) and 0.01 M citrate/Na_2SO_4 (dashed line).

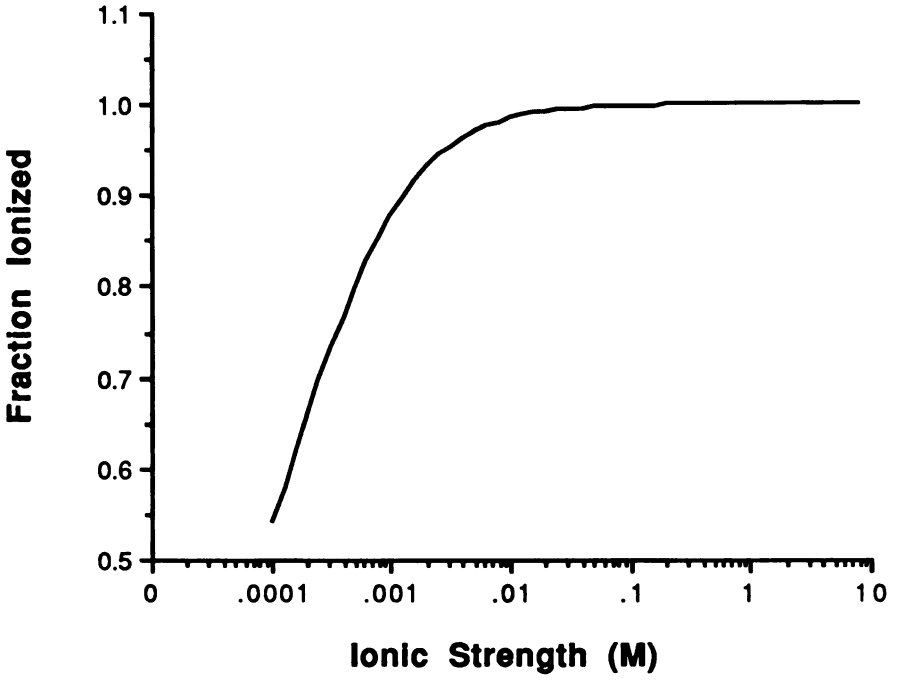

Figure 5.9. Fraction of gel amine groups ionized for HCl/NaCl solutions at pH 4.0 computed as a function of ionic strength from the Donnan theory using a simple proton mass action law (eqn. 5.9).

0.056% Cit^{-3} in the external solution (see Appendix 5.A). The relative abundance of the multivalent counterions will be greater in the gel due to the Donnan effect. As NaCl is added to increase the ionic strength, stoichiometric equivalents of Cl^- from the external solution will exchange for the mono, di and trivalent citrate anions in the gel. To the extent that is exchange process occurs, Π_{ion} increases. The maximum in the citrate/NaCl curve at approximately I'=0.07 M signals the near completeness of the exchange process (virtually all gel counterions are Cl^-). A further increase in I' causes a reduction in Π_{ion} in parallel with the HCl/NaCl curve. The observed swelling in citrate/NaCl solutions (Figure 5.3) shows remarkable qualitative agreement with the predictions, with the maximum occurring at approximately I'=0.06 M (approximately 0.07 M predicted).

For citrate/Na_2SO_4 solutions, Π_{ion} monotonically decreases with increasing ionic strength without showing a maximum, as in the citrate/NaCl curve. In this case, addition of Na_2SO_4 results in the exchange of 2 equivalents of Cit^- and 1 equivalent of Cit^{-2} from the gel for each equivalent of SO_4^{-2} that enters the gel from the solution. In contrast to the citrate/NaCl case, this stoichiometry of exchange results in a decrease in the mobile ion concentration in the gel and thus the ion swelling pressure. The observed swelling data of Figure 5.3 in citrate/Na_2SO_4 solutions shows an initial small increase as Na_2SO_4 is added, but then decreases with a further increase in ionic strength. The small initial increase in swelling is not predicted by the theory and could involve nonideal partitioning of the multivalent ions, or the ability of Cit^{-2} and of Cit^{-3} ions to provide electrostatic crosslinks in the gel which are eliminated as they exchange for SO_4^{-2}.

It should be noted that other accounts of nonmonotonic swelling as a function of ionic strength have been reported for ionic gels containing weak acid groups (8,12). The initial increase in swelling in these gels has been attributed to ion exchange between salt

cations in the solution with free hydronium ions in the gel, which in turn, leads to an increased ionization of the fixed carboxyl groups through proton mass action (8).

Figure 5.10 shows the correlation of Π_{ion} (computed with constant H) with the corresponding values of gel hydration for both the pH-dependent data of Figure 5.2 and the ionic strength dependent data of Figure 5.3. The correlation appears to be an approximately linear, monotonically increasing function and implies that this relationship exists regardless of the solutions conditions that were used to vary H. It should be pointed out that this correlation is only semi-quantitative because the magnitude of Π_{ion} will depend on the value of H (0.70) employed in the calculation of ρ^o and the value of the gel ionization constant K ($10^{-7.7}$).

5.5.2 Quantitative Predictions

A more stringent test of the Donnan theory in predicting the swelling behavior of the MMA/DMA gel is to incorporate the observed values of gel equilibrium hydration (H) in the computation of Π_{ion}. For a given set of conditions (pH, ionic strength, electrolyte solution), the measured value of gel hydration (H) for the MMA/DMA gel was used directly in the calculation of ρ^o_{net} using eqn. 5.10. Validity of the correlation will be evidenced if Π_{ion} turns out to be a monotonically increasing function of H, regardless of the conditions that determine the equilibrium hydration. Thus, an increase in H should correlate with an increase in the predicted value of Π_{ion}.

Figure 5.11 shows the resulting plot of Π_{ion} with the observed equilibrium gel hydration. A correlation is essentially nonexistent. The computed values of Π_{ion} appear to have little quantitative relationship with H. In the region of the highest gel hydration where the theory should be most valid, Π_{ion} decreases as H increases which is physically unrealistic.

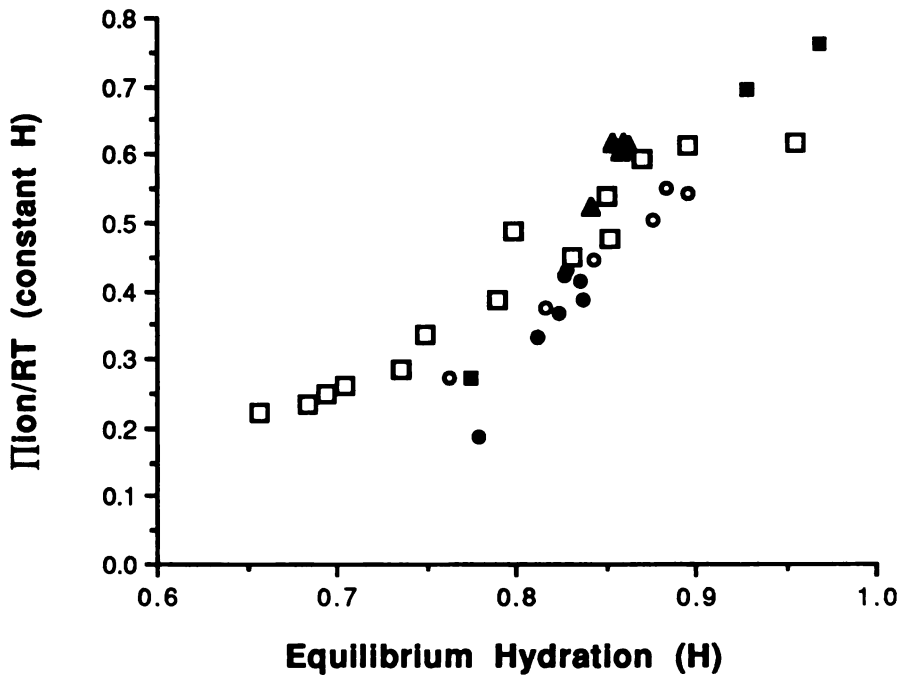

Figure 5.10. Computed Π_{ion} (constant H) as a function of observed equilibrium hydration for the pH and ionic strength dependent data presented in Figures 5.2 and 5.3. HCl/NaCl ionic strength data at pH 4.0 (■), 0.01 M citrate/NaCl ionic strength data at pH 4.0 (○), 0.01 M citrate/Na_2SO_4 ionic strength data at pH 4.0 (●), HCl/NaCl pH data (▲) and 0.01 M citrate/NaCl pH data (❑).

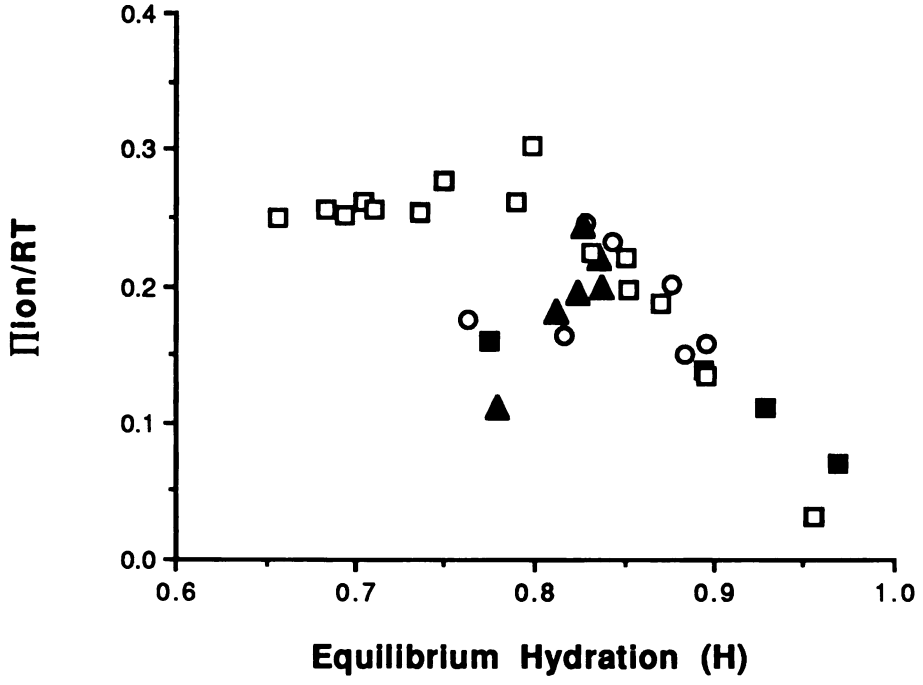

Figure 5.11. Computed Π_{ion} (based on observed values of membrane hydration H) as a function of observed equilibrium hydration for the pH and ionic strength dependent data presented in Figures 5.2 and 5.3. HCl/NaCl ionic strength data at pH 4.0 (■), 0.01 M citrate /NaCl ionic strength data at pH 4.0 (○), 0.01 M citrate/Na_2SO_4 ionic strength data at pH 4.0 (▲) and the pH data in 0.01 M citrate/NaCl and HCl/NaCl (□).

Ricka and Tanaka found the theory to be quantitatively consistent in predicting the swelling behavior of lightly ionized polyacrylamide gels in monovalent salt solutions (8). These gels hydrate much more extensively (30-100 fold greater) than the MMA/DMA gel studied here and contain approximately a six fold lower content of ionizable groups (5.2 mole% versus 30 mole%). It is apparent that conditions of applicability of the theory outlined in Subsection 5.2.3 apply to the case of swelling in the derivatized polyacrylamide gels, but are significantly violated in the MMA/DMA gel. Swelling in the present case is probably not extensive enough to invoke ideal solution behavior. For example, a gel swollen to a typical value of 80% water (H=0.80) will contain 20% polymer by weight. The dielectric constant of the gel interior, in such circumstances, will be lower than that of the external solution and will reduce the activities of the ions (they become less osmotically active) which will cause deviations from ideal Donnan partitioning. The exact magnitude of these effects has not been assessed.

Another difficulty that arises in applying the theory is knowing how the interior environment of the gel affects the ionization of weak electrolyte species such as the gel amine groups and all citrate species. Simple mass action laws were used to describe ionization processes which were each based on a single (invariant) equilibrium constant. This treatment neglects the changes in the ionization constants that arise due to dielectric effects of the gel internal phase, which will change as a function of gel hydration, the electrostatic interactions between charged groups that are known to affect ionization (10-12), and the fact that the pK's used apply to aqueous solutions under dilute conditions (water concentration of 55.5 M). It is expected that the ionization of weak electrolytes will be suppressed (decrease in K of the gel and an increase in the three K's of citrate) as gel swelling decreases, or as ρ_{net} increases reflecting the increased difficulty in ionizing these groups. Therefore, the simple mass action law as implemented is expected to cause ρ_{net} to be overestimated.

The invariance of gel swelling in the various chloride salts (Figure 5.4A) is in accordance with the Donnan Theory. Because the gels are swollen and ionized under the same conditions (pH 4.0 and I'=0.1 M), gel coions (cations of the chloride salts) are expected to be relatively (Donnan) excluded from the gel interior and thus should exert little impact on the ion swelling pressure and equilibrium swelling. Under these conditions, Π_{ion} is primarily determined by the gel counterion which, in the data of Figure 5.4A, is Cl^- in each case.

Gel swelling is strongly affected by the identity of the counterion (anions of the sodium salts) as shown in Figure 5.4B, which is not predicted by Donnan theory. Furthermore, these effects correlate strongly with the position of the anion in the Hofmeister or lyotropic series (20-21). This series identifies a certain "order of effectiveness" of ions that has been found to be remarkably similar in a wide variety of physical and chemical processes. Some of these include protein stability (22), swelling of gelatin (20) and collagen (23), adsorption in gels (24-25) and in the ion-selective permeabilities of hydrogels (26). The order of anions that has emerged is:

$$SCN^-, I^-, Br^-, NO_3^-, Cl^-, SO_4^{-2}$$

These salt effects are generally regarded as resulting from the water structure perturbing effects of the ions in solution (21). Relatively small ions and multivalent ions at the end of the series are thought to be water structure-makers (kosmotropes). They order and electrostrict surrounding water molecules through ion-dipole interactions to form long range hydration shells. Large monovalent ions at the beginning of the series are thought to be water structure-breakers (chaotropes) which generate relatively weak electrostatic fields capable of perturbing only nearest neighbor water molecules.

Recent studies have shown that the order of elution of anions from a crosslinked dextran gel correlated strongly with the lyotropic series, with the ions at the beginning of

the series eluting later than those at the end (27). This was interpreted as an indication of the degree to which a given ion adsorbed to the stationary gel phase; late elution indicating a greater tendency to adsorb, rather than a simple hydrated volume effect. In the present system, the adsorption of the chaotropes to the gel could explain the trend of decreasing equilibrium swelling, because adsorption or ion-pair formation will tend to reduce the activity of the ions and thus their contribution to Π_{ion}. It should be noted that the degree of swelling in sulfate solution is lower than that predicted by the lyotropic series. This can be at least partially explained by the Donnan theory since swelling in the presence of divalent counterions at I'=0.1 M produces a lower Π_{ion} (Figure 5.8) and thus swelling (Figure 5.3).

Despite numerous shortcomings of the Donnan theory in quantitatively predicting the swelling behavior of the MMA/DMA gel, it does a reasonably good job of qualitatively predicting trends in the swelling data and so provides useful insights in to the mechanisms that determine swelling in electrolyte solutions.

5.6 Conclusions

The swelling behavior of the MMA/DMA 70/30 mole% gel as a function of solution pH is principally determined by pH with significant but secondary contributions from the valences of ionic solutes. Multivalent ions tend to decrease swelling. As a function of ionic strength, swelling is strongly dependent on ion valence in dilute solutions while at higher concentrations it is determined primarily by the solution ionic strength. Gel coions have little effect on gel swelling while swelling is strongly dependent on the presence of different counterions which correlate with the Hofmeister series. The Donnan theory has been shown to be qualitatively successful in predicting many of the observed trends in the swelling data as functions of both pH and ionic strength. However, quantitatively the theory fails to provide meaningful predictions. It is felt that the assumptions and

simplifications inherent in the theory do not apply to the case of swelling in the MMA/DMA 70/30 mole% gel.

Appendix 5.A. Calculation of Counterion Distribution in Citrate Buffer Solutions.

Citric acid (H_3Cit) is a triprotic acid (pK_1 3.06, pK_2 4.74 and pK_3 6.40) which is capable of dissociating into three anionic species: H_2Cit^-, $HCit^{-2}$ and Cit^{-3}. The relative concentrations of the three anions will depend on the pH of the solution, and can readily be computed as follows. Let f_i be the fraction of citrate species existing as any given (i^{th}) form (H_3Cit, H_2Cit^-, $HCit^{-2}$ or Cit^{-3}). It can be shown that (14):

$$f_{Cit^{-1}} = \frac{K_1 [H^+]^2}{D}$$

$$f_{Cit^{-2}} = \frac{K_1 K_2 [H^+]}{D}$$

$$f_{Cit^{-3}} = \frac{K_1 K_2 K_3}{D}$$

and

$$f_{H_3Cit} = 1 - f_{Cit^{-1}} - f_{Cit^{-2}} - f_{Cit^{-3}}$$

where

$$D = [H^+]^3 + K_1 [H^+]^2 + K_1 K_2 [H^+] + K_1 K_2 K_3$$

For $K_1 = 10^{-3.06}$, $K_2 = 10^{-4.74}$, $K_3 = 10^{-6.40}$ and a solution pH of 4.0 , we have:

$f_{Cit^{-1}} = .771$ (or 77.1%)

$f_{Cit^{-2}} = .140$ (or 14.0%)

$f_{Cit^{-3}} = .00056$ (or 0.056%)

$f_{H_3Cit} = .088$ (or 8.8%)

References

1. F. Helfferich, "Ion Exchange", Chapter 5, McGraw-Hill, New York, 1962.

2. P.J. Flory, "Principles of Polymer Chemistry", Chapter XIII, Cornell University Press, 1953.

3. R.A. Siegel in "Self-Regulating and Pulsed Drug Delivery Systems", J. Kost, Ed., CRC Press, in press.

4. H.R. Proctor, The Equilirium of Dilute Hydrochloric Acid and Gelatin, J. Chem. Soc., 105, 313 (1914).

5. H.R. Proctor and J.A. Wilson, The Acid-Gelatin Equilibrium, J. Chem. Soc., 109, 307 (1916).

6. D. Vermaas and J.J. Hermans, The Swelling of Cellulose Xanthate Gels in Dilute Salt Solutions, Rec. Trav. Chim., 67, 983 (1948).

7. F.G. Donnan, Theory of Membrane Equilibria, Chem. Rev., 1, 73 (1925).

8. J. Ricka and T. Tanaka, Swelling of Ionic Gels: Quantitative Performance of the Donnan Theory, Macromolecules, 17, 2916 (1984).

9. S.H. Gehrke, G. P. Andrews and E. L. Cussler, Chemical Aspects of Gel Extraction, Chem. Eng. Sci., 41, 8, 2153 (1986).

10. A. Katchalsky, Polyelectrolyte Gels, Prog. Biophys., 4, 1 (1954).

11. A. Katchalsky and I. Michaeli, Polyelectrolyte Gels in Salt Solutions, J. Polym. Sci., 15, 69 (1955).

12. I. Michaeli and A. Katchalsky, Potentiometric Titration of Polyelectrolyte Gels, J. Polym. Sci., 23, 603 (1957).

13. A. Shatkay and I. Michaeli, Potentiometric Titration of Polyelectrolytes with Separation of Phases, J. Phys. Chem., 70, 3777 (1966).

14. A. Martin, J. Swarbrick and A. Cammarata, "Physical Pharmacy, Physical Chemical Principles in the Pharmaceutical Sciences", 3rd Ed., Chapter 9, Lea & Febiger, 1983.

15. J. Th.G. Overbeek, The Donnan Equilibrium, Prog. Biophys. Biophys. Chem., 6, 57 (1956).

16. E.A. Guggenheim, "Thermodynamics", 5th Ed., North-Holland, Amsterdam (1967).

17. J. Grignon and A.M. Scallan, Effects of pH and Neutral Salts Upon the Swelling of Cellulose Gels, J. Appl. Polym. Sci., 25, 2829 (1980).

18. B. Schwarz and R.A. Siegel, Calculation of Liquid-Liquid Phase Behavior for Ionic Polymers, submitted.

19. R.A. Siegel and B.A. Firestone, pH-Dependent Equilibrium Swelling Properties of Hydrophobic Polyelectrolyte Copolymer Gels, Macromolecules, 21, 3254 (1988).

20. F. Hofmeister, On the Understanding of the Effect of Salts, and, On Regularities in the Precipitating Effect of Salts and Their Relationship to Their Physiological Behavior, Arch. Exptl. Path. Pharmakol. (Leipzig), 24, 247 (1888).

21. K.D. Collins and M.W. Washabaugh, The Hofmeister Effect and the Behavior of Water at Interfaces, Q. Rev. Biophys., 18, 323 (1985).

22. K. Hamaguchi and E.P. Geiduschek, The Effect of Electrolytes on the Stability of the Deoxyribonucleate Helix, J. Am. Chem. Soc., 84, 1329 (1962).

23. H. Freundlich and P.S. Gordon, The Swelling Pressure of Isinglass in Water and Aqueous Solutions, Trans. Faraday Soc., 32, 1415 (1936).

24. E. Heymann, H.G. Bleakley and A.R. Docking, Studies on the Lyotropic Series. I. The Adsorption of Salts on Methylcellulose, J. Phys. Chem., 42, 353 (1938).

25. A.R. Docking and E. Heymann, Studies on the Lyotropic Series. II. The Adsorption of Salts on Gelatin, J. Phys. Chem., 43, 513 (1939).

26. C.J. Hamilton, S.M. Murphy, N.D. Atherton and B.J. Tighe, Synthetic Hydrogels: 4. The Permeability of Poly(2-Hydroxyethyl Methacrylate) to Cations - An Overview of Solute-Water Interactions and Transport Processes, 29, 1879 (1988).

27. M.W. Washabaugh and K.D. Collins, The Systematic Characterization by Aqueous Column Chromatography of Solutes Which Affect Protein Stability, J. Biolog. Chem., 261, 12477 (1986).

28. W.H. Press, B.P. Flannery, S.A. Teukolsky and W.T. Vetterling, "Numerical Recipes, The Art of Scientific Computing", Chapter 9, pg. 254, Cambridge Univ. Press, 1986.

Chapter 6.

Kinetics of Water Sorption and Swelling

6.1 Introduction

Small molecule sorption into polymeric materials is important in many processes. The penetration of polymeric films and coatings in packaging materials by oxygen, carbon dioxide and water vapor (1), oxygen permeability in hydrogel contact lenses (2,3), the separation of small molecular weight gases using glassy polymers (4), solvent swellable gels in solvent extraction and solute recovery processes (5-7) and swelling controlled drug delivery systems (8) are some examples. All involve the penetration of polymeric phases by small molecules and are driven by simple gradients in chemical potential of the penetrating species.

When an initially dry glassy polymer is placed in a solvent of good compatibility, sorption can lead to significant volume expansion or swelling in the polymeric phase. The presence of an appreciable concentration of solvent plasticizes the polymer and causes it to undergo a glass-to-rubber transition. During the process of dynamic sorption, a sharp boundary or moving front is commonly observed separating the unsolvated glassy polymer region ahead of the front from the swollen and rubbery gel phase behind it (9). The existence of moving fronts has been attributed to the slow chain relaxation processes in the glassy state induced by the plasticizing effect of the solvent (10). Concentration profiles of penetrants in glassy nonionic polymers undergoing dynamic sorption have been quantitated by birefringence measurements (11) and microdensitometry (12,13) which often show abrupt changes in penetrant concentration indicative of the swelling front.

When sorption is accompanied by a glass-to-rubber transition, the time-course of overall penetrant uptake often deviates from classical Fickian diffusion behavior even when a concentration-dependent diffusion coefficient is employed (14,15,17). In Fickian sorption, the initial uptake into polymeric slabs is proportional to $t^{1/2}$ and is commonly observed in small molecule sorption into polymers well above T_g (16). In glassy polymers, however, sorption is often proportional to t^n where the kinetic exponent n can take on values between 1/2 and 1.0. This non-Fickian or 'anomalous' sorption behavior is generally associated with the combined effects of inward penetrant diffusion and the slow polymer relaxation processes that occur in response to penetrant invasion at the swelling front (9,14,15). Sorption that is completely rate controlled by polymer relaxation is termed Case II transport as first defined by Alfrey, Gurnee and Lloyd (9), and is characterized by a kinetic exponent of unity indicating linear sorption kinetics.

Transport processes in gels become more complex when sorption of water is accompanied by ionization of the network. Mobile counterions must enter the gel from the external solution to preserve electroneutrality and will be influenced by the resulting membrane (Donnan) potential (see Chapter 5). Thus, diffusion of mobile ions is necessarily coupled to water sorption as the gel becomes hydrated and ionized. Furthermore, when the gel is initially glassy, polymer relaxation processes will also contribute to the dynamics of sorption as discussed above.

Although several reports have appeared concerning the effects of ions on the swelling equilibria and permeability of neutral and ionized gels (18-22), little is known about the dependence of sorption and swelling kinetics of ionic gels on diffusive transport of ions. Helfferich has discussed the effect of ion diffusion on the rates of certain ion exchange reactions (23,24). In particular, it was shown theoretically that the rate of ion diffusion can be dramatically slowed, and can even become rate-limiting for subsequent ion exchange, when the resin phase contains fixed ionized groups (24). This retardation effect

can arise by either the reversible binding and localization of diffusing ions to specific functional groups of the resin (diffusion-reaction), or the Donnan exclusion of coions from the swollen gel phase resulting in a reduced concentration gradient and thus diffusional driving force. Since the swelling process in glassy hydrophobic nAMA/DMA gels is driven by network ionization, it is expected that the processes of ion transport and polymer relaxation will be important in determining sorption kinetics in these gels.

In this chapter, the results of a series of comprehensive studies on the aqueous kinetic swelling properties of nAMA/DMA copolymer gels are presented. We will focus on three general aspects that are expected to affect the kinetics of water sorption in these ionic gels: 1) the effects of gel composition (comonomer ratio and nAMA sidechain length), 2) the external solution composition (pH, ionic strength and electrolyte composition) and 3) temperature. The underlying transport processes governing the observed kinetics of sorption and swelling will also be discussed.

6.2 Experimental

6.2.1 Materials

Sodium chloride, formic acid (88% solution), glacial acetic acid (Mallinckrodt, Inc.); sodium sulfate, propionic acid, butyric acid, valeric acid (pentanoic acid), hexanoic acid, acetamide, methyl acetate (Aldrich Chemical Co.), citric acid (Fisher Scientific) and n-hexane (Fisher Scientific) were analytical reagent grade or better and were used as received. Water used in all experiments was double distilled and deionized.

6.2.2 Gel Preparation

Gel samples were prepared as thin circular disks with a dry thickness of 0.28 ($\pm$ 0.02) mm and diameter 9 mm according to the method described in Chapter 3. For the

sample geometry studies, disks of thicknesses 0.27, 0.38 and 0.83 (+- 0.02) mm and diameter 7 mm were prepared.

6.2.3 Swelling Kinetic Experiments

Each swelling kinetic experiment was conducted in 2 liters of aqueous buffer solution at a specified pH and ionic strength, thermostated to constant temperature. The large solution volume assured that the solution composition (pH, ionic strength) would not change over the course of the sorption experiment due to ion absorption by the gel. All experiments were conducted at 25 °C unless otherwise indicated. In general, 0.01 M citrate buffer was used and NaCl was added to adjust the ionic strength to the desired level. Unbuffered solutions contained 0.1 M of the respective strong electrolyte at pH 4.0. Solutions of the n-carboxylic acids (formic, acetic, butyric, valeric and hexanoic) were prepared with the same conjugate base (A^-) concentration of 0.0012 M. Stirring was provided by a motorized stirring plate which rotated a magnetic stir bar (5.5 cm x 1 cm) placed at the bottom of the flask. The experimental set-up used in all swelling kinetic experiments is shown in Figure 6.1.

In each experiment, preweighed, initially dry gel disks in duplicate were suspended in a porous basket which was immersed in the buffer solution. The basket was easily removable to facilitate sampling of the disks. Periodically, the samples were removed from the solution and weighted after the excess surface water was removed by blotting with a laboratory tissue. The disks were then returned to the buffer solution. Solution pH was measured before and after every experiment and was found to be constant to within 0.03 pH unit in every case.

The extent of swelling for each sample disk at time t is expressed as the swelling ratio (SR):

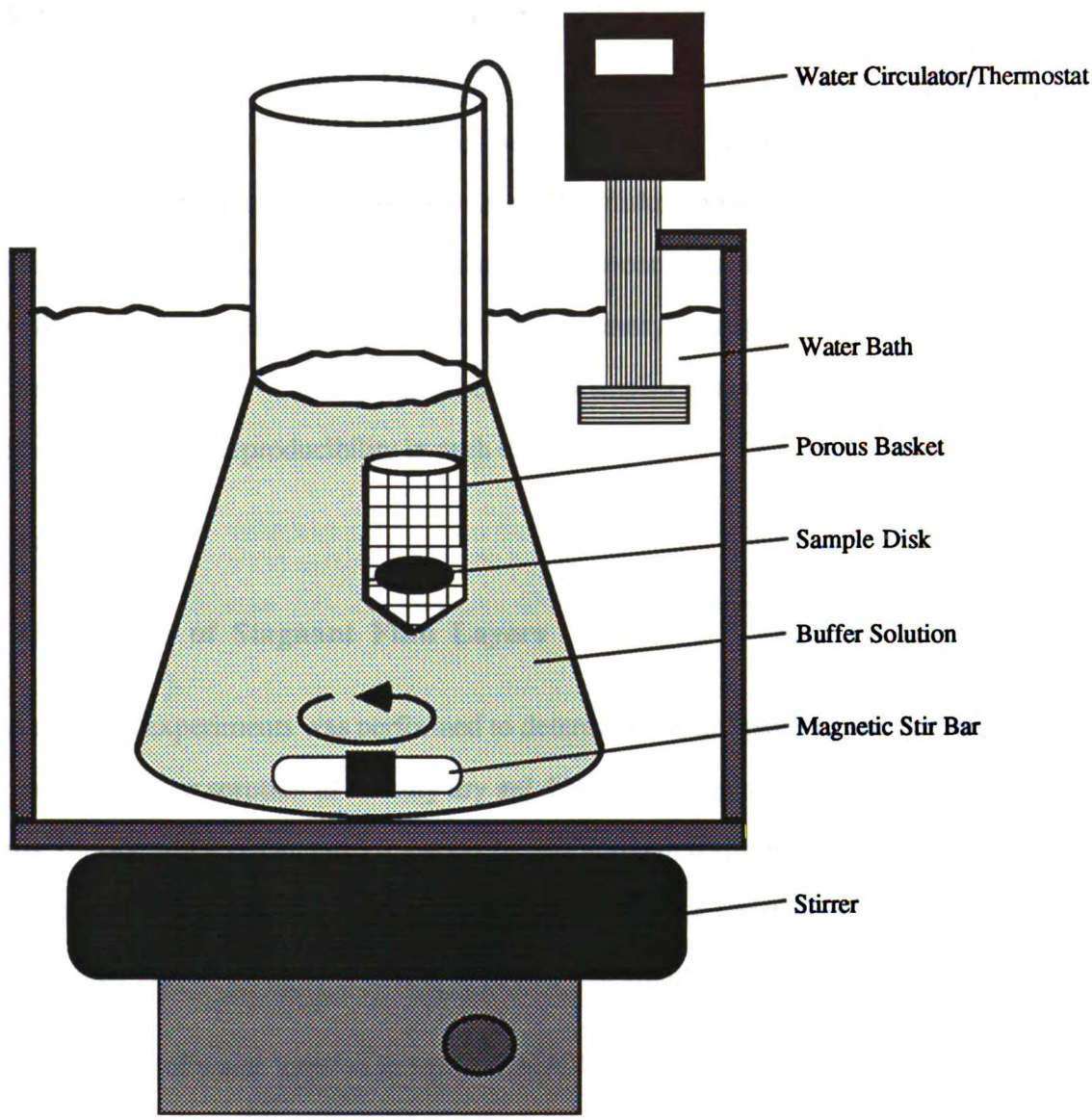

Figure 6.1. Experimental setup used for all swelling kinetic experiments.

$$SR(t) = \text{g water sorbed at time t / g dry gel} \qquad (6.2)$$

and is calculated as $(W_t-W_o) / W_o$ where W_t and W_o are the sample weights at time t and in the dry (initial) state, respectively. The swelling ratio expressed in this manner is the amount of water sorbed at any time normalized to the dry weight of the sample. This normalization eliminates the effect of surface area of the disks, and is useful when all samples have the same initial thickness. All data plots for each kinetic experiment show the mean swelling ratio for the duplicate samples with the corresponding standard error bars inserted for each time point. The error bars are usually smaller than the size of the symbols used indicating excellent reproducibility in each experiment.

6.3 Results

6.3.1 Elimination of Stagnant Film Layers

A series of experiments was performed to determine the influence of stirring speed on the kinetics of water sorption in initially dry gel disks. Unstirred or stagnant film layers on the disk surface add resistances to transport (e.g. of ions) in addition to those provided by the disk itself (23). It is therefore necessary to eliminate these resistances by maintaining 'well-stirred' conditions during each sorption experiment.

The kinetics of water sorption in MMA/DMA 70/30 disks (0.27 mm x 9 mm) were determined as a function of (constant) stirring rate at solution pHs of 3.0 and 4.0. Stagnant surface layers should be most pronounced under conditions of rapid water sorption. The MMA/DMA 70/30 mole% gel, which shows the most rapid sorption kinetics at any pH (results shown below), was thus used for these experiments. The stirring rate was set to a predetermined value as measured by a stroboscope tachometer, which measured the

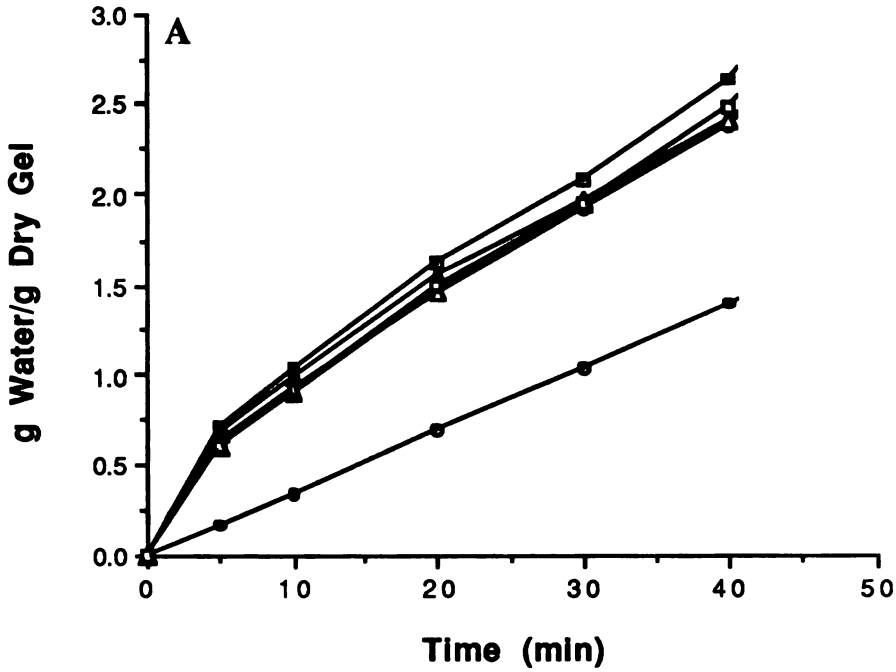

Figure 6.2 A. Effect of stirring rate on initial water sorption kinetics of the MMA/DMA 70/30 mole% gel at pH 3.0 at 25 °C. No stirring (●), 205 rpm (□), 230 rpm (○), 315 rpm (Δ), 430 rpm (■) and 600 rpm (▲).

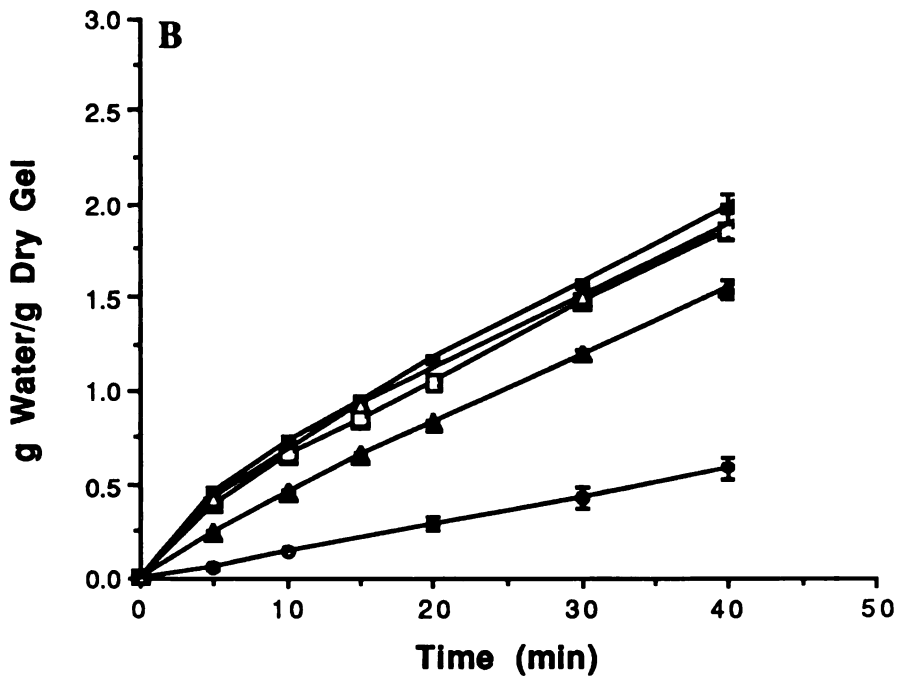

Figure 6.2 B. Effect of stirring rate on initial water sorption kinetics of the MMA/DMA 70/30 mole% gel at pH 4.0 at 25 °C. No stirring (●), 170 rpm (▲), 220 rpm (Δ), 390 rpm (□) and 525 rpm (■).

rotation speed (rpm) of the main shaft of the motorized stirring unit. The results of these experiments are shown in Figure 6.2 A and B.

Sorption kinetics under static conditions (no stirring) were significantly slower than under conditions of stirring at each pH. This indicates the influence of stagnant films. Furthermore, as the stirring rate is increased to speeds in excess of approximately 200 rpm, the sorption curves appear to converge into a single curve. This is interpreted as indicating the elimination of stagnant films. All subsequent sorption experiments were conducted with stirring speeds of 450 rpm or more to insure 'well-stirred' conditions.

6.3.2 Effect of Gel Composition

The effects of varying gel comonomer ratio and n-alkyl ester sidechain length on the aqueous sorption kinetics are shown in Figures 6.3 and 6.4, respectively. Several features of these sorption curves are apparent and are characteristic of water sorption in glassy nAMA/DMA gels (see below). The transient portion of each curve is generally biphasic, or sigmoidal, characterized by an initial phase of relatively slow water uptake followed by an accelerated phase observed just prior to the establishment of swelling equilibrium. Sorption kinetics for MMA/DMA gels of various comonomer ratios at a constant pH of 3.0 are presented in Figure 6.3. Gels containing 70/30, 78/22, 82/18 and 86/14 mole% MMA/DMA were prepared. The initial sorption rate decreases sharply as the content of the hydrophobic comonomer (MMA) increases. The 70/30 mole% gel has an initial sorption phase duration of about 1 hr., the 78/22 gel 2 hrs. and the 82/18 gel a duration of about 3.5 hrs. The 86/14 gel has a very slow sorption rate which was still in progress after 6 hrs. The final swelling equilibrium greatly decreases as MMA content increases, as was discussed in Chapter 4.

The effect of the n-alkyl ester sidechain length of the nAMA comonomer on sorption kinetics at a constant pH of 3.0 is presented in Figure 6.4. The gels used in this

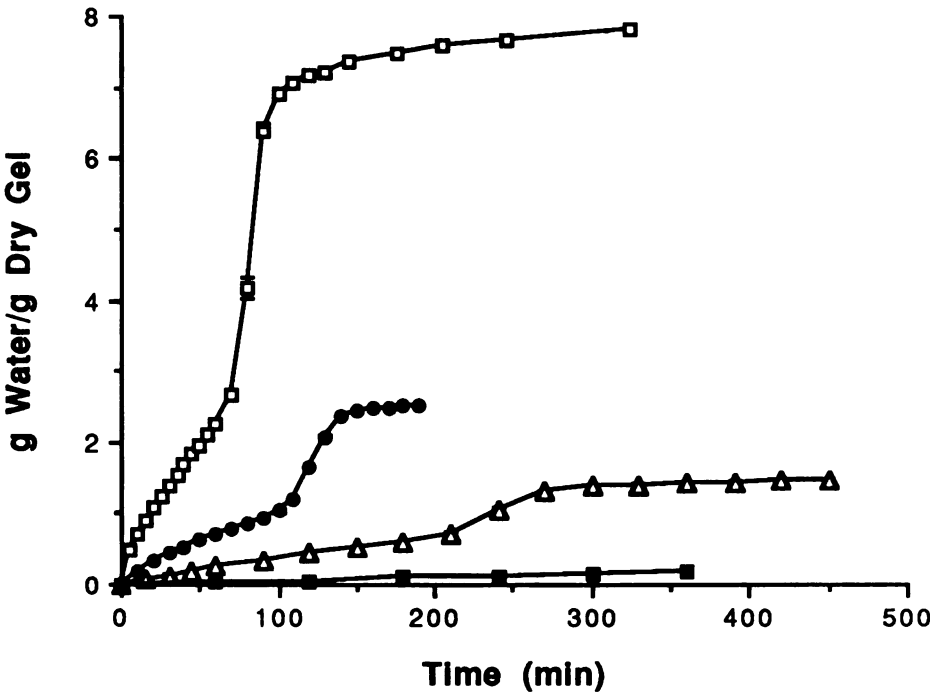

Figure 6.3. Effect of comonomer ratio on the swelling kinetics of MMA/DMA gels in 0.01 M citrate buffer at pH 3.0, I'=0.1 M and 25 °C. 70/30 mole% (❑), 78/22 mole% (●), 82/18 mole% (Δ) and 86/14 mole% (■).

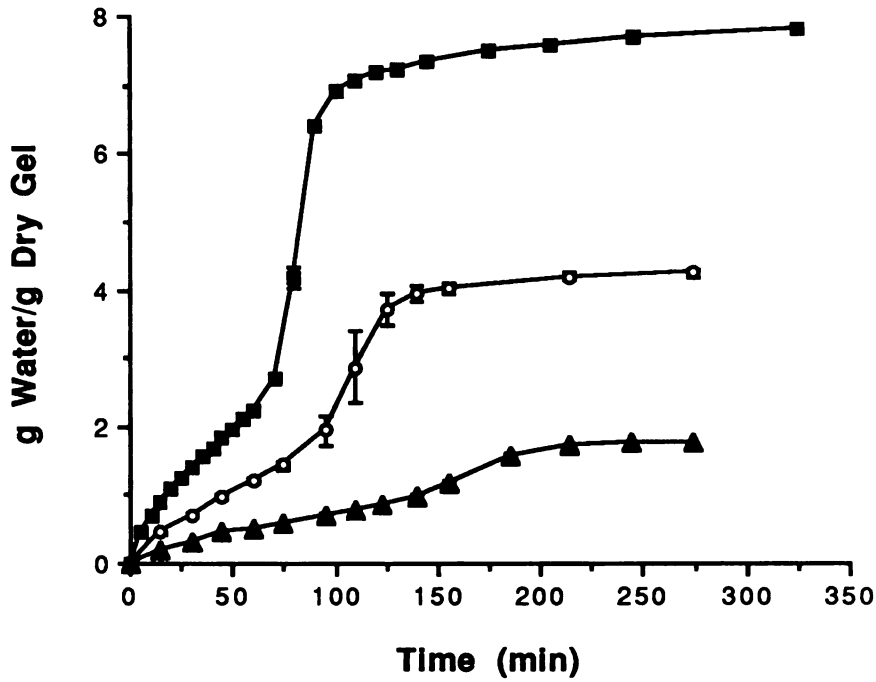

Figure 6.4. Effect of n-alkyl ester sidechain length on the swelling kinetics of nAMA/DMA gels in 0.01 M citrate buffer at pH 3.0, I'=0.1 M and 25 °C. MMA/DMA-C_1 (■), EMA/DMA-C_2 (○) and PMA/DMA-C_3 (▲). All gels had a constant comonomer ratio of 70/30 mole%.

experiment all had nAMA/DMA comonomer ratios of 70/30 mole% and differed only in the sidechain length of the nAMA comonomer. Shown are the sorption curves for gels with nAMA sidechain lengths of C_1 (MMA/DMA), C_2 (EMA/DMA) and C_3 (PMA/DMA). The initial sorption rate is observed to dramatically decrease as nAMA sidechain length increases. The initial phase of sorption is prolonged as both the initial rate and the final extent of swelling decrease.

6.3.3 Effect of Sample Thickness

In order to determine the effect of sample disk geometry on the observed biphasic kinetic sorption profiles, sorption profiles of MMA/DMA 70/30 mole% gel disks prepared in three different thicknesses (0.27, 0.38 and 0.83 mm) and constant diameter (7 mm) were measured at pH 5.0 and 25 °C. The results are presented in Figure 6.5. To account for the contribution of different disk geometries, the sorption data have been normalized by the initial surface area of each disk. Sorption is thus expressed as: g water/mm^2 original surface area. Figure 6.5 indicates that the normalized sorption rates are identical and that the duration of the initial phase increases in approximate proportion to the initial disk thickness: onset of the accelerated phase being earliest for the 0.27 mm disk and most delayed for the 0.83 mm disk.

6.3.4 pH Dependence

The influence of solution pH on the water sorption kinetics of the MMA/DMA 70/30 mole% gel is shown in Figure 6.6 in which the swelling ratio (g water/g dry gel) is plotted as a function of time. The rate of water uptake during the initial sorption phase is highly pH-dependent. As pH is reduced, the rate of initial sorption, which is essentially zero at pH 7.0, sharply increases. At pH 5.0 swelling equilibrium is achieved in about 3

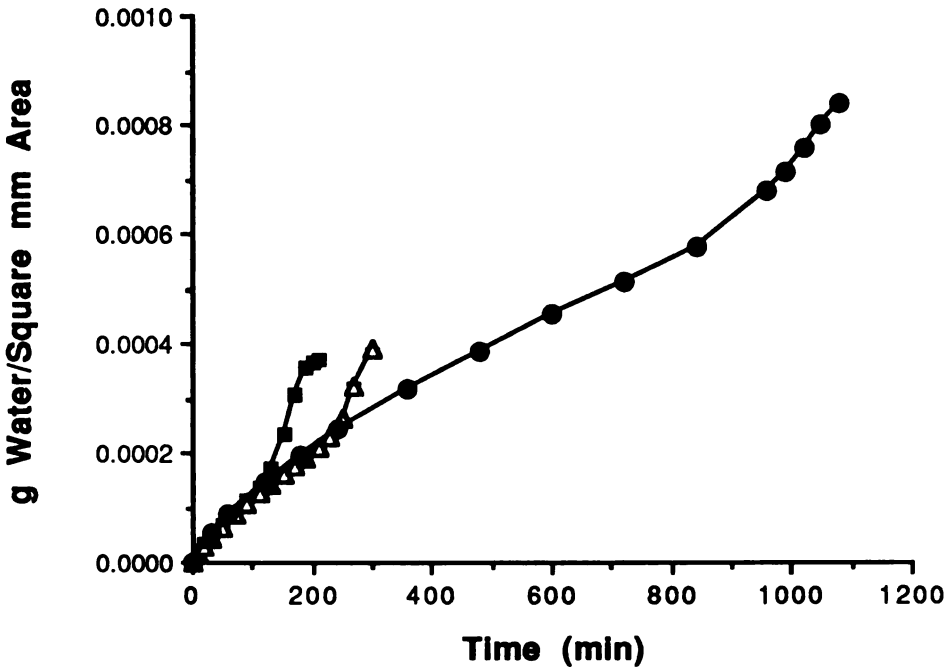

Figure 6.5. Effect of disk thickness on the swelling kinetic profile of the MMA/DMA 70/30 mole% gel in 0.01 M citrate buffer at pH 5.0, I'=0.1 M and 25 °C. Disk thicknesses are 0.27 mm (■), 0.38 mm (Δ) and 0.83 mm (●).

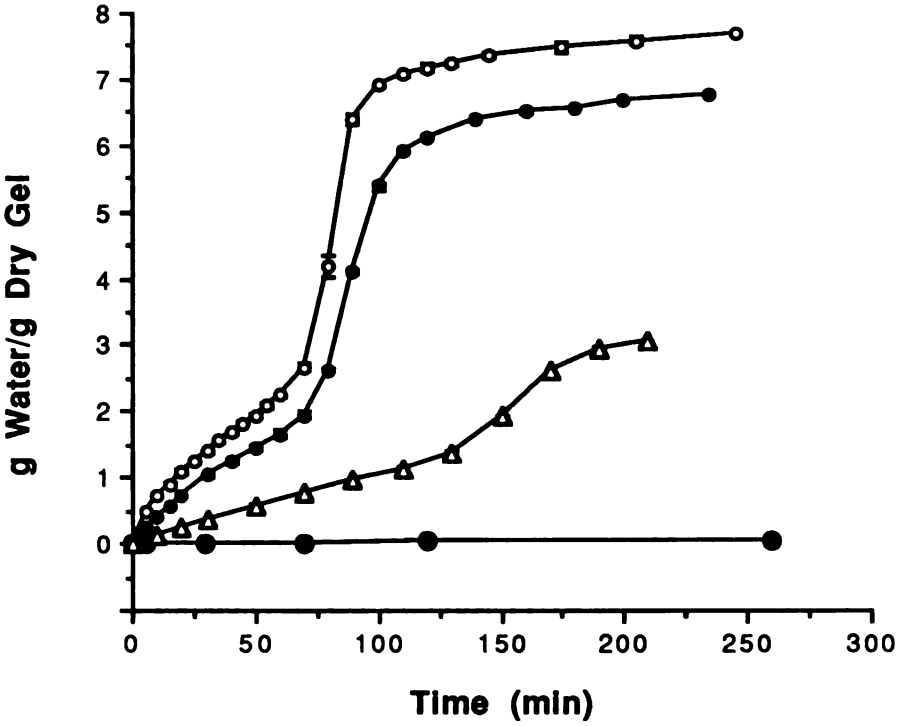

Figure 6.6. Effect of solution pH on the swelling kinetics of the MMA/DMA 70/30 mole% gel in 0.01 M citrate buffer at I'=0.1 M and 25 °C. pH 3.0 (○), pH 4.0 (●), pH 5.0 (Δ) and pH 7.0 (●).

hrs. while at pH 3.0 it is reached in about 90 min. In addition, the duration of the initial sorption phase decreases with a reduction in pH.

6.3.5 Temperature Dependence

The sorption kinetics of the 70/30 mole% MMA/DMA and BMA/DMA gels at pH 4.0 measured as a function of temperature are presented in Figures 6.7 and 6.8, respectively. Sorption kinetics for each gel were measured at six temperatures between 10 and 60 °C, inclusive. All solution pHs were measured at the temperature of the experiment and were calibrated with respect to standard buffers at the same temperature.

Whereas both copolymers have initial water sorption rates that increase significantly with temperature, it is evident that the general sorption profiles for the BMA/DMA gel (Figure 6.8) differ markedly from those of Figures 6.3, 6.4, 6.6 and 6.7. The characteristic biphasic sorption behavior exhibited by the glassy gels with shorter sidechains (MMA/DMA, EMA/DMA and PMA/DMA at all comonomer ratios) is conspicuously absent from the BMA/DMA sorption profiles. These curves have initial sorption phases that extend out to 70-80% of the equilibrium value without showing any rate acceleration. It is significant to note that the BMA/DMA 70/30 gel has the lowest glass temperature (31.1 °C, (Chapter 4)) of all the gels studied here which is near or below all of the experimental temperatures investigated in this study. In spite of these differences, the initial sorption rate increases significantly with temperature. For example, the duration of the initial sorption phase for the MMA/DMA gel is approximately 2 hrs. at 10 °C but decreases to 30 min. at 60 °C. The accompanying equilibrium swelling ratio increases from 5.0 at 10 °C to in excess of 8.0 at 60 °C. The trends for the temperature dependence of the sorption curves of the BMA/DMA gel are qualitatively similar to those of MMA/DMA in both sorption rate and extent, though the swelling curves for BMA/DMA are monophasic, and the swelling ratios are significantly lower than those for MMA/DMA.

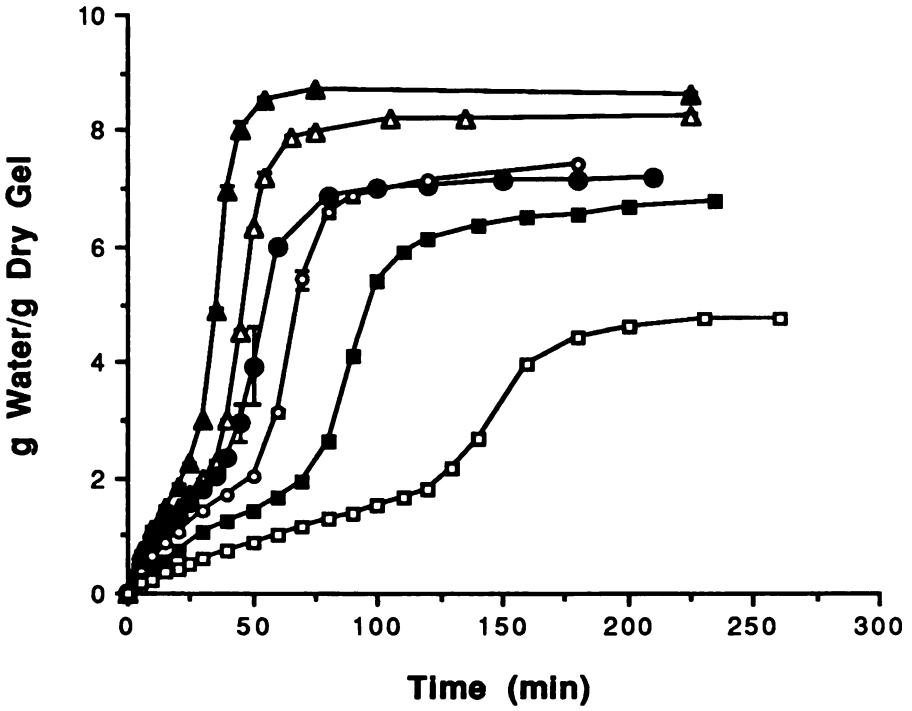

Figure 6.7. Temperature dependence of the swelling kinetics of the MMA/DMA 70/30 mole% gel in 0.01 M citrate buffer at pH 4.0 and I'=0.1 M. 10 °C (□), 25 °C (■), 35 °C (○), 42 °C (●), 50 °C (Δ) and 60 °C (▲).

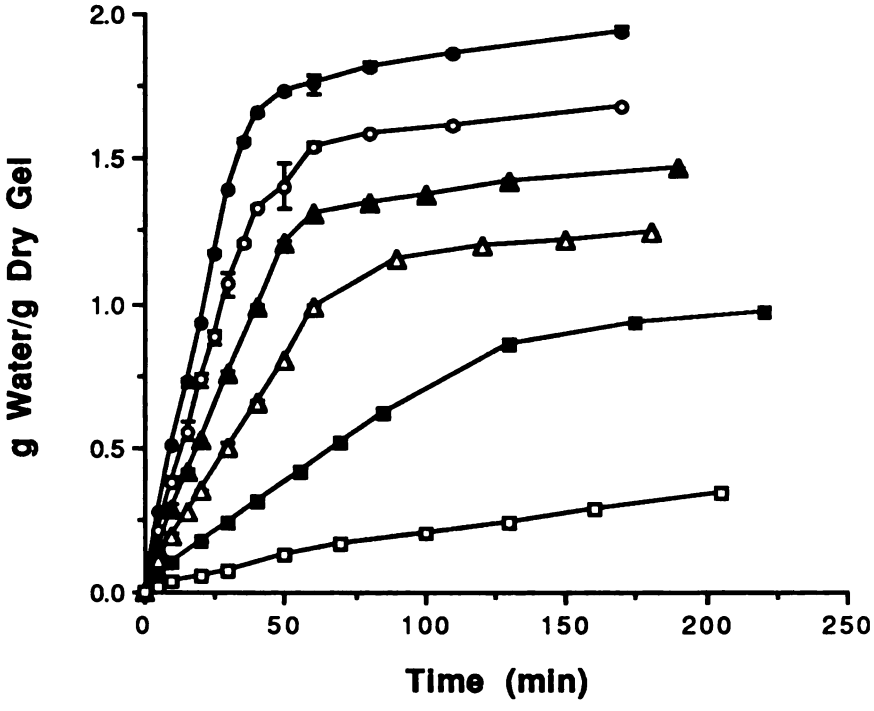

Figure 6.8. Temperature dependence of the swelling kinetics of the BMA/DMA 70/30 mole% gel in 0.01 M citrate buffer at pH 4.0 and Γ=0.1 M. 10 °C (❑), 25 °C (■), 35 °C (Δ), 42 °C (▲), 50 °C (○) and 60 °C (●).

6.3.6 Ionic Strength Dependence

The effects of solution ionic strength (Γ) on water sorption kinetics in the MMA/DMA 70/30 gel in both buffered citrate and dilute HCl solutions at a constant pH of 4.0 are shown in Figures 6.9 and 6.10, respectively. The solutions contained added NaCl to adjust the ionic strength to the desired level. Figure 6.9 indicates that the initial rate of water sorption is a nonmonotonic function of solution ionic strength in buffered citrate solutions. Sorption rate increases with ionic strength up to Γ=0.056 M but then decreases as Γ is increased further. This nonmonotonicity closely parallels or 'tracks' the observed equilibrium swelling ratio (indicated as asymptotes for each curve in Figure 6.9) over this range of ionic strength. The basis for the nonmonotonic behavior of the equilibrium swelling ratio versus ionic strength has been discussed in Chapter 5. It is interesting to observe that although the initial sorption rates and final equilibria are similar in Γ=0.013 M and 0.306 M solutions, the acceleration point is reached considerably earlier at the lower ionic strength.

Similar nonmonotonic sorption behavior is observed in NaCl solutions (no citrate) as a function of Γ as shown in Figure 6.10. However, two important differences are noted in comparing the sorption data of Figure 6.10 with that of Figure 6.9. First, sorption kinetics are significantly slower in NaCl solutions than in citrate/NaCl solutions at the same pH and ionic strength. This suggests that the rate and mechanism of sorption depends strongly on the identity of the involved ions. This will be investigated further in Subsection 6.3.8. Second, the nonmonotonicity in sorption rate in NaCl solutions does not correlate with the final swelling ratio which monotonically decreases over this range in Γ, as indicated in Table 6.1. At present we have no explanation for this phenomenon.

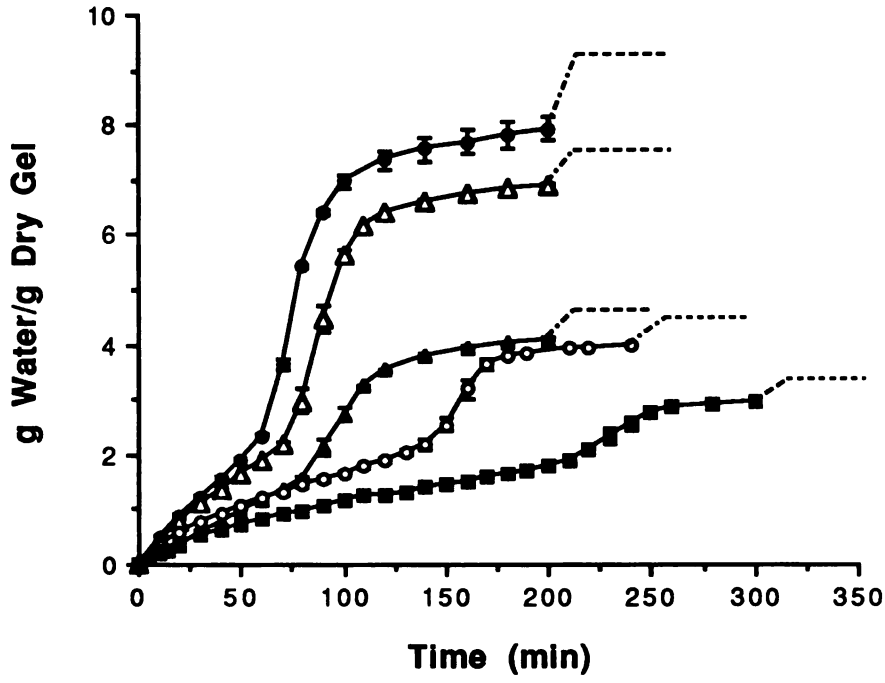

Figure 6.9. Effect of solution ionic strength (I') on the swelling kinetics of the MMA/DMA 70/30 mole% gel at pH 4.0 and 25 °C in 0.01 M citrate buffer. NaCl was added to adjust the ionic strength to the final level. I'=0.013 M (no added NaCl) (▲), I'=0.056 M (●), I'=0.106 M (Δ), I'=0.306 M (○) and I'=0.506 M (■). Dashed lines indicate final swelling equilibria.

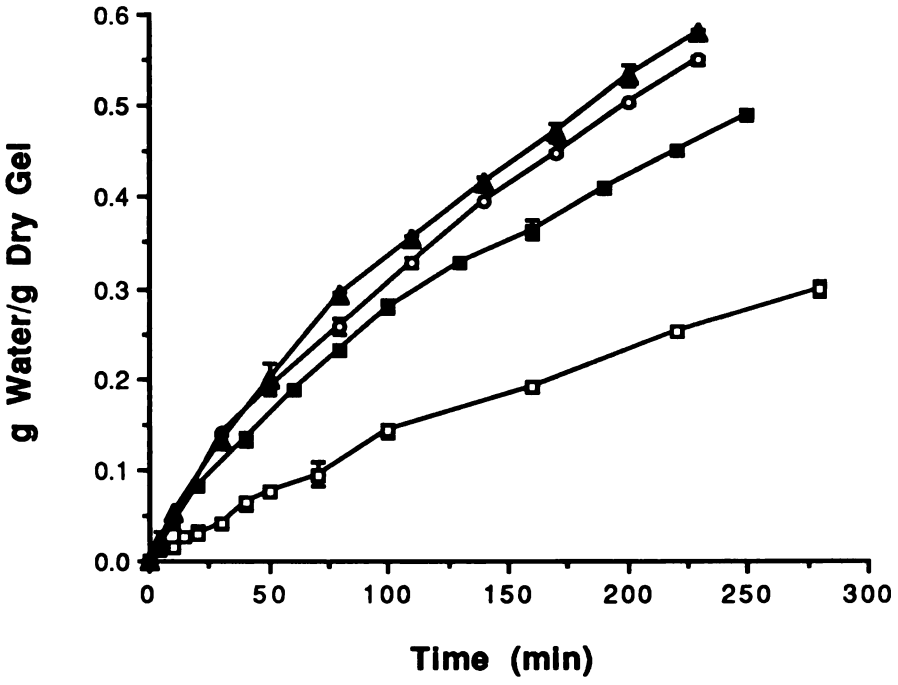

Figure 6.10. Effect of solution ionic strength (I') on the swelling kinetics of the MMA/DMA 70/30 mole% gel at pH 4.0 and 25 °C in dilute HCl solution. NaCl was added to adjust the ionic strength to the final level. I'=0.0064 M (□), I'=0.05 M (○), I'=0.10 M (▲) and I'=0.50 M (■).

Table 6.1. Equilibrium Swelling Ratio and Ordinal Swelling Rates of the MMA/DMA 70/30 Gel in NaCl solution as a Function of Solution Ionic Strength at pH 4.0.

Γ (M)	Equilibrium Swelling Ratio (g water/g dry gel)	Rank Order of Initial Sorption Rate
0.0064	27.6	4 (slowest)
0.05	13.8	2
0.10	8.1	1 (fastest)
0.50	3.3	3

6.3.7 Analysis of Kinetic Exponents

In order to obtain a more quantitative understanding of the nature of the sorption kinetics in nAMA/DMA gels, the initial phase sorption data of each experiment were fit by a rate equation of the form;

$$SR(t) = k\, t^{n} \qquad (6.1)$$

where SR(t) is the measured sample swelling ratio at time t, k is the swelling rate constant and n is the kinetic exponent. Eqn. 6.1 is a phenomenological rate law, where the kinetic exponent n provides insight into the type of sorption mechanism that is operative. For example, for Fickian kinetics in which the rate of penetrant diffusion is rate-limiting, n=0.5, whereas values of n between 0.5 and 1.0 indicate the contribution of non-Fickian processes such as polymer relaxation. Values of n were obtained by plotting ln(SR) versus ln(t) for data points up to the sorption inflection, and computing the linear regression coefficients. The exponent n was obtained as the slope of the resulting regression line. The 95% confidence limits for n were also computed. Figure 6.11 shows a log/log plot of

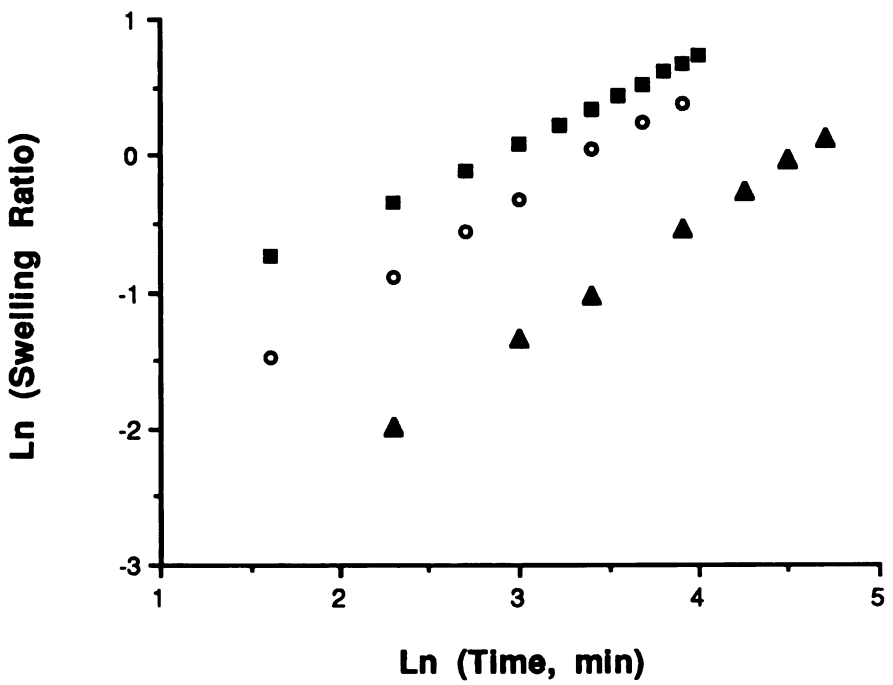

Figure 6.11. Example of a typical log-log plot of the initial swelling kinetic data used to compute the kinetic exponent n from eqn. 6.1. The exponent n is obtained as the slope of each line. Data are for the MMA/DMA 70/30 mole% gel at pH 3.0 (■), pH 4.0 (○) and pH 5.0 (▲) in 0.01 M citrate buffer at 25 °C and I'=0.1 M.

the initial sorption data for the MMA/DMA 70/30 mole% gel at pHs of 3.0, 4.0 and 5.0 (data from Figure 6.6).

The resulting values of the kinetic exponent n in 0.01 M citrate buffer are tabulated in Tables 6.2 through 6.4 as functions of nAMA/DMA comonomer ratio, n-alkyl ester sidechain length and pH, respectively. The data of Tables 6.2-6.4 indicate that the initial phase water sorption kinetics are generally non-Fickian. Furthermore, sorption appears to approach Case II behavior (n increases towards unity) as the solution pH is increased or the hydrophobic (MMA) comonomer content increases. In each case, n increases as final swelling decreases which corresponds to a decrease in solution/gel compatibility. The effect of n-alkyl ester sidechain length appears not to have a systematic effect on the kinetic exponent (Table 6.4) although final swelling sharply decreases as sidechain length increases.

The temperature dependence of the kinetic exponent n for the 70/30 MMA/DMA gels in 0.01 M citrate buffer at pH 4.0 are indicated in Figure 6.12. In the case of the MMA/DMA sorption, n decreases monotonically with temperature indicating that water sorption becomes increasingly Fickian at elevated temperatures. The values of n for the BMA/DMA gel shows the opposite temperature dependence with n increasing and approaching Case II sorption behavior as temperature increases. This behavior for the BMA/DMA gel is noteworthy, since the T_g of the dry gel is 31 °C. A contrast can be drawn with nonionized gels which, at temperatures above T_g, display Fickian sorption kinetics.

Sorption kinetics of the BMA/DMA gel were also measured in n-hexane at various temperatures in order to see whether Fickian behavior would be observed when sorption proceeds in the absence of gel ionization. Figure 6.13 shows the resulting sorption profiles in n-hexane at 25, 35 and 45 °C while the corresponding values of n are indicated in Figure

Table 6.2. Effect of Comonomer Ratio on the Kinetic Exponent n in 0.01 M Citrate Buffer.

Gel	Composition (mole%)	pH	n (± 95%CI)
MMA/DMA	70/30	3.0	0.616 (± 0.014)
MMA/DMA	78/22	3.0	0.708 (± 0.012)
MMA/DMA	82/18	3.0	0.865 (± 0.021)
MMA/DMA	86/14	3.0	1.220 (± 0.133)
MMA/DMA	70/30	4.0	0.814 (± 0.037)
MMA/DMA	78/22	4.0	0.881 (± 0.025)
MMA/DMA	82/18	4.0	0.994 (± 0.051)

Table 6.3. Effect of n-Alkyl Sidechain Length on the Kinetic Exponent n in 0.01 M Citrate Buffer.

Gel	Composition (mole%)	pH	Chain Length	n (± 95%CI)
MMA/DMA	70/30	3.0	1	0.616 (± 0.014)
EMA/DMA	70/30	3.0	2	0.716 (± 0.036)
PMA/DMA	70/30	3.0	3	0.661 (± 0.060)
MMA/DMA	70/30	4.0	1	0.814 (± 0.037)
EMA/DMA	70/30	4.0	2	0.816 (± 0.030)
PMA/DMA	70/30	4.0	3	0.864 (± 0.099)
BMA/DMA	70/30	4.0	4	0.801 (± 0.037)

Table 6.4. Effect of Solution pH on the Kinetic Exponent n in 0.01 M Citrate Buffer.

Gel	Composition (mole%)	pH	n (± 95%CI)
MMA/DMA	70/30	3.0	0.616 (± 0.014)
MMA/DMA	70/30	4.0	0.814 (± 0.037)
MMA/DMA	70/30	5.0	0.883 (± 0.023)
MMA/DMA	78/22	3.0	0.708 (± 0.012)
MMA/DMA	78/22	4.0	0.881 (± 0.025)
MMA/DMA	82/18	3.0	0.865 (± 0.021)
MMA/DMA	82/18	4.0	0.994 (± 0.051)
EMA/DMA	70/30	3.0	0.716 (± 0.036)
EMA/DMA	70/30	4.0	0.816 (± 0.030)
EMA/DMA	70/30	4.5	0.837 (± 0.055)
EMA/DMA	70/30	5.0	1.020 (± 0.059)
PMA/DMA	70/30	3.0	0.661 (± 0.060)
PMA/DMA	70/30	4.0	0.864 (± 0.099)
PMA/DMA	70/30	4.5	0.939 (± 0.064)

6.12. The values of n for n-hexane sorption in the BMA/DMA gel appear to be fairly invariant over this temperature range and are reasonably close to 0.5 indicating a predominantly Fickian sorption mechanism. It should be noted that the exponents appear to be consistently above 0.5, but the deviation is small.

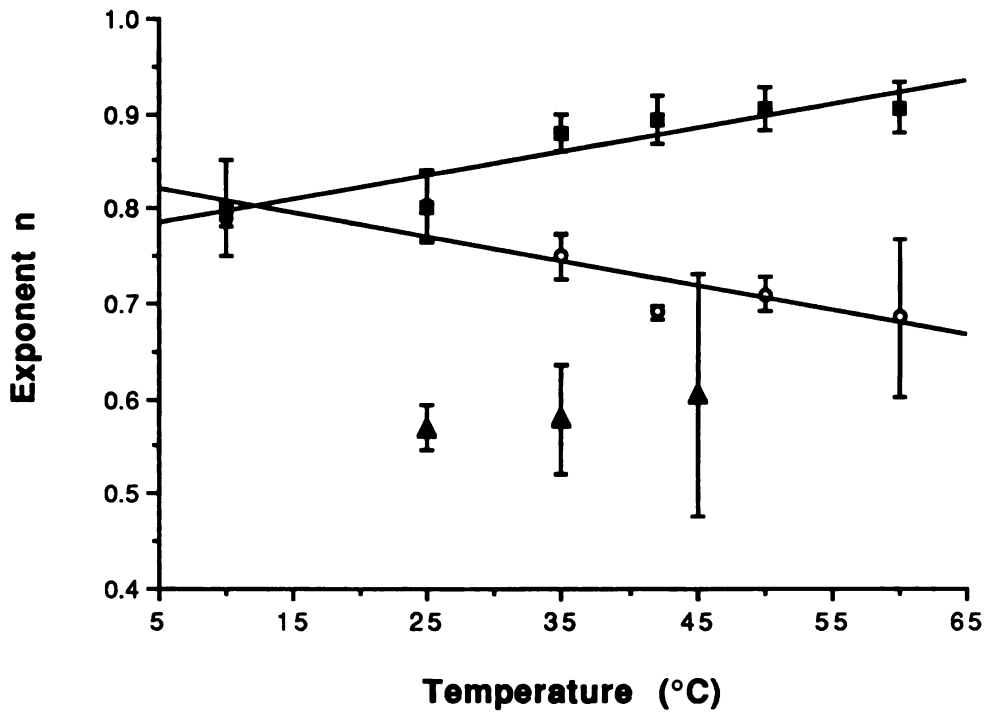

Figure 6.12. Temperature dependence of the kinetic exponent n for the MMA/DMA 70/30 mole% gel in 0.01 M citrate buffer at pH 4.0 (○), BMA/DMA 70/30 mole% gel in 0.01 M citrate buffer at pH 4.0 (■) and for the BMA/DMA 70/30 mole% gel in n-hexane (▲).

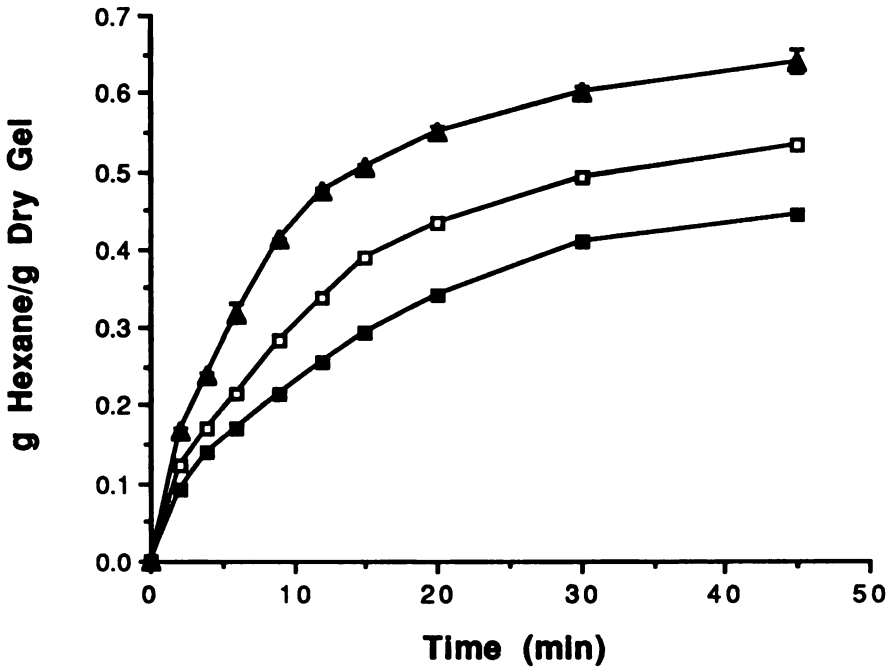

Figure 6.13. Swelling kinetics of the BMA/DMA 70/30 mole% gel in n-hexane at 25 °C (■), 35 °C (❑) and 45 °C (▲).

6.3.8 Effect of Solution Electrolyte Composition

The data presented in Figures 6.9 and 6.10 indicate that the kinetics of water sorption are strongly influenced by the specific ions in solution and are not simply determined by solution pH and ionic strength alone. In an effort to elucidate the basis for these ionic effects, additional sorption data were obtained in solutions of various chemical compositions including: nonionic compounds structurally related to buffer ions employed, a homologous series of n-alkyl carboxylic acids and a series of strong electrolyte sodium salts.

The first mechanism considered for the rate enhancement observed in buffered solutions was the organic structure of buffer species employed. Organic anions, in addition to serving as gel counterions, may be capable of specific (hydrophobic) interactions with the network chains that could result in a plasticization effect. This mechanism was tested by two experimental approaches. The first involved measuring sorption kinetics in an acetate buffer and then in unbuffered aqueous solutions containing equimolar neutral compounds structurally related to acetic acid. The neutral compounds tested were methyl acetate and acetamide, the structures of which are indicated in Figure 6.14. If a plasticization mechanism is involved, then neutral, structurally related

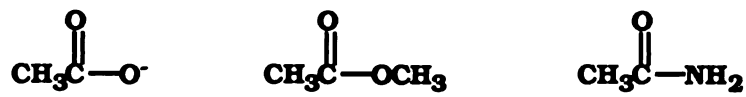

acetate ion methyl acetate acetamide

Figure 6.14. Structures of acetate ion and the two structurally related nonionic compounds methyl acetate and acetamide.

compounds could produce the same effect. The second experiment involved the effect of aqueous solutions containing a series of n-alkyl carboxylic acids of increasing chain

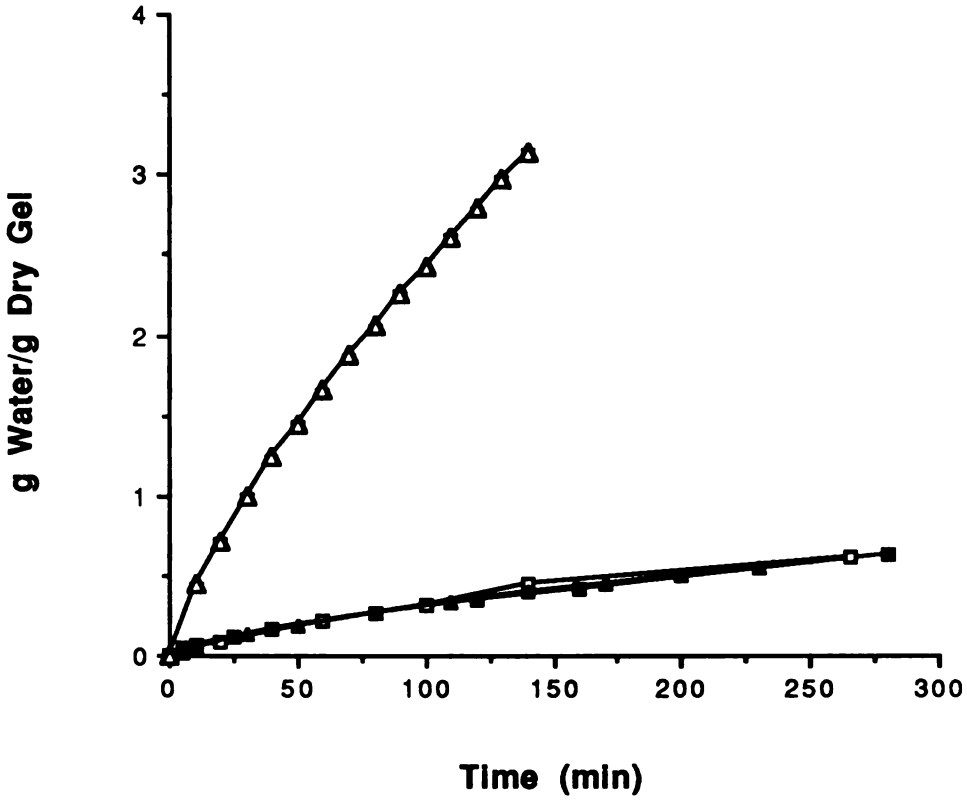

Figure 6.15. Effect of nonionic additives on the swelling kinetics of the MMA/DMA 70/30 mole% gel at pH 4.0, Γ=0.1 M and 25 °C. 0.01 M acetate buffer (Δ), 0.01 M acetamide (■), 0.01 M methyl acetate (❑) and dilute HCl (▲).

lengths. If the counterion interacts with the gel via its organic backbone, then the sorption rate should increase with carboxylate chain length since more hydrophobic contacts can be made per molecule of acid.

Sorption in the presence of 0.01 M acetate buffer, unbuffered methyl acetate (0.01 M) and acetamide (0.01 M) solutions at pH 4.0 and I'=0.05 M (NaCl) are shown in Figure 6.15. As a comparison, the sorption curve in NaCl (pH 4.0, I'=0.05 M) from Figure 6.10 is also included. The nonionic compounds have no effect on the sorption rate, which is similar in both cases to that in NaCl solution alone. Sorption in acetate buffer, however, is clearly faster and comparable to that in 0.01 M citrate buffer at pH 4.0 (Figure 6.9).

Aqueous solutions of n-alkyl carboxylic acids were prepared with equimolar conjugate base [A^-] concentrations of 0.0012 M (no corrections for activity coefficients were made). This was done to normalize the counterion concentration across acids of various pK_a values. The results, shown in Figure 6.16, indicate that sorption rate

Table 6.5. Equilibrium Swelling of the MMA/DMA 70/30 Gel in n-Alkyl Carboxylic Acid Solutions at pH 4.0.

Carboxylic Acid	pK_a	Equilibrium Swelling Ratio (g water/g dry gel ± SD)
Formate (C1)	3.75	not determined [a]
Acetate (C2)	4.76	30.5 (± 0.2)
Butyrate (C4)	4.82	29.5 (± 0.3)
Valerate (C5)	4.86	27.5 (± 0.2)
Hexanoate (C6)	4.80	20.5 (± 0.3)

[a] Equilibrium swelling could not be determined due to an unstable solution pH.

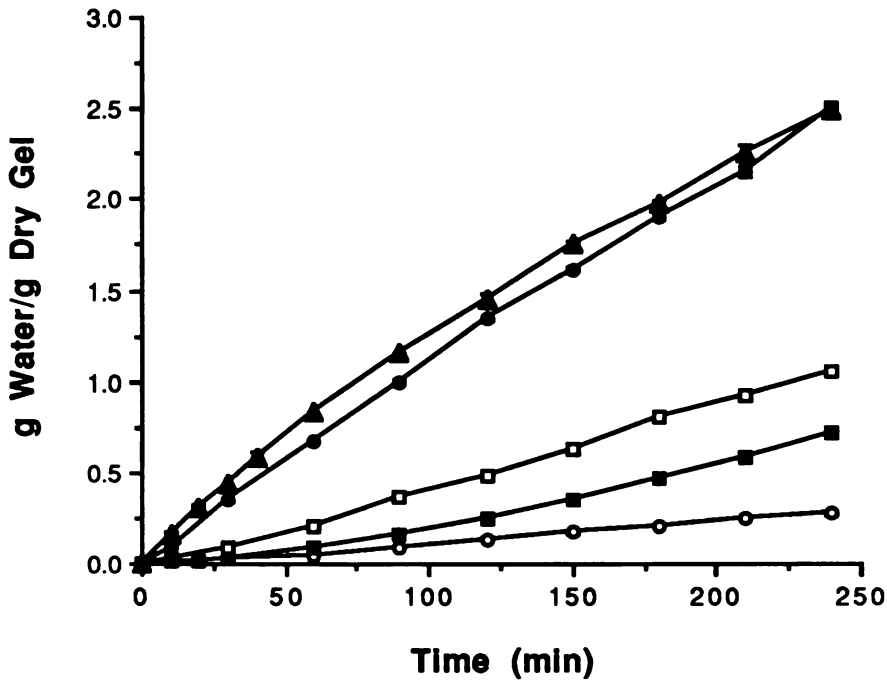

Figure 6.16. Swelling kinetics of the MMA/DMA 70/30 mole% gel in the presence on n-alkyl carboxylic acids of various chain lengths at pH 4.0 and an equivalent conjugate base concentration of 0.0012 M. Formate-C1 (○), acetate-C2 (■), butyrate-C4 (□), valerate-C5 (●) and hexanoate-C6 (▲).

systematically increases with increasing chain length of the carboxylate anion. These data suggest that gel counterions with appreciable hydrophobic character are able to interact with the gel and accelerate the rate of water sorption. In addition, as shown in Table 6.5, the final swelling equilibria in the presence of these acids decreases with increasing acid chain length, and are significantly greater than in citrate buffer solution at the same pH and ionic strength as reported in Chapter 4.

6.4 Discussion

It is well known that penetrant sorption in glassy nonionic gels often exhibits non-Fickian or anomalous kinetics when significant swelling of the polymeric phase occurs (9-17). Deviation from Fickian behavior is attributed to the contribution of network chain relaxation processes that are induced by the plasticizing effect of the penetrant (9,14,15). Thus, the overall rate of penetrant sorption in nonionic glassy gels is generally controlled by two processes: polymer chain relaxation and the inward diffusion of penetrant from the solution. In glassy gels that are both ionizable and hydrophobic, the processes that control water sorption kinetics are more complex than those of neutral, hydrophilic glassy gels. In the former case, there are four coupled transport/reaction processes that can contribute to the overall rate and mechanism of water sorption: 1) water diffusion into the hydrating gel, 2) diffusion of mobile ions, 3) ionization of the DMA groups through a proton binding reaction and 4) relaxation of ionized polymer chains. Diffusion of water and ions are necessarily coupled in nAMA/DMA gels because sorption is driven by gel ionization which requires the concomitant entry of mobile counterions to preserve electroneutrality. Thus, in contrast to penetrant sorption in nonionizable gels, transport of mobile ions into the gel phase is a requisite step that adds to the complexity of the overall sorption process.

Three important observations strongly suggest that transport of mobile ions in these gels plays a central role in determining the rate and non-Fickian nature of water sorption:

1) the strong dependence of sorption rate on counterion structure (strong versus weak electrolyte, hydrophobicity), 2) the correlation of sorption rate with swelling endpoint in the presence of weak electrolytes, and the absence of this correlation in strong electrolyte solutions (Table 6.1), and 3) in rubbery BMA/DMA 70/30 gels water sorption in citrate buffer is non-Fickian but n-hexane sorption is essentially Fickian (Figure 6.12). It is evident that the non-Fickian behavior of sorption in nAMA/DMA gels cannot simply be attributed to the polymer relaxation processes as with nonionic glassy gels.

A working hypothesis for the cause of the non-Fickian kinetics is the following. Due to the hydrophobic nature of these gels in the unionized state, water and ions will have difficulty penetrating appreciably into the unswollen unionized polymer phase due to dielectric exclusion. Thus, the process of hydration and ionization of the chains which leads to gel swelling probably proceeds by a moving front mechanism regardless of whether the gels are initially glassy or rubbery. The ionization of the amine groups must be preceded by a hydration process which is probably confined to the immediate region of the front, and resembles a surface ionization process (the surface being at the position of the moving front). This mechanism is inherently non-Fickian since the characteristic length of the 'reaction zone' where hydration and ionization of the gel occurs does not change as the sorption process advances into the dry gel. This suggestion is supported by the finding that water sorption in the rubbery BMA/DMA gel is inherently non-Fickian (Figure 6.12), whereas sorption of n-hexane in the same gel, which is not driven by gel ionization, is essentially Fickian in nature. Of course, in the case of initially glassy nAMA/DMA gels, the relaxation of the chains as they become plasticized will also contribute to non-Fickian sorption behavior.

The moving front mechanism in initially glassy gels is also supported by the fact that the sorption curves shown in Figures 6.3-6.7 and 6.9 are sigmoidal, characterized by an initial phase of relatively slow water uptake followed by an accelerated phase. Such

sigmoidal profiles have been widely reported for sorption of organic penetrants into glassy nonionic polymers (25-28), and the accelerated phase has been termed 'super-Case II' transport by Jacques et al. (25). In the present system, the time of onset of the accelerated phase increases in approximate proportion to the sample disk thickness (Figure 6.5). Furthermore, it has been shown that the fractional release of caffeine from dynamically swelling gels in aqueous solution is proportional to the fractional water uptake at any time t (29). These results are consistent with the moving penetrant front mechanism of sorption discussed by Jacques et al. (25), Alfrey et al. (9) and Peterlin (30) for penetrant sorption in glassy polymers.

A moving front separates the swollen gel phase from the unswollen glassy core, as illustrated in Figure 6.17. The presence of the penetrant in the swollen phase lowers the glass temperature so that the gel in this region becomes rubbery and elastic. The remaining glassy core constrains swelling to the direction normal to the front. In particular, when the sample has a disk geometry with a large aspect ratio (as in the present work), the glassy core constrains swelling to essentially one dimension. When the two fronts meet at the sample midplane the intact core vanishes, and subsequent swelling is unconstrained and occurs in 3-dimensions. This characterizes the accelerated or super-Case II sorption phase. During the initial sorption phase, the penetrant fronts are far from the midplane of the sample, and sorption can be regarded as if it is occurring into a semi-infinite medium.

The glass temperatures of the gels studied here were determined by differential scanning calorimetry as reported in Chapter 4. For all of the gels that show biphasic sorption behavior, the T_g is above the temperature of the experiment (the lowest is 51.6 °C for the PMA/DMA 70/30 gel), indicating that the unhydrated gels, and therefore the cores, are glassy. The sorption curves of the BMA/DMA gel shown in Figure 6.8, however, are not biphasic. The T_g for this gel is 31.1 °C which is below most of the experimental temperatures indicating that the gel is rubbery. It does not contain a glassy core and thus

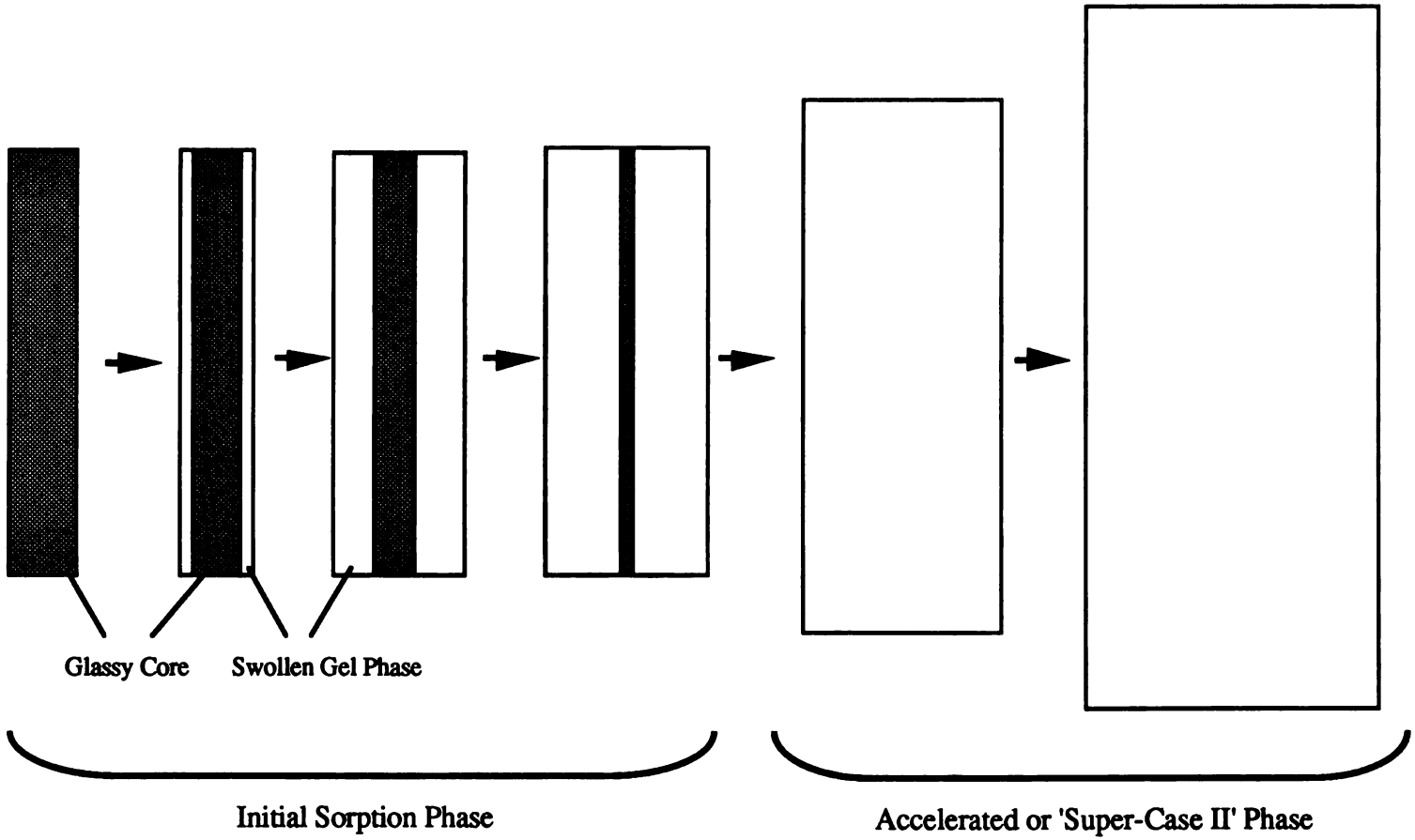

Figure 6.17. Illustration of the moving front mechanism of swelling in glassy gels. During the initial phase of water sorption, a moving front separating an outer swollen gel phase from an inner glassy core invades the material from the surface (swelling from the edges is neglected). Swelling is constrained to the direction normal to the front by the presence of the glassy core, which decreases in thickness as swelling proceeds. As the two swelling fronts meet at the sample midplane, the intact core vanishes and subsequent swelling occurs in three dimensions and at a faster rate due to the absence of the constraining core. This characterizes the accelerated or 'super-Case II' phase of swelling.

does not undergo the super-Case II acceleration phenomenon. However, water sorption kinetics in this gel are still non-Fickian and it is hypothesized that water sorption still proceeds by a moving front mechanism.

The sorption data of Figures 6.9 and 6.10 indicate that solution ionic composition profoundly affects the water sorption kinetics under conditions of identical pH and ionic strength. The initial sorption rate is significantly increased in the presence of organic electrolytes such as citrate or n-alkyl carboxylates compared with that in simple NaCl solutions. However, addition of nonionizable organic compounds such as methyl acetate or acetamide has no effect on sorption rate (Figure 6.15). In addition, the enhancement affected by organic electrolytes increases with increasing carbon chain length (Figure 6.16). A reasonable explanation for the effect of electrolyte composition on sorption kinetics is that the development of an outer charged gel layer during the course of sorption creates a diffusional resistance to the further entry of mobile ions. The resistance is created by the Donnan exclusion of coions (of which hydronium ion is the most important in the present case) which necessarily retards the rate of entry of counterions through electric coupling of ion fluxes (23,24). Thus Donnan exclusion sufficiently reduces the hydronium ion flux such that it ultimately limits the rate of amine group ionization at the swelling front and subsequent gel swelling. Similarly, Gehrke and Cussler (44) found that the swelling kinetics of a weak acid polyacrylamide hydrogel in alkaline solution were rate-limited by H^+/Na^+ ion exchange process due to the Donnan exclusion of hydroxide ions.

However, this Donnan barrier can be circumvented if the solution contains weakly acidic compounds. The protonated unionized form of the weak acid can "carry" hydrogen ions across the swollen Donnan layer without feeling the effects of the Donnan potential. Once at the swelling front, the hydrogen ion can be transferred to an as yet unionized network amine group which serves as a hydrogen ion acceptor (pK_a of the amine group is probably above that of the weak acid making the hydrogen ion transfer favorable). The

ionized carrier (conjugate base) thus becomes a counterion to the gel. This is quite similar to the mechanism by which salts of weak acids and bases circumvent other types of diffusional barriers such as natural lipid bilayers (31-32). Transfer of a hydrogen ion from ammonium ion to acetate produces unionized ammonia and acetic acid which can readily permeate bilayer membranes (32). This mechanism is consistent with the finding that water sorption kinetics are significantly faster in weak acid buffers (citrate or acetate) than in simple strong electrolyte solutions such as NaCl. Furthermore, the inability of nonionizable organic compounds to enhance the rate is consistent with this mechanism since they cannot serve as hydrogen ion carriers.

The increase in water sorption rate observed as pH decreases in citrate solutions (Figure 6.6) is also consistent with the hydrogen ion carrier theory. As solution pH decreases, the ionization equilibrium of citrate will shift to produce more undissociated citrate species (active carriers) which will increase the diffusional flux of carriers into the gel. It should be noted that decreasing pH will also serve to increase the diffusional flux of hydronium ions, but this effect is probably of minor consequence because of the relative exclusion of hydronium ions that is expected from the gel phase. The effect of pH on sorption kinetics in unbuffered NaCl solutions, however, has not been determined experimentally. In addition, the data of Table 6.1 indicates that the initial sorption rate of the MMA/DMA 70/30 gel in unbuffered NaCl solutions at pH 4.0 is not driven by the swelling stress that exists between the constrained swollen gel phase and the glassy core in the vicinity of the swelling front, as was proposed in some models of penetrant sorption into nonionic polymers (10,15,43). The swelling stress, which increases as the solvent concentration in the swollen gel phase increases, creates a time-dependent mechanical deformation of the glassy core which induces the advancement of the swelling front. The initial sorption rate does not correlate with the final swelling equilibrium (Table 6.1) which would be expected if a stress mechanism were operative.

The data of Figure 6.16 and Table 6.5 indicate that gel/organic counterion interactions are also involved. Increasing the hydrophobicity of the carboxylate simultaneously increases the water sorption rate and decreases gel swelling equilibrium. Carboxylates with longer hydrocarbon chains probably can concentrate at the hydrophobic swelling front and increase the sorption rate by plasticizing the chains, although the exact mechanism is poorly understood. As stated earlier, the carboxylate solutions were prepared with the same conjugate base (A^-) concentration which, because of the differences in pK_a's of the shorter chain (C_1-C_4) carboxylates (Table 6.5), will result in differences in the concentration of unionized (carrier) acid species and suggests the simultaneous effect of active carrier concentration. However, the largest sorption rate enhancements are observed with the longer chain (C_4-C_6) carboxylates which have virtually identical pK_a's. The decrease in the final swelling equilibrium probably results from carboxylate adsorption to network chains through hydrophobic contacts or by ion-pairing with the ionized gel amine groups. Adsorption of n-alkyl carboxylic acids (33) and sodium alkyl sulfonates (34) to anion exchange resins has been shown to increase sharply with an increase in length of the alkyl group.

As shown in Figures 6.3 and 6.4, sorption rate is strongly affected by gel comonomer ratio and nAMA sidechain length. As gel/solution compatibility decreases (as indicated by a reduction in the extent of swelling at equilibrium) either through an increase in the hydrophobic comonomer (MMA) content or an increase in the nAMA sidechain length the initial sorption rate decreases. Furthermore, sorption becomes more non-Fickian with increasing MMA comonomer content (n increases towards unity, Table 6.2). This trend is in accord with the sorption behavior of various organic penetrants in epoxy polymers as reported by Kwei and Zupko (35). It was found that as compatibility decreased for any penetrant/polymer pair, the sorption rate decreased and the kinetic exponent increased towards unity. However, Franson and Peppas observed Fickian water

sorption kinetics (n=0.5) in glassy poly(HEMA-co-MMA) and poly(HEMA-co-N-vinyl pyrrolidone) copolymers over a wide range of comonomer ratios (36).

The temperature dependence of the water sorption mechanism for the MMA/DMA gel shown in Figure 6.10, in which the kinetic exponent n decreases with temperature (indicating sorption becomes more Fickian), conforms with behavior that is typically observed in organic penetrant sorption into glassy materials (12-13,37-39). The explanation for such behavior centers on the fact that the rate of relaxation of chains undergoing a glass to rubber transition is known to increase sharply with increasing temperature, with activation energies estimated to be 20-60 kcal/mole (40-42). Conversely, Fickian diffusion processes are significantly less activated (E_{act}= 5-10 kcal/mole (13)) and are not as susceptible to rate enhancements due to increases in ambient temperature. As temperature increases, the rate of chain relaxation increases rapidly and plays a diminishing role relative to diffusion in the overall sorption process. This is consistent with the observed reduction in the exponent n towards 0.5 with increasing temperature for the MMA/DMA gel.

The temperature dependence of the exponent n for the rubbery BMA/DMA gel in aqueous solution (Figure 6.12), however, cannot be explained by the argument employed for the glassy MMA/DMA gel. The exponent n in the former case increases with temperature indicating that sorption becomes increasingly non-Fickian at elevated temperatures. One explanation of this trend is that because the hydrophobic effect increases in strength with increasing temperature, there is a stronger exclusion of water from the unhydrated polymer phase which causes a sharpening of the moving front and an increase in the kinetic exponent n.

6.5 Conclusions

The kinetics of water sorption in initially dry nAMA/DMA gels in aqueous solution have been shown to be very sensitive to gel composition (comonomer ratio and nAMA sidechain length), solution composition (pH, ionic strength and ionic composition) and temperature. Sorption rates increase significantly with decreasing pH, increasing temperature, decreasing nAMA content and decreasing nAMA sidechain length. Sorption curves in initially glassy gels are biphasic, which is consistent with a moving front mechanism, whereas sorption in initially rubbery gels is monophasic. Regardless of the T_g of the gel, sorption is generally non-Fickian in nature. Because water sorption is driven by gel ionization, ion transport plays an important role in determining the rate and mechanism of sorption. It is suggested that the Donnan exclusion of coions (including hydronium ions) accounts for the fact that sorption kinetics in solutions of strong electrolytes is quite slow. In the presence of weak electrolytes such as citrate or acetate, sorption kinetics are much faster presumably due to the ability of unionized species to carry hydrogen ions into the gel.

References

1. G.A. Gordon and P.R. Hsia in "Permeability of Plastic Films and Coatings to Gases, Vapors, and Liquids", H.P. Hopfenberg, Ed., p. 261, Polymer Science and Technology, Vol. 6, Plenum Press, New York, 1974.

2. W-H. Yang, V.F. Smolen and N.A. Peppas, Oxygen Permeability Coefficients of Polymers for Hard and Soft Contact Lens Applications, J. Memb. Sci., 9, 53 (1981).

3. B.J. Tighe in "Hydrogels in Medicine and Pharmacy", N.A. Peppas, Ed., Vol. III, Chapter 3, CRC Press, 1987.

4. V. Stannett in "Diffusion in Polymers", J. Crank and G.S. Park, Eds., Chapter 2, Academic Press, 1968.

5. E.L. Cussler, M.R. Stokar and J.E. Varberg, Gels as Size Selective Extraction Solvents, AIChE. J., 30, 578 (1984).

6. R.F.S. Freitas and E.L. Cussler, Temperature Sensitive Gels as Extraction Solvents, Chem. Eng. Sci., 42, 1, 97 (1987).

7. S.H. Gehrke, G. P. Andrews and E. L. Cussler, Chemical Aspects of Gel Extraction, Chem. Eng. Sci., 41, 8, 2153 (1986).

8. "Recent Advances in Drug Delivery Systems", J.M. Anderson and S.W. Kim Eds., Plenum Press, New York, 1984.

9. T. Alfrey, E.F. Gurnee and W.G. Lloyd, Diffusion in Glassy Polymers, J. Polym. Sci., C, 12, 249 (1966).

10. J.H. Petropoulous and P.P. Roussis, The Influence of Transverse Differential Swelling Stresses on the Kinetics of Sorption of Penetrants by Polymer Membranes, J. Memb. Sci., 3, 343 (1978).

11. E.F. Gurnee, Measurement of Concentration Gradients in Swelling Crosslinked Polymer Beads, J. Polym. Sci., A2, 5, 799 (1967).

12. N.L. Thomas and A.H. Windle, Case II Swelling of PMMA Sheet in Methanol, J. Memb. Sci. 3, 337 (1978).

13. N.L. Thomas and A.H. Windle, Transport of Methanol in Poly(Methyl Methacrylate), Polymer, 19, 255 (1978).

14. G.S. Park in "Diffusion in Polymers", J. Crank and G.S. Park, Eds., Chapter 5, Academic Press, 1968.

15. N.L. Thomas and A.H. Windle, Polymer, A Deformation Model for Case II Diffusion, 21, 613 (1980).

16. H. Fujita in "Diffusion in Polymers", J. Crank and G.S. Park, Eds., Chapter 3, Academic Press, 1968.

17. J. Crank, "The Mathematics of Diffusion", 2nd Edition, Chapter 11, Oxford University Press, 1975.

18. I. Ohmine and T. Tanaka, Salt Effects on the Phase Transition of Ionic Gels, J. Chem. Phys., 77, 5725 (1982).

19. J. Ricka and T. Tanaka, Phase Transition in Ionic Gels Induced by Copper Complexation, Macromolecules, 18, 83 (1985).

20. M.R. Van De Mark and N.D. Lian, Use of Organic Cosolvents for Enhanced Leaching of HEMA/MAA Copolymers, J. Polym. Sci., Part C, 25, 327 (1987).

21. C.J. Hamilton, S.M. Murphy, N.D. Atherton and B.J. Tighe, Synthetic Hydrogels: 4. The Permeability of Poly(2-Hydroxyethyl Methacrylate) to Cations - An Overview of Solute-Water Interactions and Transport Processes, Polymer, 29, 1879 (1988).

22. J. Kopecek, J Vacik and D. Lim, Permeability of Membranes Containing Ionogenic Groups, J. Polym. Sci., A1, 9, 2801 (1971).

23 F. Helfferich, "Ion Exchange", Chapter 6, McGraw-Hill, New York, 1962.

24. F. Helfferich, Ion-Exchange Kinetics. V. Ion Exchange Accompanied by Reactions, J. Phys. Chem. 69, 4, 1178 (1965).

25. C.H.M. Jacques, H.P. Hopfenberg and V. Stannett in "Permeability of Plastic Films and Coatings to Gases, Vapors, and Liquids", H.P. Hopfenberg, Ed., p. 73, Polymer Science and Technology, Vol. 6, Plenum Press, New York, 1974.

26. E. Bagley and F.A. Long, Two Stage Sorption and Desorption of Organic Vapors in Cellulose Acetate, J. Am. Chem. Soc., 17, 2172 (1955).

27. P. Drechsel, J.L. Hoavd and F.A. Long, Diffusion of Acetone into Cellulose Nitrate Films and Study of Accompanying Orientation, J. Polym. Sci., 10, 2, 241 (1953).

28. R.H. Holley. H.B. Hopfenberg and V. Stannett, Anomalous Transport of Hydrocarbons in Polystyrene, Polym. Eng. Sci., 10, 6, 376 (1970).

29. R.A. Siegel, M. Falamarzian, B.A. Firestone and B.C. Moxley, pH-Controlled Release from Hydrophobic/Polyelectrolyte Copolymer Hydrogels, J. Contr. Rel., 8, 179 (1988).

30. A. Peterlin, Diffusion in a Network with Discontinuous Swelling, J. Polym. Sci., B, 3, 1083 (1965).

31. H. Davson and J.F. Danielli, "The Permeability of Natural Membranes", University Press, Cambridge, 1943.

32. P. Mitchell in "Membranes and Ion Transort", Vol. 1, E.E. Bittar, Ed., Chapter 7, Wiley-Interscience, 1970.

33. S. Peterson and R.W. Jeffers, Equilibria Between Aliphatic Acids and a Strong Base Anion Exchanger, J. Am. Chem. Soc., 74, 1605 (1952).

34. Y. Ihara, Effect of Inorganic Salt on Adsorption of Sodium Alkyl Sulphates and Fatty Acid Sodium Salts from Aqueous Solution onto Ion Exchange Resins, J. Appl. Polym. Sci., 36, 891 (1988).

35. T.K. Kwei and H.M. Zupko, Diffusion in Glassy Polymers. I, J. Polym. Sci. A2, 7, 867 (1969).

36. N.M. Franson and N.A. Peppas, Influence of Copolymer Composition on Non-Fickian Water Transport Through Glassy Copolymers, J. Appl. Polym. Sci., 28, 1299 (1983).

37. L. Nicolais, E. Drioli, H.B. Hopfenberg and D. Tidone, Characterization and Effects of n-Hexane Swelling of Polystyrene Sheets, Polymer, 18, 1137 (1977).

38. L. Nicolais, E. Drioli, H.B. Hopfenberg and G. Caricati, Diffusion Controlled Penetration of Polymethyl Methacrylate Sheets by Monohydric Normal Alcohols, J. Memb. Sci., 3, 231 (1978).

39. H.B. Hopfenberg, R.H. Holley and V. Stannett, The Effect of Penetrant Activity and Temperature on the Anomalous Diffusion of Hydrocarbons and Solvent Crazing in Polystyrene Part I. Biaxially Oriented Polystyrene, Polym. Eng. Sci., 9, 4, 242 (1969).

40. C.H.M. Jacques and H.B. Hopfenberg, Kinetics of Vapor and Liquid Transport in Glassy Polyblends of Polystyrene and Poly(2,6-dimethyl-1,4-Phenylene Oxide). Part II, Polym. Eng. Sci., 14, 449 (1974).

41. H.B. Hopfenberg, L. Nicolais and E. Drioli, Relaxation Controlled (Case II) Transport of Lower Alcohols in Poly(Methyl Methacrylate), Polymer, 17, 3, 195 (1976).

42. A.S. Michaels, H.J. Bixler and H.B. Hopfenberg, Controllably Crazed Polystyrene: Morphology and Permeability, J. Appl. Polym. Sci., 12, 991 (1968).

43. J. Crank, A Theoretical Investigation of the Influence of Molecular Relaxation and Internal Stress on Diffusion in Polymers, J. Polym. Sci., 11, 151 (1953).

44. S.H. Gehrke and E.L. Cussler, Mass Transfer in pH-Sensitive Hydrogels, Chem. Eng. Sci., 44, 559 (1989).

Chapter 7.

Swelling Reversibility and the Mechanism of Gel Deswelling

7.1 Introduction

The primary purpose of the present chapter is to investigate the dynamic swelling properties of hydrated gels as driven by step changes in solution pH, particularly in the vicinity of the swelling phase transition. Attention will be placed on the reversibility of swelling given step pH perturbations of various magnitudes and the effect these perturbations have on the kinetics and mechanisms of gel deswelling. The understanding of such dynamic properties is of vital importance for the technological utilization of gels that display discontinuous volume transitions.

7.2 Experimental

7.2.1 Materials

Sodium chloride, sodium dihydrogen phosphate monohydrate (Mallinckrodt, Inc.), citric acid (Fisher Scientific) were all analytical reagent grade and were used without further purification. Water used in all experiments was double distilled and deionized. Gel samples (MMA/DMA and BMA/DMA 70/30 mole%) were prepared as thin circular disks (0.28 x 7 mm) according to the method described in Chapter 3.

7.2.2 Swelling Studies

Each kinetic swelling experiment was conducted in 2 liters of buffer solution of known pH and ionic strength according to the method of Chapter 6. In general, 0.01 M citrate buffer was used for buffers below pH 7.0, while 0.01 M phosphate buffer was used

for buffers above pH 7.0. The total ionic strength of all buffer solutions was adjusted to 0.1 M with NaCl.

7.2.3 Caffeine Release Experiments

Release of caffeine from hydrated dynamically deswelling gel disks was monitored in 100 ml of either 0.01 M citrate buffer pH 5.2 or 0.01 M phosphate buffer pH 8.0 at 25 °C. The ionic strength of all buffers was adjusted to 0.1 M with NaCl. Stirring was provided in all release experiments by a magnetically driven stir bar. The appearance of caffeine in the solution was quantitated by UV spectrophotometry at 272 nm.

7.3 Results and Discussion

7.3.1 Swelling Dynamics Induced by Changes in Solution pH

A series of experiments were performed to measure the dynamics and reversibility of swelling of a hydrated gel given step perturbations in solution pH. Figure 7.1 shows the effect of cycling the solution pH between 5.0 and 6.0 on the swelling dynamics of the MMA/DMA 70/30 gel. Upon transferring the gel disk to pH 6.0 solution (at time zero), rapid deswelling immediately occurs and a new swelling equilibrium is nearly attained within 20 min. Returning the pH to 5.0 (at 110 min) immediately initiates the swelling process and the original equilibrium hydration is virtually re-attained in 20 min. Successive cycles indicate that swelling is fully reversible and reproducible between pH 5.0 and 6.0, at least over the time-period observed.

Gel deswelling, as driven by successive step increases in solution pH, is indicated in Figure 7.2. Each pH increment corresponds approximately to a 0.5 pH unit increase. The gel was initially brought to swelling equilibrium at pH 5.0, and was then transferred to a series of buffer solutions of successively increasing pH. The gel responds to each

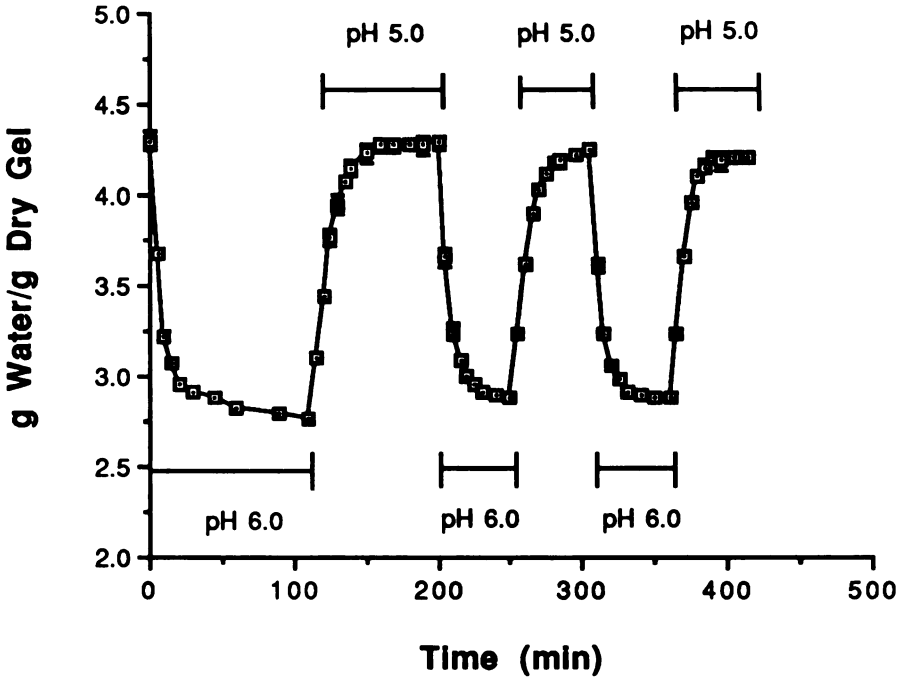

Figure 7.1. Changes in the swelling state of the MMA/DMA 70/30 mole% gel brought about by cycling the solution pH between 5.0 and 6.0 in 0.01 M citrate buffer. Gel was initially equilibrated to pH 5.0.

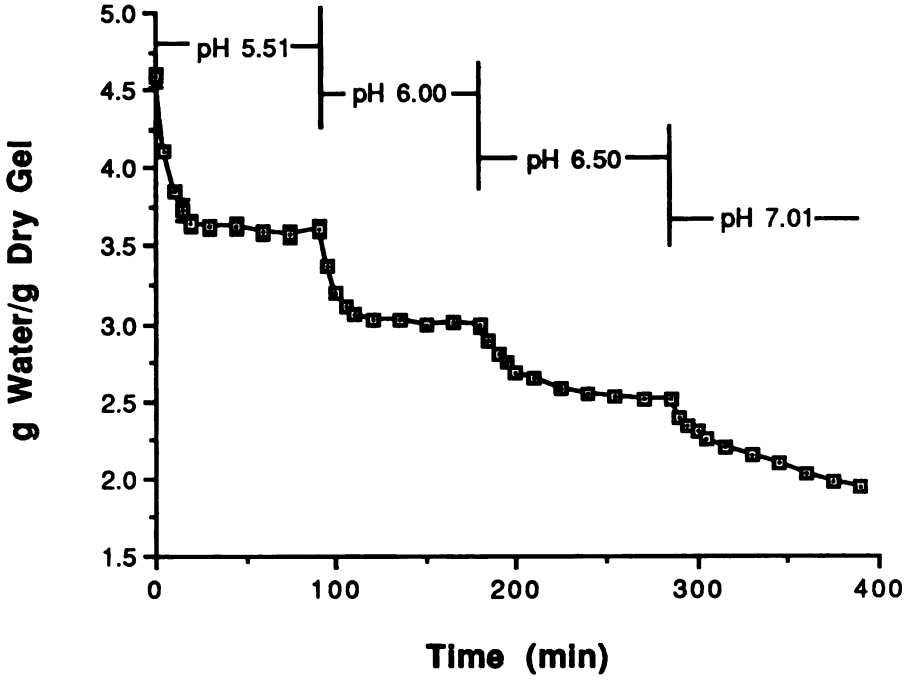

Figure 7.2. Deswelling of the MMA/DMA 70/30 mole% gel as driven by successive step increases in solution pH of approximately 0.5 pH unit.

increase in solution pH by immediately deswelling. However, the initial deswelling kinetics become progressively slower as the solution pH increases. Swelling equilibrium is attained in each interval (approximately 100 min) except at pH 7.01, where the process was still in progress after 100 min.

In another set of experiments, the effect of the magnitude of the pH perturbation on the rates of deswelling and swelling in hydrated gels was examined. Gel disks were initially brought to swelling equilibrium at pH 5.0, and then transferred (at time zero) to solutions of higher pH. Gel deswelling was monitored for a period of 30-75 min, after which time the disks were returned to the original pH 5.0 solution to initiate reswelling. Results for the deswelling and reswelling phases are shown in Figures 7.3A and 7.3B, respectively. For each curve, the pH of the deswelling solution is indicated. Swelling appears to be fully reversible for changes in pH of up to 3 pH units (pH 5.0-8.0). Regardless of the extent of deswelling, the gels essentially reattain swelling equilibrium when returned to pH 5.0 solution. However, the rates of deswelling appear to depend markedly on the magnitude of the pH change. For instance, deswelling in pH 5.26, 5.70, 6.05 and 6.52 solutions is initially rapid and the gels come to their new equilibria, as determined by the buffer pH, in about 30 min (60 min for the pH 6.52 solution). At higher final pHs, the deswelling rate is significantly decreased and the gels do not reach equilibrium for times exceeding 70 min.

Figure 7.4 shows the time-course of deswelling for a MMA/DMA 70/30 gel, initially equilibrated to pH 5.2, and transferred to pH 8.0 solution at time zero. The initial rate of deswelling is obviously quite rapid for the first 60 min., but then appears to enter a slower secondary deswelling phase during which gel hydration decreases very slowly. After 17 hrs. at pH 8.0, gel hydration remains significantly above the 'equilibrium' value as displayed in Figure 7.4.

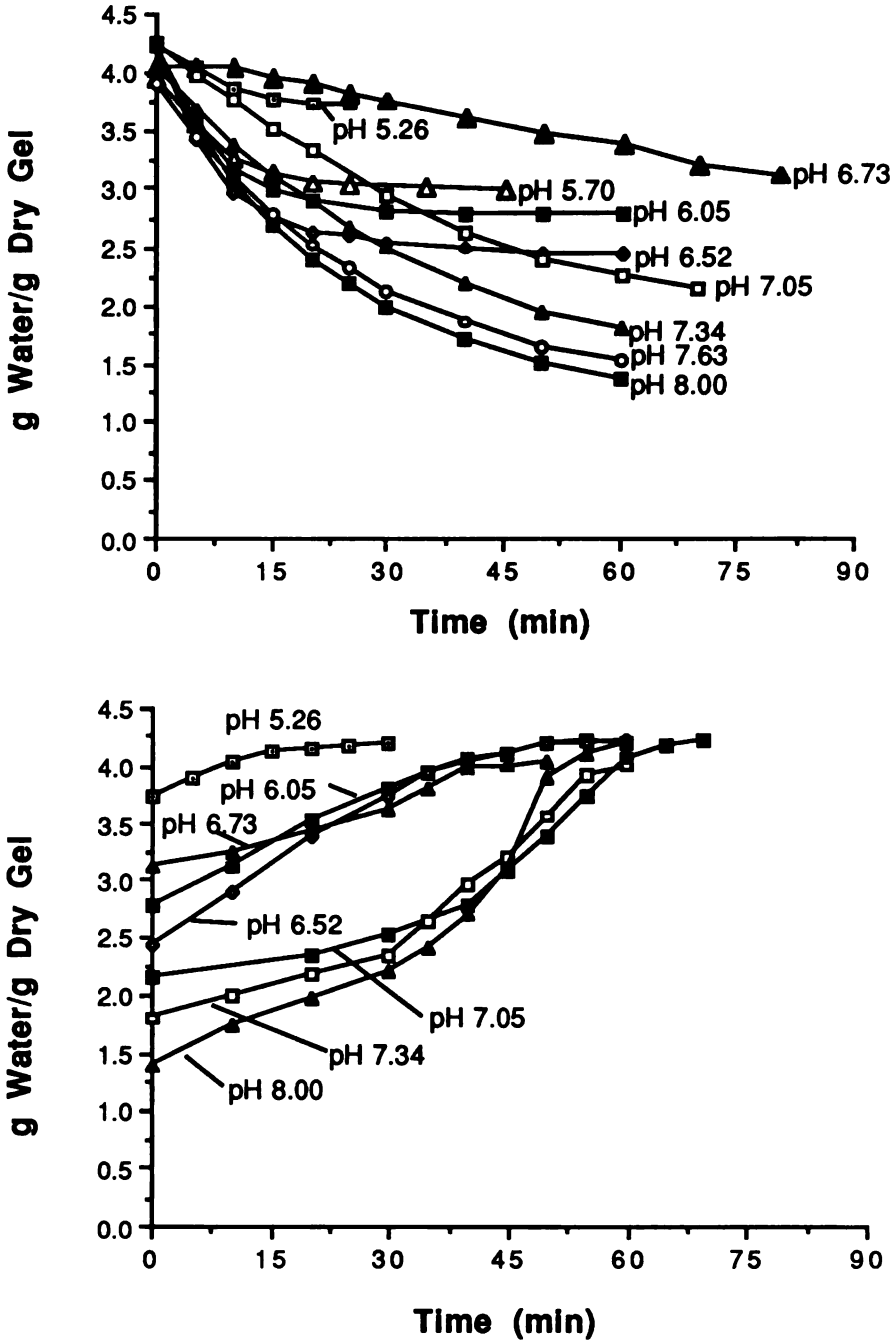

Figure 7.3. A (top), Effect of the magnitude of a step increase in solution pH on the kinetics of deswelling of the MMA/DMA 70/30 mole% gel. Gels were initially equilibrated to pH 5.0. B (bottom), Reswelling initiated by placing the gels back in pH 5.0 buffer.

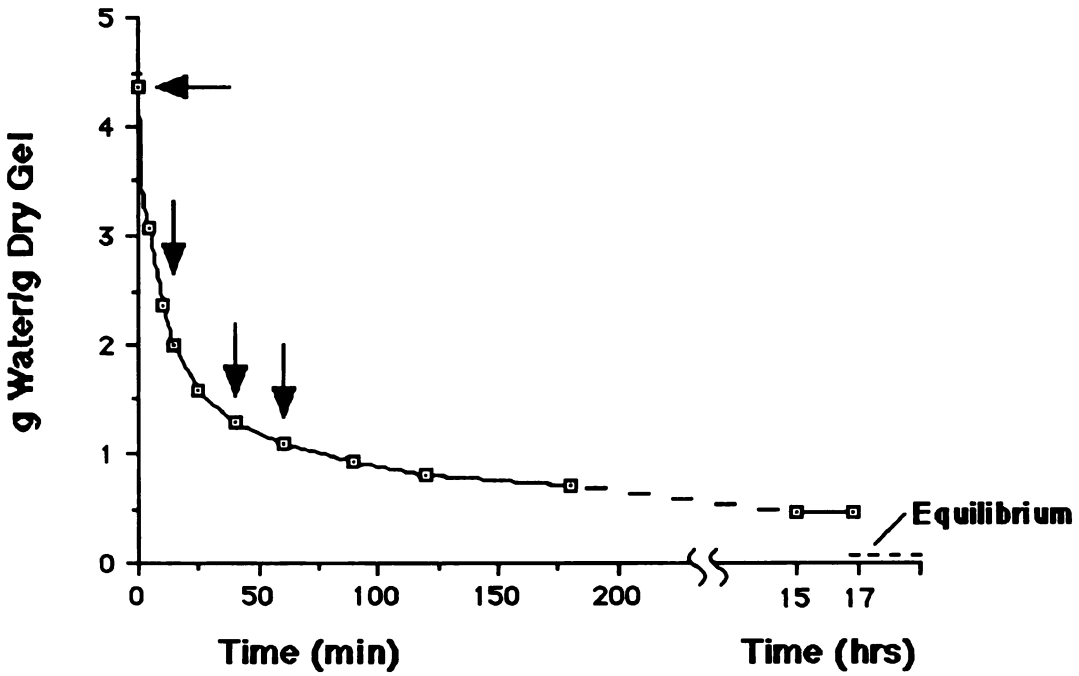

Figure 7.4. Time-course of deswelling of the MMA/DMA 70/30 mole% gel in pH 8.0 buffer solution at 25 °C. Gel was swollen to equilibrium at pH 5.2 and transferred to pH 8.0 buffer at time zero. Arrows indicate time points when caffeine release was monitored in experimental results of Figure 7.8.

7.3.2 Mechanisms of Gel Deswelling

The data in Figures 7.1 through 7.4 indicate that if the final pH does not traverse the transition pH (pH_t) of 6.6 (Chapter 4), the gel remains swollen and swelling equilibrium is reattained rapidly for both swelling and deswelling processes. Such perturbations in solution pH below pH_t cause relatively small changes in the network ion osmotic pressure as driven by the redistribution of mobile ions between the gel and the solution by diffusion (1). However, when the final solution pH is above pH_t, the kinetics of deswelling become more complicated and considerable slowing is apparent. Furthermore, two different phases of kinetic slowing can be observed depending on the final pH. Initial-phase slowing is observed when the final pH approaches pH_t as shown in Figure 7.3A. A late-phase slowing process becomes evident as the final pH is increased away from pH_t, while the initial-phase slowing disappears as shown in the pH 8.0 deswelling curve of Figure 7.4.

We now investigate the possible transport mechanisms that could give rise to the kinetic deswelling phenomena observed when the transition pH is traversed. For initial-phase slowing, we consider kinetic slowing that can arise in the vicinity of a phase transition. For late-phase slowing, two mechanisms are proposed and experimentally tested: gel surface collapse leading to skin formation and the process of gel vitrification. These mechanisms will be considered individually.

7.3.2.A Slowing Near a Transition Point. Tanaka and Fillmore demonstrated that the swelling and deswelling processes of a highly swollen polyacrylamide gel are determined by the cooperative diffusion of the polymer network in water, which is related to the bulk counterflow of water through the network (2). This finding is in direct contrast to the view that gel deswelling is rate-limited by the diffusion of water molecules in the gel (3). Tanaka et al. have also shown that the important transport parameter is the cooperative

diffusion coefficient of the network, which is defined as the ratio of the elastic modulus of the network to the friction coefficient between the network and the fluid (4,5).

If the swollen gel undergoes a first-order volume phase transition as induced by a change in a system variable (e.g. temperature), then it has been shown that the cooperative diffusion coefficient of the network is greatly diminished when the final state is in the vicinity of the swelling transition (6-8). This phenomenon is analagous to 'critical slowing' and causes the kinetics of such swelling or deswelling processes to become very slow (8).

An explanation for this slowing phenomenon is illustrated in Figure 7.5 where free energy of a swollen gel is schematically depicted as a function of volume for six cases of gel deswelling. For a gel at equilibrium, the global minimum in the free energy curve defines the equilibrium volume. When a sudden change in some external variable (e.g. temperature, pH etc.) is invoked, the minimum in the free energy curve is shifted along the volume axis. The gel, which is now no longer at equilibrium, imbibes or expells solvent which corresponds to a fall down the free energy curve towards the new minimum. The driving force, and thus the rate of the process, is proportional to the derivative of the free energy with respect to volume (slope). When the final state does not cross a transition point (cases A-C), the derivative is finite and the deswelling process occurs with a finite rate. When the final state lies across, but close to, the transition point (case D), a large composition change is thermodynamically dictated but the system encounters a substantial kinetic barrier which decreases the rate. The magnitude of the barrier decreases as the final pH increases past the transition pH (compare cases D-F). This is similar to 'critical slowing' which occurs when the initial and final states are close to the critical point of the transition and the free energy curve connecting the two states has a zero derivative.

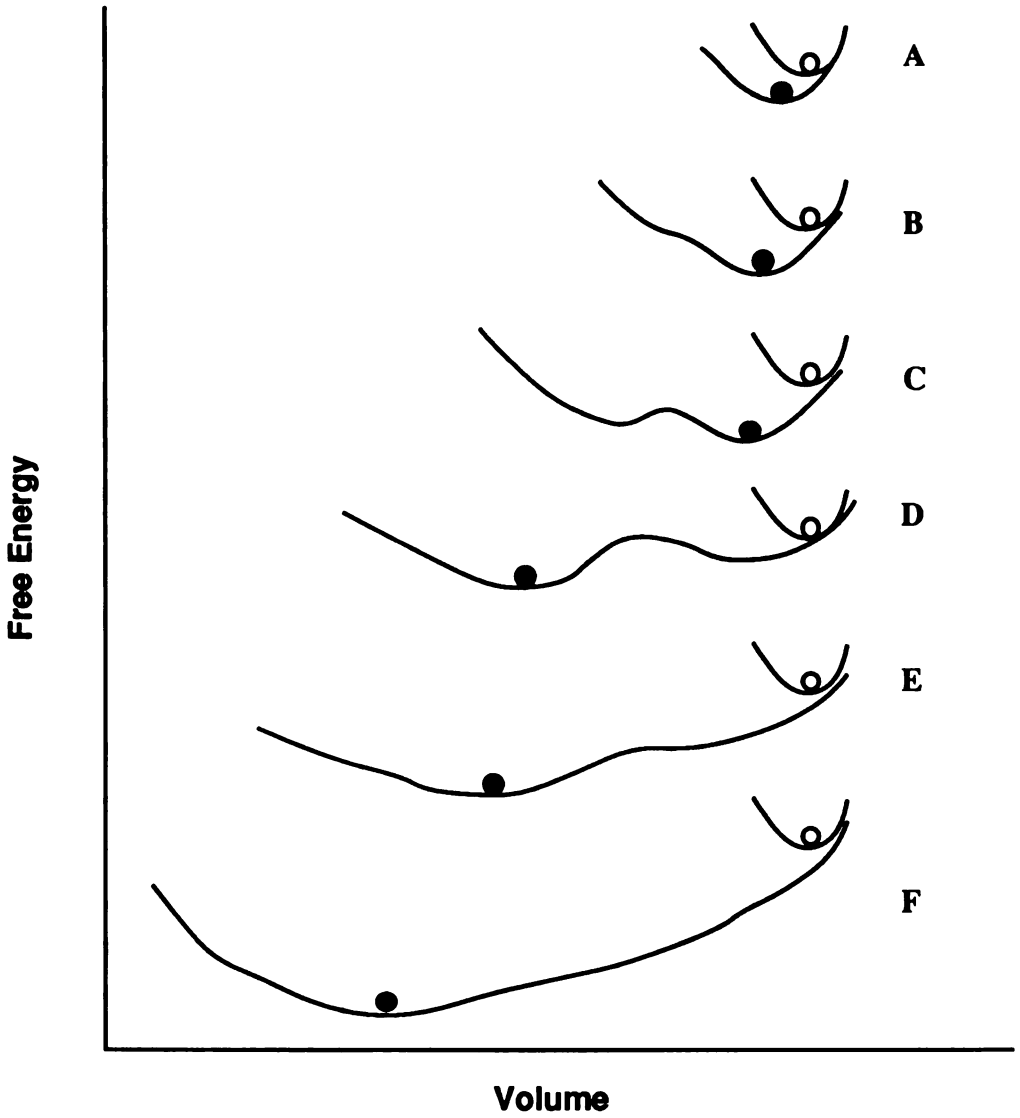

Figure 7.5. Illustration of the origin of kinetic slowing in the vicinity of the swelling transition. Shown is a representation of the free energy surface of the system as a function of gel volume for six cases of deswelling, all starting from the same initial state (signified by ○). The global minimum in free energy defines the equilibrium volume of the gel. When the solution pH is suddenly increased, the minimum in the free energy curve shifts to a smaller volume. The gel, which is now no longer at equilibrium, expells solvent (deswells) which corresponds to a fall down the free energy curve towards the new global minimum (signified by ●). When the final pH remains below the transition pH (cases A-C), the change in volume is relatively small and the gel deswells rapidly. When the final pH is above the transition pH (cases D-F), the new equilibrium lies at much smaller volume dictating a large change in swelling. The gel now encounters a kinetic barrier to collapse (phase separation) whose magnitude decreases as the final pH increases past the transition pH. Adapted from (8).

In the case of the MMA/DMA 70/30 gel, the swelling isotherm exhibits what is believed to be a discontinuous, first-order volume transition near pH 6.6 (Chapter 4). If in fact this is a first-order transition, then it can be expected that deswelling processes should become progressively slower as the final pH approaches pH_t from above. This mechanism was investigated by fitting an empirical exponential decay function of the form (8):

$$SR(t) = A\, e^{-kt} \tag{7.1}$$

to the initial portion of each deswelling curve of Figure 7.3A, where SR(t) is the swelling ratio at time t and k is a rate constant characterizing the deswelling rate. The obtained rate constants (k) are listed in Table 7.1 and are plotted as a function of final solution pH as

Table 7.1. Deswelling Rate Constants as a Function of Final Solution pH Obtained by Fitting Eqn. 7.1 to the Data of Figure 7.3A.

Final pH	Deswelling Rate Constant (k) (min^{-1})	R^2
5.26	0.00852	1.00
5.70	0.0188	0.997
6.05	0.0277	0.992
6.52	0.0355	0.989
6.73	0.00391	0.998
7.05	0.0120	0.999
7.34	0.0154	0.996
7.63	0.0199	0.996
8.00	0.0247	0.987

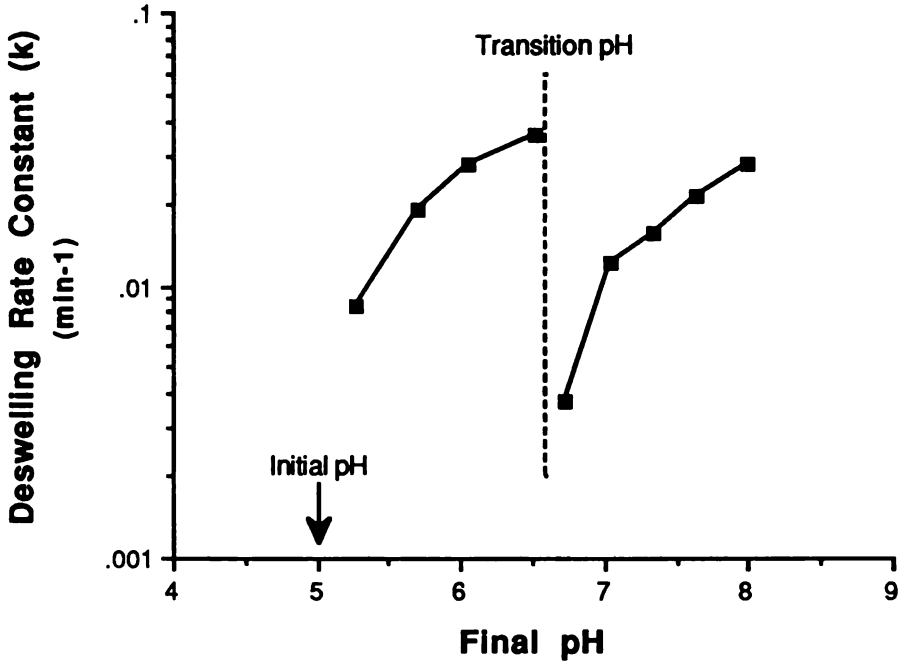

Figure 7.6. Deswelling rate constants (k) obtained by fitting eqn. 7.1 to the data of Figure 7.3A. There is an apparent discontinuity in k near pH 6.6 which corresponds to the pH of the swelling phase transition.

shown in Figure 7.6 (initial pH being 5.0). The results of Table 7.1 and Figure 7.6 show that k abruptly changes in the vicinity of pH 6.6. As the final pH approaches pH 6.6 from above, k decreases by nearly an order of magnitude. Presumably, further slowing would occur if the final pH could be adjusted even closer to the pH_t. When the final pH is increased away from the transition pH, k increases to magnitudes that are comparable to those where no transition has taken place. Thus, it is seen that the observed initial-phase slowing only occurs for final pH values that are above, but close to, the transition pH. These data provide evidence that the initial-phase slowing is due to a mechanism caused by the proximity to a swelling phase transition, and that the swelling transition observed for the MMA/DMA 70/30 gel (Chapter 4) is in fact a first-order transition. However, this mechanism does not explain the late-phase kinetic slowing that is observable when the final pH is well above pH_t.

7.3.2.B Surface Collapse. At all pHs above pH_t, the equilibrium state of the gel is a dense, hydrophobic structure. It is conceivable that, upon exposure to solution at high pH, network chains on the surface of the swollen gel collapse to form a compact layer or 'skin'. The formation of a compact surface layer could effectively seal off the gel interior from the external solution and prevent further efflux of water and exchange of ions. This could explain the fact that the rate of deswelling at pHs well above pH_t is initially rapid, but decreases sharply after a period of time because an impermeable skin may require finite time to form. Similar slowing phenomena were reported for hydrogels that undergo reversible thermal collapse by Matsuo and Tanaka (8) and Bae et al. (9). They found that gel deswelling, initiated by a step increase in the solution temperature through the LCST of the gel, was initially rapid, but leveled off after several hours to a value of gel hydration that was well in excess of the equilibrium value. They attributed the late-phase kinetic slowing to the formation of a collapsed surface layer, although experimental verification of this mechanism was not provided.

The surface collapse hypothesis was experimentally tested in the present case by measuring the diffusional release of a small marker molecule, initially located in the interior of a hydrated gel, during various stages of dynamic deswelling (10). Evidence for transport limitations would be manifest in a decrease in the rate of release of the marker as gel deswelling progresses. Caffeine was used as the marker molecule for three reasons: 1) it is small (MW 194) and water soluble, 2) it is uncharged at all experimental pHs which avoids the effects of Donnan partitioning or other electrostatic interactions with the gel, and 3) it has an appreciable molar extinction coefficient at 272 nm which facilitates quantitation.

The release experiments were performed as illustrated in Figure 7.7. Gel disks were brought to swelling equilibrium at pH 5.2 in a 0.01 M citrate buffer solution that contained 10 mg/ml caffeine. This allowed caffeine to partition into the gel but did not affect the equilibrium swelling ratio. Swollen, caffeine loaded disks were then transferred to 100 ml of 0.01 M phosphate buffer pH 8.0 also containing 10 mg/ml caffeine. The samples were allowed to deswell in this solution for various durations (0, 15, 40 or 60 min) but were not depleted of their caffeine payloads. Samples were then removed, lightly blotted and placed in 100 ml of caffeine-free phosphate buffer at pH 8.0. The subsequent appearance of caffeine in the buffer was monitored by periodically sampling aliquots of the solution and measuring the optical density at 272 nm. The '0 min' sample was transferred from the pH 5.2 caffeine solution directly to the pH 8.0 caffeine-free release solution and corresponded to the case where gel deswelling and caffeine release commence concurrently. An additional (control) experiment was performed by monitoring caffeine release from a gel sample loaded with caffeine at pH 5.2 and transferred to fresh caffeine-free buffer at pH 5.2 (no gel deswelling). In addition, the deswelling of a gel equilibrated to pH 5.2 and transferred to pH 8.0 buffer was measured.

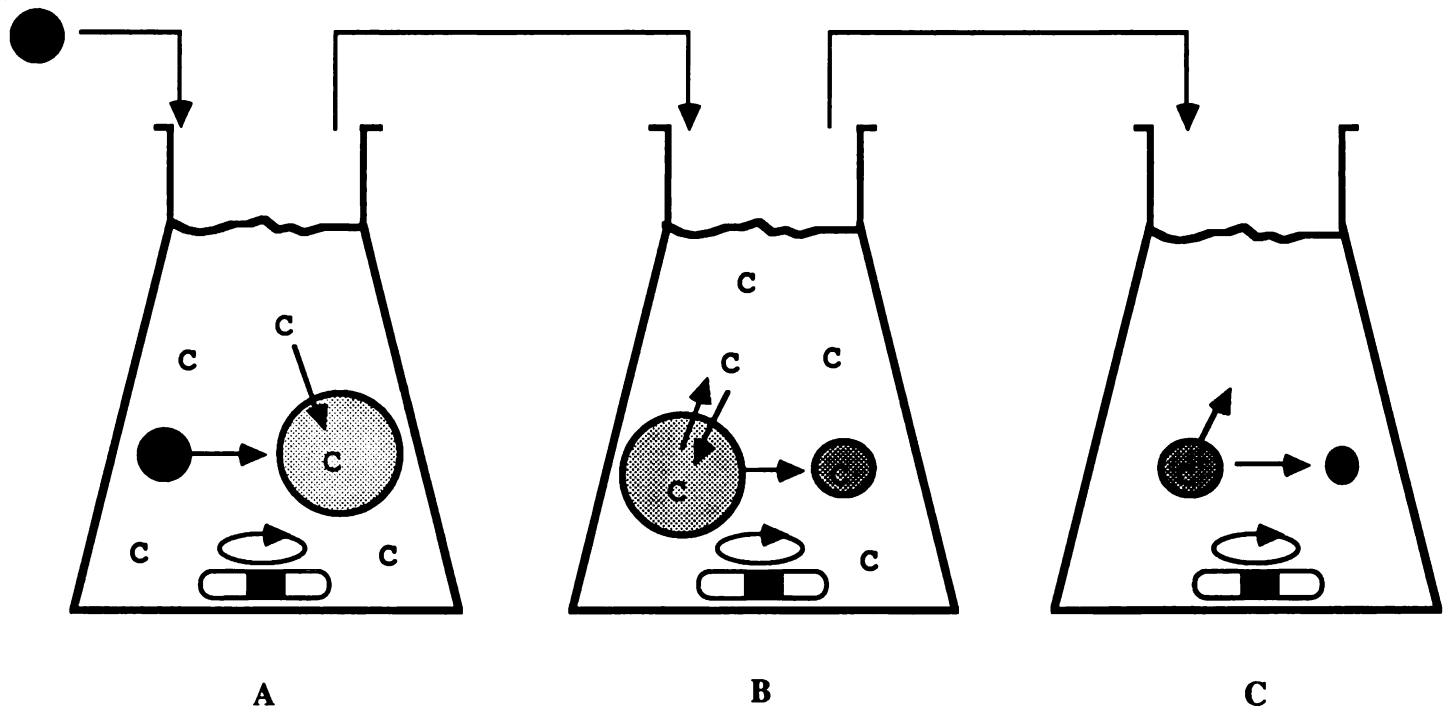

Figure 7.7. Procedure of caffeine release experiments. A, Dry gel disk is placed in pH 5.2 buffer containing 10 mg/ml caffeine (signified by C). Gel swells and caffeine partitions into the gel interior. B, The swollen, caffeine loaded disk is transferred to pH 8.0 buffer also containing 10 mg/ml caffeine. Disk deswells but is not depleted of its caffeine payload. C, The partially deswollen disk is transferred to fresh pH 8.0 caffeine-free buffer, and the rate of appearance of caffeine from the dynamically deswelling disk is monitored by UV spectrophotometry at 272 nm.

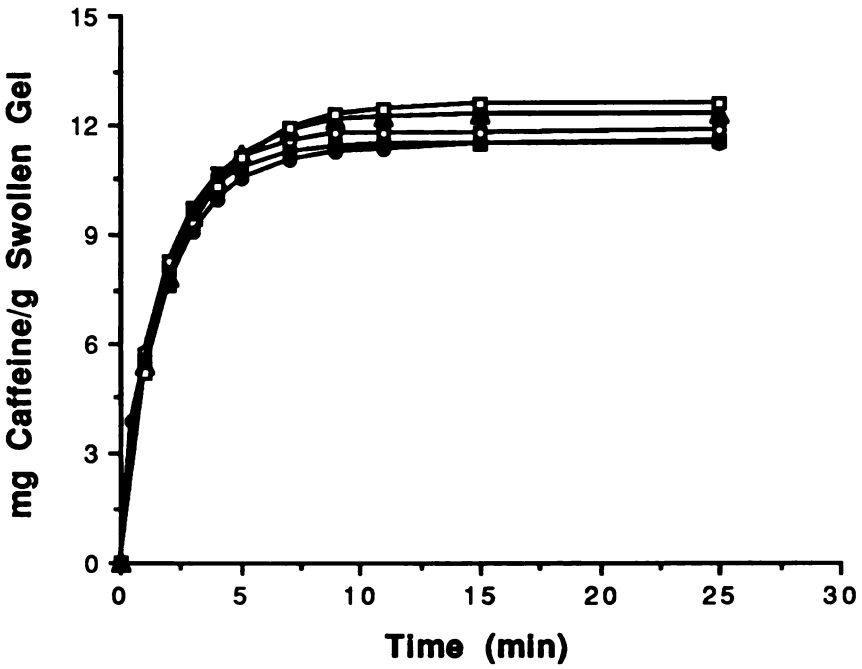

Figure 7.8. Release of caffeine in pH 8.0 buffer from hydrated dynamically deswelling gel disks at various stages of collapse. Experimental procedure is illustrated in Figure 7.4 and 7.7. Control (release into pH 5.2 buffer) (●), 0 min. collapse (■), 15 min. collapse (○), 40 min. collapse (▲) and 60 min. collapse (❑).

The results of the caffeine release experiments are shown in Figure 7.8. The arrows in the deswelling curve of Figure 7.4 indicate the points on the deswelling curve where caffeine release was monitored. The release data indicate that transport of caffeine from gels undergoing concurrent deswelling is unaffected by the duration of deswelling at pH 8.0 up to 60 min. All release curves superimpose on that for the equilibrated, non-deswelling (control) gel at pH 5.2. Release in all cases was complete in about 8 min. Although the deswelling process (Figure 7.4) has slowed down considerably after 60 min and remains significantly above its equilibrium swelling ratio of 0.11, the release data show no evidence for the existence of a diffusional barrier to caffeine. It was further found that the total amount of caffeine released linearly correlated with the initial water content of disks of different thicknesses. This confirms that caffeine is being released from the full volume of the disk and is not simply a surface release phenomenon. Since the diffusivity of water is expected to be greater than that for caffeine, it is concluded that a diffusional barrier to water transport is not contributing to the slow late-phase deswelling kinetics observed.

7.3.2.C Gel Vitrification. Another source of late-phase slowing could involve the process of gel vitrification as the internal water content of the gel becomes sufficiently low. It is well known that the glass temperatures of polymeric materials are lowered by the presence of solvent, which can induce a glass-to-rubber transition if T_g is lowered sufficiently below ambient temperature (ref. 10 Chapter 6). The glass temperature of the MMA/DMA 70/30 gel in the dry state is 91 °C (Chapter 4), which indicates that it is glassy at room temperature. MMA/DMA gels at equilibrium at pHs above the transition are hard and brittle and appear to have retained the glassy character of the dry state. This suggests that, at some point during the process of deswelling at high pH, an initially swollen gel will become kinetically limited as it approaches glassy compositions.

This mechanism was tested by measuring the deswelling kinetics of a swollen gel at temperatures well above its dry state T_g. This eliminates any possible contribution from slowing due to vitrification. The BMA/DMA 70/30 gel was chosen for this purpose because it has a T_g of 31 °C (Chapter 4), and the deswelling experiment was conducted at 50 °C. Figure 7.9 indicates the time course of deswelling of the BMA/DMA gel, initially brought to equilibrium at pH 5.2 and then placed in pH 8.0 buffer at time zero. As observed in the MMA/DMA deswelling curve (Figure 7.4), the kinetics of deswelling proceed rapidly for the first 50-60 min. but sharply level-off thereafter. After 17 hrs at pH 8.0, the measured swelling ratio (0.26) remained well above the equilibrium value of 0.01. Subsequent caffeine release experiments also showed that skin formation was not occuring during deswelling of the BMA/DMA gel at 50 °C and pH 8.0. These experiments strongly indicate that late-phase slowing is common to glassy and rubbery polyelectrolyte gels alike and thus cannot be attributed to a vitrification process.

7.3.2.D Other Possible Late-Phase Slowing Mechanisms. Although we are presently unable to experimently confirm a single causative mechanism for late-phase kinetic slowing, several other potential mechanisms can be proposed.

A possible source of slowing could result from the difficulty in expelling water that hydrates the network chains through hydrogen bonds and dipole/dipole interactions. It is well known that a significant fraction of the internal water content of a wide variety of tissues, synthetic membranes and swollen hydrogels exhibits properties that are distinct from bulk water (11-17). Differential scanning calorimetry measurements indicate that some hydrogel water does not freeze when taken well below 0 °C (12-14), and NMR spin-lattice relaxation studies reveal classes of water in poly(N-vinyl-2-pyrrolidone-co-methyl methacrylate) and polyhydroxyethyl methacrylate (pHEMA) hydrogels that have widely differing

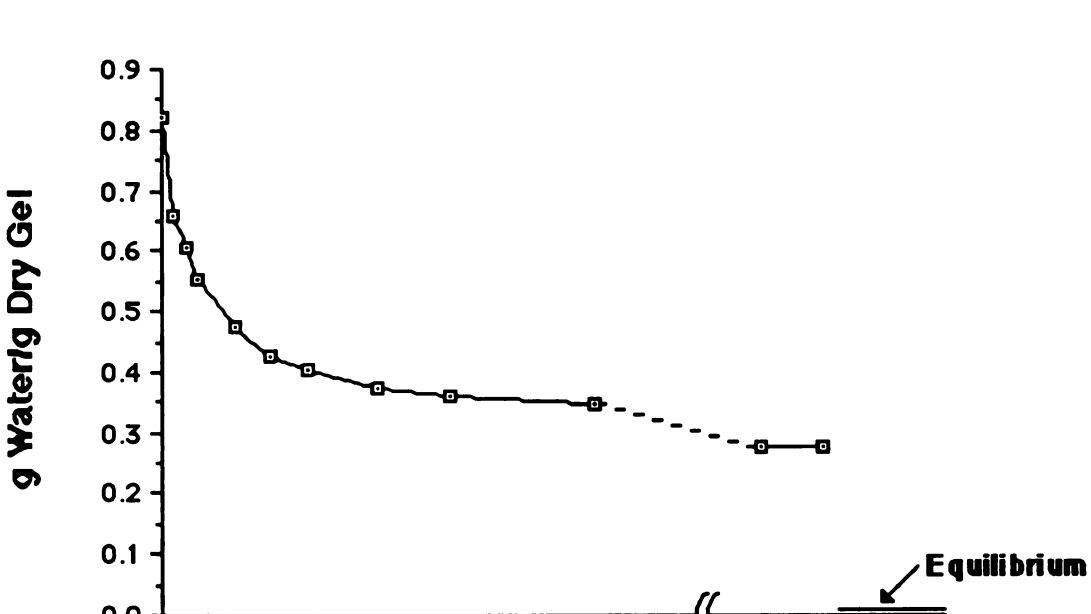

Figure 7.9. Time-course of deswelling of the BMA/DMA 70/30 mole% gel in pH 8.0 buffer at 50 °C. Gel was swollen to equilibrium at pH 5.2 buffer and transferred to pH 8.0 buffer at time zero.

translational mobilities (15-16). Furthermore, the presence of fixed charges and ions in hydrated ionic membranes can significantly reduce the bulk water content (17). Evidence that this anomalous water strongly interacts with the network comes from the finding that freezable, bulk-like water is not detectable in pHEMA until the gel reaches a certain minimum hydration (12-14,16). Apparently, water that first enters the gel becomes strongly associated with the chains which prevents it from freezing. Bulk water does not appear until the network chains are sufficiently hydrated.

In the process of deswelling from an extensively swollen state, the more mobile 'bulk' water component is expected to be expelled first. This process probably occurs rapidly (provided that the final state is not close to a transition point) and is most likely rate-limited by the cooperative diffusion of the network. Once the gel is depleted of bulk water, the deswelling process could abruptly slow down due to the lower mobility of the bound water component, which could contribute to rate-limiting the process.

The last mechanism that we consider for kinetic slowing is based on proton diffusion-reaction. In response to a step increase in external pH, transient proton diffusion within the gel may be delayed by reversible binding to unprotonated or 'free' amine groups on the gel. If the gel free amine group concentration exceeds the proton concentration inside the gel, which will likely be the case at high pH, then transient proton diffusion may be slowed by several orders of magnitude due to such binding. Nussbaum and Grodzinsky have shown that proton diffusion-reaction determines the rate at which force transients develop in stretched collagen membranes that are exposed to step perturbations in solution pH (18).

7.4 Conclusions

It is been demonstrated in this chapter that the swelling and deswelling processes of swollen MMA/DMA 70/30 gels are rapid and highly reversible given step-changes in solution pH that do not traverse the transition pH of 6.6. However, when the final pH traverses the transition pH, the kinetics of deswelling become more complicated. Two different phases of kinetic slowing are observed which depend on the proximity of the final pH to the transition pH (pH_t). Early-phase slowing becomes more pronounced as the final pH approaches pH_t, which was shown to be consistent with a critical slowing phenomenon. When the final pH is well above pH_t, deswelling is initially rapid but then is followed by a late-phase slowing process. Although a causitive mechanism was not found for late-phase slowing, it was shown that mechanisms including surface collapse or gel vitrification are not involved. Other mechanisms such as bound water or proton diffusion-reaction were proposed.

References

1. F. Helfferich, "Ion Exchange", Chapter 6, McGraw-Hill, New York, 1962.

2. T. Tanaka and D. Fillmore, Kinetics of Swelling of Gels, J. Chem. Phys., 70, 1214 (1979).

3. T. Tanaka, Kinetics of Phase Transition in Polymer Gels, Physica A, 140, 261 (1986).

4. T. Tanaka, L.O. Hocker and G.B. Benedek, Spectrum of Light Scattered from a Viscoelastic Gel, J. Chem. Phys., 59, 9, 5151 (1973).

5. T. Tanaka, S.-T. Sun, Y. Hirokawa, S. Katayama, J. Kucera, Y. Hirose and T. Amiya, Mechanical Instability of Gels at the Phase Transition, Nature, 325, 796 (1987).

6. T. Tanaka, S. Ishiwata and C. Ishimoto, Critical Behavior of Density Fluctuations in Gels, Phys. Rev. Lett., 38, 14, 771 (1977).

7. A. Hochberg, T. Tanaka and D. Nicoli, Spinodal Line and Critical Point of an Acrylamide Gel, Phys. Rev. Lett., 43, 3, 217 (1979).

8. E. Sato Matsuo and T. Tanaka, Kinetics of Discontinuous Volume-Phase Transition of Gels, J. Chem. Phys., 89, 3, 1695 (1988).

9. Y.H. Bae, T. Okano, R. Hsu and S.W. Kim, Thermo-Sensitive Polymers as On-Off Switches for Drug Release, Makromol. Chem. Rapid Comm., 8, 481 (1987).

10. B.A. Firestone and R.A. Siegel, Dynamic pH-Dependent Swelling Properties of a Hydrophobic Polyelectrolyte Gel, Polym. Comm., 29, 204 (1988).

11. M.S. Jhon and J.D. Andrade, Water and Hydrogels, J. Biomed. Mater. Res., 7, 509 (1973).

12. H.B. Lee, M.S. Jhon and J.D. Andrade, Nature of Water in Synthetic Hydrogels I. Dilatometry, Specific Conductivity, and Differential Scanning Calorimetry of Polyhydroxyethyl Methacrylate, J. Coll. Inter. Sci., 51, 2, 225 (1975).

13. P.H. Corkhill, A.M. Jolly, C.O. Ng and B.J. Tighe, Synthetic Hydrogels: 1. Hydroxyalkyl Acrylate and Methacrylate Copolymers - Water Binding Studies, Polymer, 28, 1758 (1987).

14. W.E. Roorda, J.A. Bouwstra, M.A. de Vries and H. Junginger, Thermal Behavior of Poly Hydroxy Ethyl Methacrylate p(HEMA) Hydrogels, Pharm. Res., 5, 11, 722 (1988).

15. F.X. Quinn, E. Kampff, G. Smyth and V.J. McBrierty, Water in Hydrogels. 1. A Study of Water in Poly(N-vinyl-2-Pyrrolidone/Methyl Methacrylate) Copolymer, Macromolecules, 21, 3191 (1988).

16. G. Smyth, F.X. Quinn and V.J. McBrierty, Water in Hydrogels. 2. A Study of Water in Poly(Hydroxyethyl Methacrylate), Macromolecules, 21, 3198 (1988).

17. M. Tasaka, S. Suzuki, Y. Ogawa and M. Kamaya, Freezing and Nonfreezing Water in Charged Membranes, J. Memb. Sci., 38, 175 (1988).

18. J.H. Nussbaum and A.J. Grodzinsky, Proton Diffusion-Reaction in a Protein Polyelectrolyte Membrane and the Kinetics of Electromechanical Forces, J. Memb. Sci., 8, 193 (1981).

Chapter 8.

Unresolved Issues and Suggestions for Future Work

The C_1-C_3 nAMA/DMA gels studied in this work have T_gs that are well in excess of ambient temperature and thus exist in the glassy state when dry (Chapter 4). The glassy property has made the study of the equilibrium and kinetic swelling properties of these gels somewhat problematic. For example, it is difficult to establish whether the low gel hydrations of the C_1-C_3 nAMA/DMA gels observed at pHs above the swelling transition reflect true equilibria or result from the exceedingly slow response time of chains in the glassy state. In addition, the non-Fickian aqueous sorption kinetics observed in dry gels are, in part, due to the glassy state (Chapter 6). The determination of T_gs of gels as a function of hydration by differential scanning calorimetry would be valuable in establishing when a gel would undergo the glass-to-rubber transition due to the plasticizing effect of water. Hydrated gels whose T_g are just below ambient temperature will exist in the rubbery state and will achieve swelling equilibria relatively rapidly. This would indicate an upper bound to the extent of swelling of gels in the glassy state.

A more satisfying approach to this problem would be to 'design out' the glassy property inherent in the shorter chain nAMA/DMA gels. This could be readily accomplished by replacing the glass-forming n-alkyl methacrylate (nAMA) monomer with an n-alkyl acrylate (nAA) in the synthesis of copolymer gels with DMA. The nAA monomer structure, shown in Figure 8.1, differs from that of the nAMA monomer in the absence of the α-methyl group. This structural difference results in a dramatic lowering of the T_gs of the corresponding homopolymers, as listed in Table 8.1, as well as a reduction in hydrophobicity. The reduction in hydrophobicity, however, could be compensated for

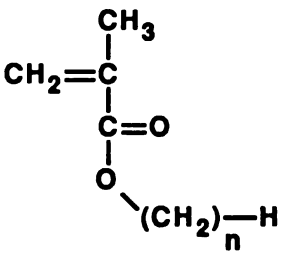

n-alkyl methacrylate (nAMA)

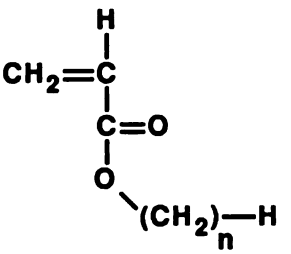

n-alkyl acrylate (nAA)

Figure 8.1. Structures of the n-alkyl methacrylate and n-alkyl acrylate monomeric units. The α-methyl group is absent in the nAA structure.

by increasing the length of the n-alkyl ester group. Gels produced by copolymerizing an nAA with DMA will be rubbery since the resulting T_g of the copolymer generally will lie somewhere between the T_gs of the two homopolymers (recall that poly(DMA) has a T_g of 19 °C, see Chapter 4).

Table 8.1. Comparison of Glass Temperatures of Some Poly(nAA) and Poly(nAMA) Homopolymers.

n-Alkyl Group	T_g of Poly(nAA) (°C) (from Ref. (1))	T_g of Poly(nAMA) (°C) (from Table 4.2)
methyl	9	104
ethyl	-22	66
n-butyl	-55	19

As discussed in Chapter 5, implementation of the Donnan theory required the knowledge of the gel charge density (ρ_{net}). The simple proton mass action law (eqn. 5.9) used to describe the ionization equilibrium of the gel in the theory was an oversimplification. It neglected to account for the the changes in the gel ionization constant that arise due to dielectric effects of the gel internal phase, which will change as a function

of gel hydration, and the electrostatic interactions between the charged groups. In future attempts to model the equilibrium swelling behavior of nAMA/DMA gels, the degree of ionization of the amine groups will have to be measured experimentally through the use of a technique which can distinguish between the ionized and unionized forms of the amine, such as NMR spectroscopy. Alternatively, the incorporation of permanently charged cationic groups into the gel, such as quaternary ammonium groups, would make the direct computation of ρ_{net} straightforward since the charged state of the gel would be independent of solution conditions.

Further studies are necessary to test the hydrogen ion carrier theory proposed to explain the swelling kinetic rate enhancement observed in the presence of weak electrolytes in Chapter 6. The postulated mechanism involves the ability of protonated unionized buffer species to transport hydrogen ions across the swollen gel layer to the swelling front. Diffusion of hydronium ions, themselves, across the swollen gel phase is expected to be slow due to Donnan exclusion. The rate of water sorption is thus predicted to vary directly with the concentration of the unionized form of the buffer. The theory could be tested by determining the sorption kinetics in a series of weak acid buffers of different pK_a's at constant solution pH and total concentration, which would result in different unionized species concentrations. In addition, this experiment would allow the contributions of solution pH and of the unionized buffer species to the overall sorption rate to be separated. Since other chemical properties of the buffer species (hydrophobicity) were shown in Chapter 6 to affect the sorption rate, it is important to employ a series of acids of chemically similar structure, such as the substituted acetic acids, in order to minimize specific interactions between the buffer and the gel phase.

References

1. E.A. Collins, J. Bares and F.W. Billmeyer, Jr., "Experiments in Polymer Science", Chapter 9, pp. 222-223, Wiley, 1973.